High Performance Conducting Polymer Coatings for Enhanced Electrochemical Properties

by

Amit Nautiyal

A dissertation submitted to the Graduate Faculty of
Auburn University
in partial fulfillment of the
requirements for the Degree of
Doctor of Philosophy

Auburn, Alabama
December 15, 2018

Keywords: conducting polymers, anticorrosive coating, ion exchange, energy storage

Approved by

Xinyu Zhang, Chair, Associate Professor, Chemical Engineering
Maria Auad, Professor, Chemical Engineering
Xiaoyuan Lou, Associate Professor, Materials Engineering
Russell Mailen, Assistant Professor, Aerospace Engineering
Asha-Dee Celestine, Assistant Professor, Aerospace Engineering

Abstract

The dissertation focuses on performance of conducting polymer as a coating that can used as anticorrosive agent, ion-exchange membrane and electrodes for energy storage devices. There are mainly two ways to synthesize conducting polymers: *chemical* and *electrochemical* polymerization. The most commonly used method is chemical oxidative polymerization. However, the conducting polymer produced via chemical method can have impurities because of the presence of oxidants. This can affect the uniformity of the coating and as a result their performance. In this study, we adopted electrochemical polymerization to improve the purity of conducting polymer coating. Besides, the polymerization time can be reduced to few minutes instead of few hours. Moreover, we can control the thickness of the coating and can have *in-situ* deposition on any surface.

There are several factors such as electrolyte composition, concentration of monomer, electrochemical technique and deposition potentials that affects formation of conducting polymer film that directly influences its homogeneity and compactness as a coating and its electrochemical performance. Adhesion is important for good coating thus cannot be overstated. There are four projects covered in this dissertation.

The first project (chapter 2) discussed the effect of various acidic medium on passivation of steel and electropolymerization of polypyrrole. The coating morphology was compared when

coating produced using various doping agents. Further, the integrity of the coating was evaluated by testing their adhesion and was enhanced. Additionally, the harsh bleach treatment was performed multiple times and thermal stability of the produced coating was tested. Moreover, the corrosion performance of the coating was investigated in salt solution (mimicking marine environment).

The second project (chapter 3) focuses on the electropolymerization of polyaniline on stainless steel. The reversible change in oxidation states of polyaniline was used to study the electrochemical exchange of anion from the produced coating. Additionally, the coating adhesion was evaluated and enhanced using bio-adhesives. Further, this study was applied to study the anion transport from the solution to the coating to understand the electrochemical activity of the polyaniline.

The third project discusses the use of sulfur based conducting polymers as anticorrosive coatings. The thiophene derivatives have limited work in the field of corrosion therefore, poly (3,4-ethylenedioxythiophene) was used to study its anticorrosive properties for steel. The electropolymerization potential was optimized for better corrosion performance. The effect of counter-ion used for poly (3,4-ethylenedioxythiophene) as anticorrosive coating was studied.

The fourth project focused on the effect of various dopant acids on electrochemical performance of polyaniline as electrode material for pseudocapacitors. The electrochemical testing involves charge storage, cycling stability that can be affected by size of the dopant used.

Acknowledgments

Firstly, I would like to thank to my advisor Dr. Xinyu Zhang for the continuous support towards my doctoral study and related research, for his patience, motivation, and immense knowledge. His advice helped me in all the time of research and writing of this thesis.

Besides my advisor, I would like to acknowledge the insightful comments and encouragement provided by my committee members, Dr. Maria Auad, Dr. Xiaoyuan Lou, Dr. Russell Mailen and Dr. Asha-Dee Celestine in writing this dissertation.

I would like to thank Dr. Tung-Shi Huang and his student Dr. Mingyu Qiao for collaborating with us, who provided us an opportunity to explore our research in different areas. Special thanks to Department of Polymer and Fiber and Department of Chemical Engineering to provide welcoming environment and to USDA, without their precious support it would not be possible to conduct this research. I thank my fellow group members for the challenging discussions which inspired me to widen my research from various perspectives. I am truly grateful to Jonathan Cook for his insights in every stage of my research and for keeping the work environment lively.

At last, I would like to express my sincere gratitude to my parents, Mr. Satyapal Singh and Mrs. Lata who made countless sacrifices to help me get to this point and supported me throughout the years. My brothers, Sumit and Abhishek for their continuous motivation to finish my study with expediency. My wife, Komal who stood by me through all my struggles, my fits of resentment and always supported me in the moments when there was no one to answer my queries.

Table of Contents

List of Tables

List of Illustrations

List of Abbreviations

CP	Conducting polymer
PAni	Polyaniline
PPy	Polypyrrole
PEDOT	Poly (3,4-ethylenedioxythiophene)
PTh	Polythiophene
PA	Polyacetylene
PPP	Polyparaphenylene
SWCNT	Single Walled Carbon Nanotubes
CNT	Carbon Nanotubes
DNA	Deoxyribonucleic acid
p-TSA	p-Toluenesulfonic acid
SA	Sulfuric acid
CSA	Camphor sulfonic acid
SDS	Sodium dodecylsulfate
SDBS	Sodium dodecylbenzene sulfonate
DA	Decanoic acid
MIC	Microbially induced corrosion
CS	Carbon steel

SS	Stainless steel
DI	Deionized water
SRB	Sulfate-reducing bacteria
SHE	Standard Hydrogen Electrode
MSE	Mercury Sulfate Electrode
SEM	Scanning Electron Microscopy
LSV	Linear Sweep Voltammetry
OCP	Open Circuit potential
BPB	Butterfield's phosphate buffer
CMC	Critical micelle concentration
S. aureus	Staphylococcus aureus
PA	Phytic acid
PhAc	Phosphoric acid
EIS	Electrochemical Impedance Spectroscopy
L	Leucoemeraldine
E	Emeraldine
P	Pernigraniline
EB	Emeraldine base
ES	Emeraldine salt
LH	Protonated leucoemeraldine
EH	Protonated emeraldine
PH	Protonated pernigraniline
Sf	Sulfates

Ph	Phosphates
CV	Cyclic voltammetry
DAm	Dopamine
EDLC	Electrochemical double layer capacitor

Chapter 1

Conducting polymers: synthesis and their applications

1.1 Introduction

Mostly, materials can be categorized into three types based on their electrical properties: conductor, semiconductor and insulators. A material is considered as conductor with electrical conductivity greater than 10^3 $S \cdot cm^{-1}$ and are termed as metals whereas if electrical conductivity of a material is less than 10^{-7} $S \cdot cm^{-1}$ then it is termed as an insulator. However, if conductivity of a material lies in between those two then the class of material is known as semiconductors. Their conductivity ranges from 10^{-4} - 10^3 $S \cdot cm^{-1}$ depending upon the degree of doping. Organic polymers typically are described as sigma (σ) and pi (π) bonds. The σ-bonds are immobile due to the covalent bonds between the carbon atoms. These polymers are saturated macromolecules and were considered as excellent electrical insulators. On the other hand, conjugated polymers have π-electrons that are localized unlike σ-electrons.

Generally, polymers were used for insulation purposes until late 1970s it was changed by Alan G. MacDiarmid, Hideki Shirakawa and Alan J. Heeger by the discovery of conducting polyacetylene whose conductivity can be reached as high as 10^3 $S.cm^{-1}$ by iodine doping. [1] This unforeseen discovery broke the traditional concept of polymers to be viewed as insulators and commenced the new area of conducting polymers that sometimes known as “synthetic metals”. They have become

the leading material in polymer science and a variety of conducting polymers (CP) have been developed ever since their discovery including polyaniline (PAni), polypyrrole (PPy), poly(3,4-ethylenedioxythiophene) (PEDOT), polythiophene (PTh), polyacetylene (PA), polyparaphenylene (PPP) and others as shown in figure 1.

1.1.1 Structure and properties. The unique electrical properties of conducting polymers arise from their chemical structure. The common feature in all conducting polymer systems is alternating single and double bonds along the backbone coupled with atoms providing p-orbitals for a continuous orbital overlap (e.g. N, S etc.) that makes them intrinsically conducting. This creates the conjugated system by overlapping π-orbitals that provides the path for charge carriers to move along polymeric chain. The conjugation give rise to delocalization of electrons that gives rigidity to their planar structure. Although conducting polymers are coupled with weak van der Waals forces, there is a strong interchain interactions provided by extended p-orbitals in the polymer. This counts for their poor solubility in many solvents. Moreover, the unsaturated polymer backbone and their proclivity to crosslink makes them thermosets. The electronic properties of a conducting polymer can be influenced by factors such as their structure, functional groups, morphology and oxidation states. They can transform from an insulator to a metal like conductor by chemical or electrochemical oxidation or reduction, this process is known as doping. The doping process changes their electrical conductivity by orders of magnitude ranging from 10^{-3} (insulator) to 10^{2} $S.cm^{-1}$ (metal). [2] The doping of conducting polymers involves partial oxidation or partial reduction to alter its electrical conductivity.

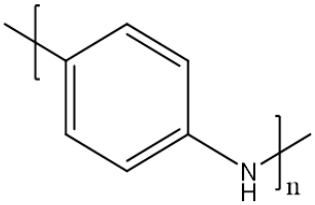

Polyaniline (PANI)

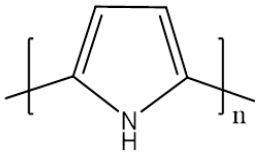

Polypyrrole (PPy)

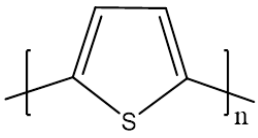

Polythiophene (PT)

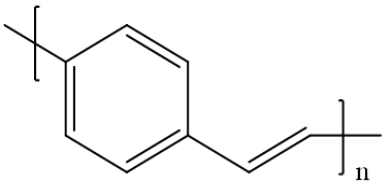

Poly (p-phenylene vinylene) (PPV)

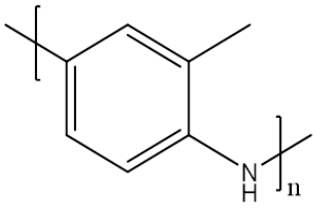

Poly (o-toluidine) (POT)

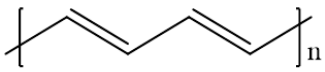

Polyacetylene (PA)

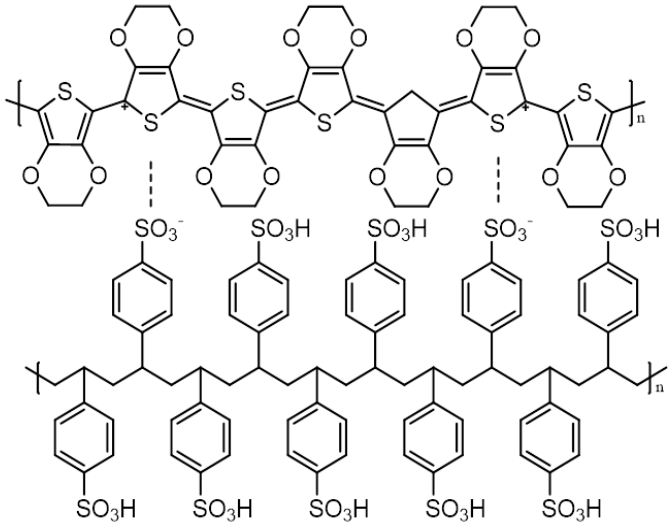

PEDOT:PSS

Poly (p-phenylene) (PPP)

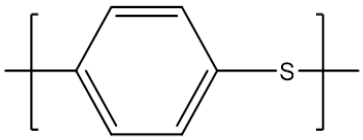

Poly (p-phenylene sulfide) (PPS)

Figure 1.1 Chemical structures of repeat unit in various conducting polymers

Oxidative doping, also known as p-doping, involves chemical treatment of the polymer with electron withdrawing group that makes it p-type material and conduct electricity predominantly through hole transport while reductive doping known as n-doping involves treating it with electron donating group that makes polymer n-type material that are primarily electron conductors. This type of doping called chemical doping. The doping can also be achieved by applying positive or negative potential to the polymer in suitable electrolyte, this is called electrochemical doping. For example, using polyacetylene, p-doping and n-doing can be written as: [1]

p-doping (*oxidation*) : $(C_2H_2)_n + \frac{3}{2} I_2 \rightarrow (C_2H_2)_n^+ + I_3^-$

n-doping (*reduction*) : $(C_2H_2)_n + Na \rightarrow (C_2H_2)_n^- + Na^+$

1.1.2 Conduction mechanism. A polymer can efficiently conduct electricity if it can satisfy two conditions: it must have charge carriers in the form of holes or electrons and free path to travel along the backbone. The charge carriers can be provided by doping the polymers that creates the electrons (n-doping) or hole (p-doping) to flow through the states created by overlapping of π-orbitals. The planar structure of conjugated polymer provides uninterrupted path for charge carriers to travel along the polymer backbone. When a conjugated polymer satisfies both these conditions, it is termed as *conducting polymer*. [3] The conductivity in conducting polymer is described by hopping mechanism where charge carriers are forced to hop from one chain to another. Therefore, to avoid any obstacle in charge transport along the backbone the polymer chains should be tightly packed to provide obstacle free path.

1.1.3 Synthesis. Conducting polymer can be synthesized mainly by two methods: chemical or electrochemical. Most of the conducting polymers have been synthesized *chemical oxidative polymerization* by oxidizing the monomer in the presence of suitable counterion (as a dopant). General oxidative polymerization involves two main steps: i) oxidation of monomer and ii) polymer chain growth. The oxidant takes an electron from monomer and forms monomer cation radical that coupled with another monomer unit to form dimer. This process leads to polymer chain growth and continues until all the reagents are consumed or reached equilibrium. Figure 2 shows the schematics of chemical oxidative polymerization of aniline. Chemical oxidative polymerization is useful when large quantity of the polymer is required. However, the polymer formed is contaminated with oxidant used and needs to be purified. *Electrochemical polymerization* method is favorable as it is directly polymerized on the conductive substrate. The polymer formed is free from oxidant impurity since potential was used to initiate the reaction. This method further eliminates the processing of conducting polymer as it was directly polymerized on the desired substrate. The method is also useful where polymer film electrodes are required. The thickness and conductivity of the polymer film can be easily controlled by proper design of experiments such as applied potential/current, type of electrolyte, type and size of dopants, temperature and techniques used for electropolymerization etc. The low potential deposition yields in short chain polymer while high potential leads to the formation of cross linked network [4,5]. The change in temperature influences the kinetics of electropolymerization and can alter the properties of resulting CP. The low temperature decreases the rate of coupling and decreases the proton elimination step. However, low temperature electropolymerization stabilizes the structure and enhances the conductivity of CP [6]. The polar solvent results in highly efficient polymer due to reduction in Columbic repulsion during coupling step.

Aniline oxidation

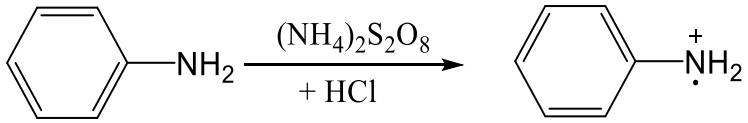

Radical coupling

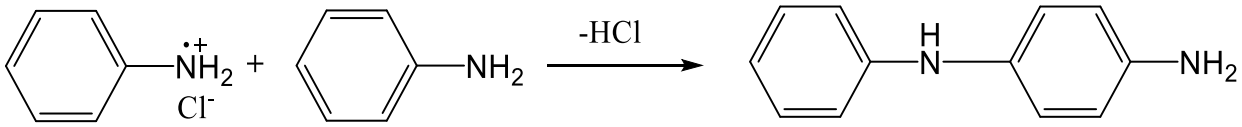

Dimer

Chain growth

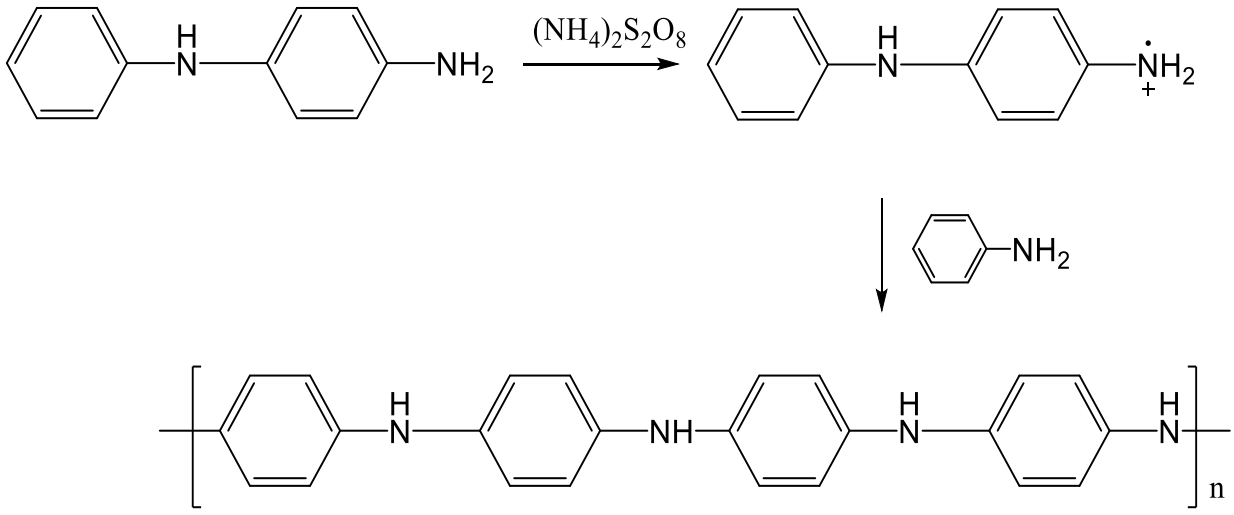

Polyaniline

Figure 1.2 Schematic presentation of mechanism of chemical oxidative polymerization of aniline.

Most electropolymerization of conducting polymer has been carried out in aqueous solution due to their low oxidation potential. The electropolymerization of conducting polymer can also be carried out in organic solvent such as acetonitrile, most widely used. However, due to its low basicity it inhibits the proton elimination step to initiate polymerization. Additionally, some organic solvents are not environmental friendly, therefore, to avoid safety hazard water is the best choice for electropolymerization of conducting polymers mainly polyaniline (PAni), polypyrrole (PPy), polythiophenes (PTh) and their derivatives. In addition to above, the conductivity and properties of the electropolymerized conducting polymer is greatly influenced by counterions (dopant) used. It was reported the electrochemical polymerization of a conducting polymer occurs in three different steps: i) monomer oxidation at anode, including formation of soluble oligomer in diffusion layer, ii) oligomer deposition, involves nucleation and growth and iii) solid state polymerization, involving polymer chain growth [7] as shown in figure 1.3. The electronic properties of a conducting polymer are significantly affected by polymerization method. The electrochemical polymerization of a conducting polymer can be carried out using different electrochemical techniques, broadly used are: cyclic voltammetry, chronoamperometry and chronopotentiometry. The three most widely used electrochemical polymerization methods to electrosynthesized conducting polymer are: potentiodynamic, potentiostatic and galvanostatic polymerization. In *potentiodynamic* polymerization, the electrode potential is regularly changes during polymerization process in cyclic manner within a certain potential range. This is carried out using cyclic voltammetry technique. The electropolymerized polymer formed had open structure and polymer chains are disorderly arranged, thus decreased conductivity. This is due to cyclic change in electrode potential on electropolymerized polymer film that undergoes continuous exchange of electrolyte and solvent in freshly form polymer film.

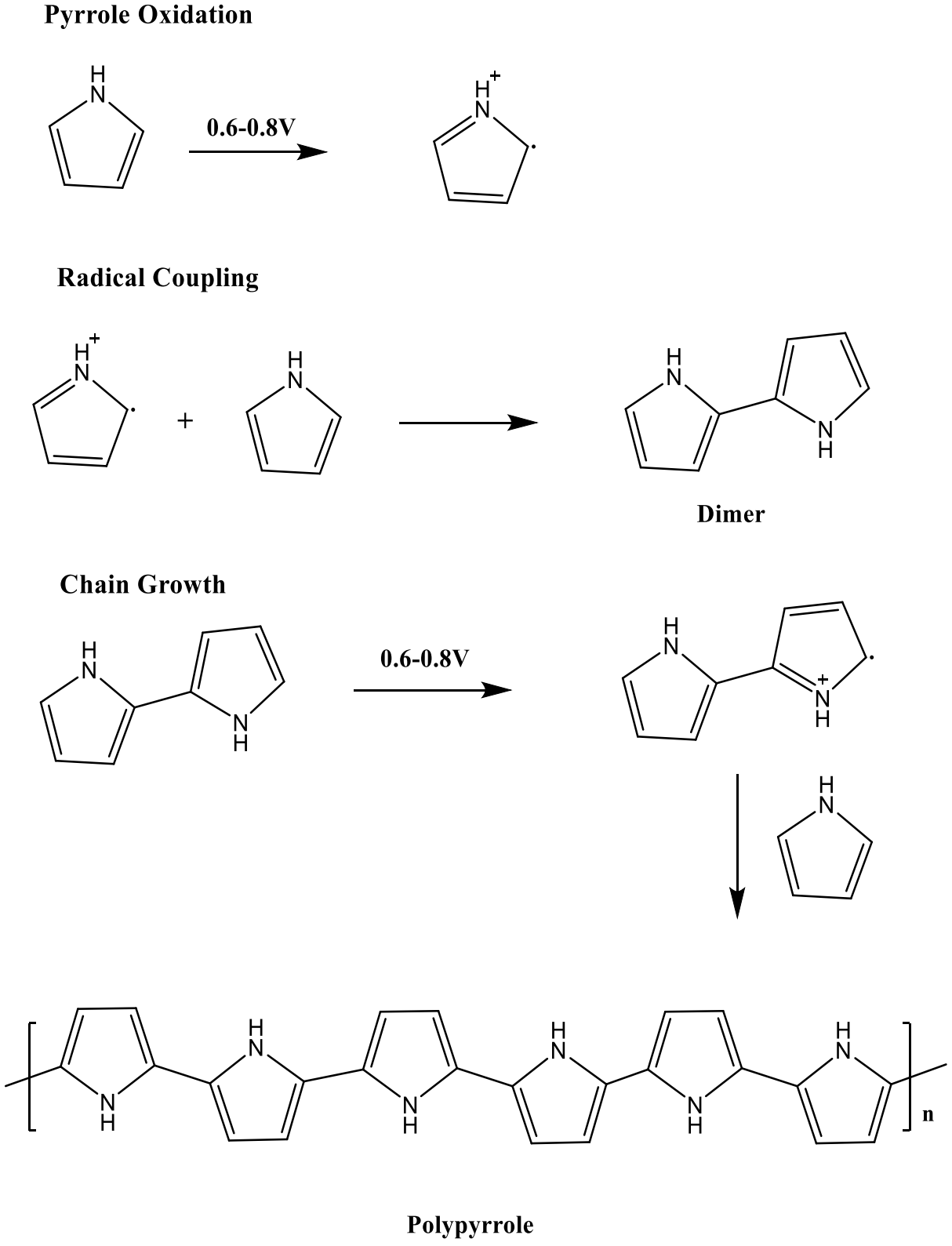

Figure 1.3 Schematic presentation of mechanism of electrochemical polymerization of pyrrole.

The electropolymerized polymer formed had open structure and polymer chains are disorderly arranged, thus decreased conductivity. This is due to cyclic change in electrode potential on electropolymerized polymer film that undergoes continuous exchange of electrolyte and solvent in freshly form polymer film. The polymer formed using this method is smooth and in its neutral state. However, polymer electrosynthesized by potentiostatic or galvanostatic polymerization are in their doped form and have high conductivity than that when electropolymerized via potentiodynamic. The polymer formed have ordered structure as they do not experience any changes after the experiment. The *potentiostatic* polymerization method is illustrated by change in current and polymerization rate with time keeping potential constant. The polymer formed is charged after the polymerization and have poor adhesion to the substrate with low homogeneity [8,9]. In contrast, the polymerization rate is constant in *galvanostatic* polymerization method by keeping current constant while measuring change in potential with time as shown in figure 1.4.

1.2 Applications

Conducting polymers can be used in variety of applications ranging from energy storage to microwave absorbing materials (fig. 1.5). They are suitable choice of materials for energy storage because of their high conductivity and reversible redox property during charging-discharging cycles. Pan *et al.* synthesized highly electrochemically active polyaniline nanostructure that showed excellent application in inkjet printing without the use of additives and good cyclability for supercapacitor electrodes [10]. Same research group fabricated the supercapacitor using polypyrrole hydrogel as electrodes and showed excellent electrochemical properties due to high electrical conductivity of polypyrrole. The polypyrrole as supercapacitor electrode provides the flexibility of the device at various radius of curvature [11].

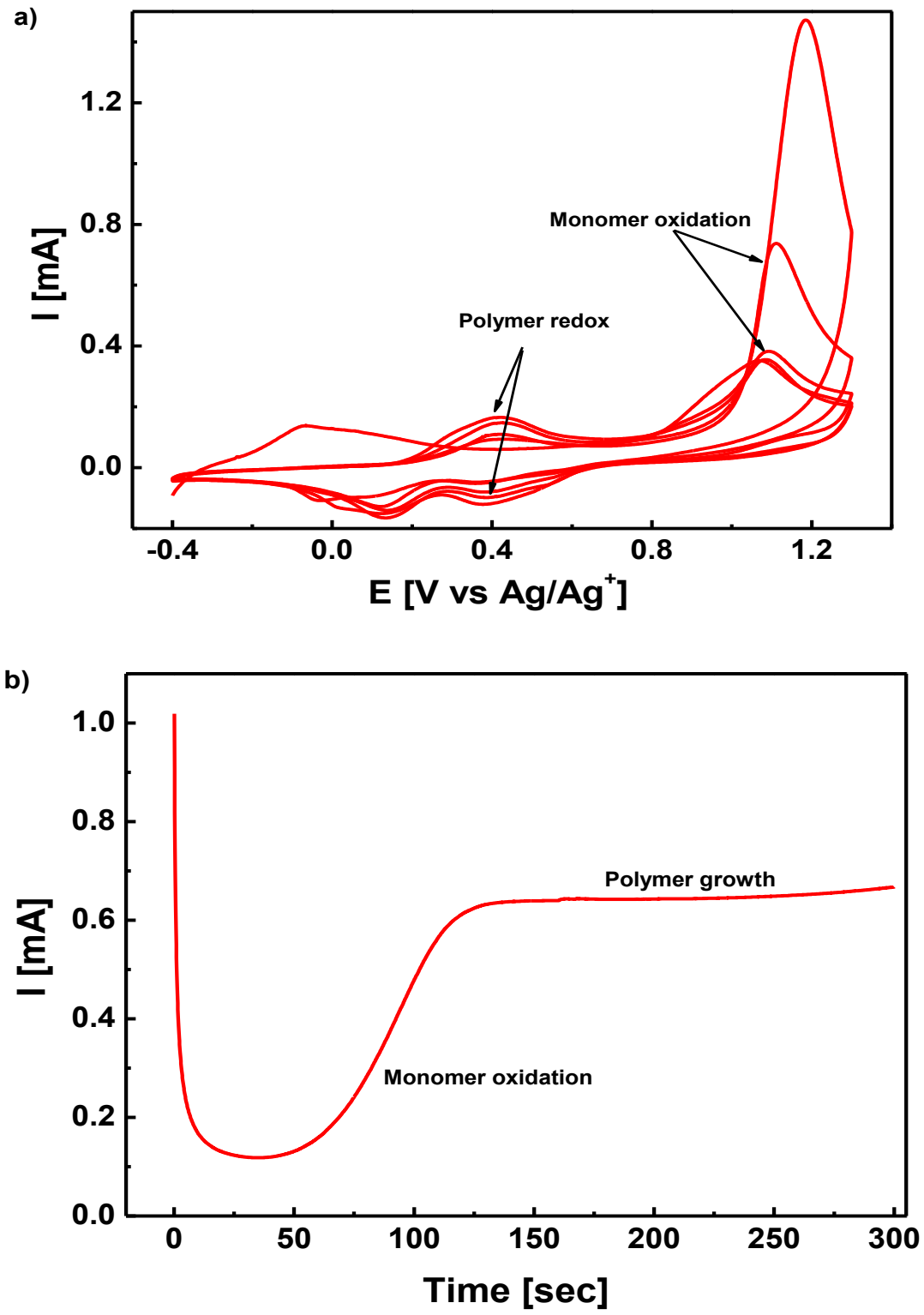

Figure 1.4 Typical electrosynthesis methods for polyaniline: a) potentiodynamic and b) potentiostatic.

Arenas *et al.* fabricated polyaniline sensor using different dopant acids. The more acidic dopants provides high sensitivity to polyaniline sensor because of high degree of protonation [12]. Besides, the using both polyaniline with single walled carbon nanotubes (SWCNT) enhances the sensing property of composite gas sensor. The presence of CP increases the conductance of the composite which NH_3 decrease it, therefore, makes them suitable for sensors [13]. Moreover, the electronic structure, chain orientation of conducting polymer makes them suitable for developing DNA sensor [14,15]. Most of the biological reactions occurs at neutral pH and conductivity of polyaniline is strongly dependent on low pH therefore, make it suitable for biosensor where change in conductivity can sense the biological reactions. Additionally, conducting polymers are considered as microwave absorbing materials that when used with suitable precursor can be used to fabricate carbon nanotubes within few seconds. Liu *at al.* used ferrocene as a precursor to carbon nanotube (CNTs) and polypyrrole as a microwave absorbing material that when exposed to microwave radiation converts ferrocene to CNTs [16]. Similar approach can be adopted to synthesize nanocarbon by carbonizing conducting polymer nanospheres by microwave radiation [17]. Moreover, conducting polymers and their derivatives were widely studied used as protective coating in corrosion protection of variety of ferrous [18,19] and non-ferrous metals [20,21]. Corrosion is defined as degradation of metal by oxidation of metal or reduction reaction takes place with metals and its surroundings. Since, corrosion is a thermodynamic process which can't be controlled, the major focus is to slow down the kinetics or alter the mechanism.

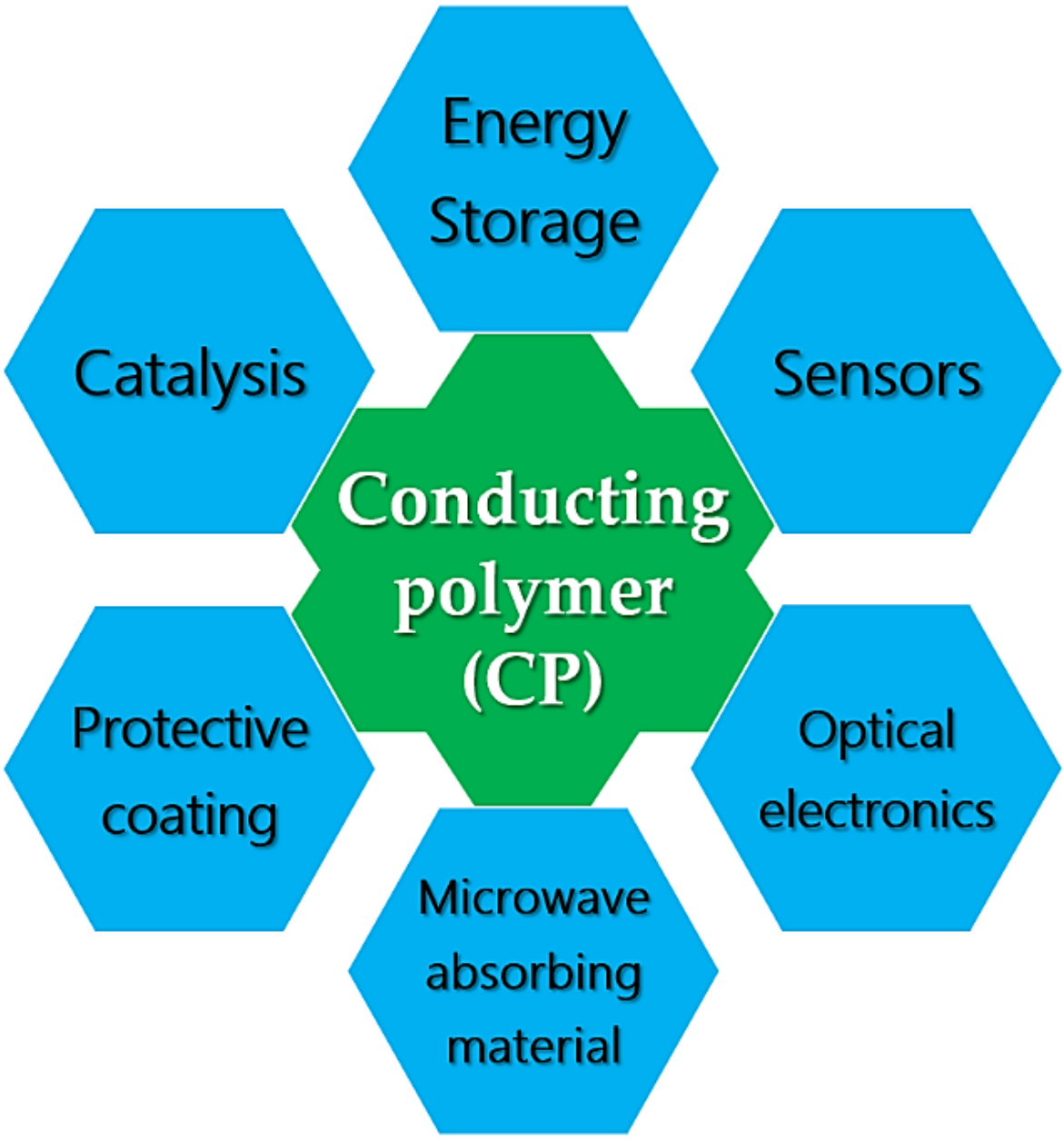

Figure 1.5 Applications of conducting polymers in different research areas.

Corrosion is recognized as electrochemical reaction involving oxidation (of metal) and reduction (with oxygen, hydrogen ion, water) reaction as shown:

Oxidation: $nM \rightarrow M^{n+} + ne^-$

Reduction: $2H^+(aq) + 2e^- \rightarrow H_2(g) \uparrow$ (acidic surroundings)

$O_2(g) + 2H_2O\,(l) + 4e^- \rightarrow 4OH^-(aq)$ (neutral/basic surroundings)

The corrosion can be suppressed by eliminating or reducing either/both above reactions. The different strategy has been developed to control the corrosion process including *cathodic protection* where the oxidation of metal is reduced by decreasing its potential. On the contrary, maintaining protective metal oxide layer (passive layer) developed by oxidizing the metal, this is *anodic protection*. Additionally, *corrosion inhibition* is provided when metal is treated with small organic substances known as inhibitors, whose main function is to prevent the metal oxidation by adsorbing completely on the metal. Besides, these three protection methods, the organic coating is most common control strategy adopted. The corrosion rate is reduced by preventing diffusion of any corrosive ion to metal/coating interface. However, the corrosive ion can diffuse through coating if defects present. Therefore, primer was applied prior to the coating to provided good adhesion to the metal surface. The one of active ingredient in primer is chromates that have harmful effect on environment. It is considered as carcinogenic and can be hazardous to many living beings including human. Consequently, conducting polymer was found out to be suitable replacement for these chromates without compensating its properties. The reversible redox and high conductivity of conducting polymers makes them appropriate coating material that provides all three protections in single layer. The polyaniline coating was most studied for corrosion protection in different

corrosive medium and showed excellent corrosion protection properties after 30days [22]. PAni can be used as direct coating, as pigment or an anti-corrosion agent in epoxy based paints that can be used to protect steel bar from rebar corrosion [23]. Similar protection was shown by polypyrrole when electrodeposited from different electrolyte medium [24]. Besides, conducting polymer can be used in microelectronics industry for copper and silver corrosion protection [25]. However, despite the presence of metal oxides present on these non-ferrous metals, they are not stronger than that of ferrous metals. Therefore, primary protection given by conducting polymer is barrier. The types of dopants used for conducting polymer plays a key role in its corrosion performance [26–28].

1.3 Challenges

It is well known that electrochemical polymerization of conducting polymer is considered as a best method to coat the metal. This is due to several advantages of electrochemical polymerization including direct deposition of conducting polymer coating can be achieved with high purity. The post processing steps has been eliminated and desired thickness can be achieved with by applied potential or current. However, the conducting polymer coating on metals can be challenging as metal dissolution occurs before electropolymerization starts due to high oxidation potential of monomers. Therefore, it is a strong desire to prevent this metal dissolution before electropolymerization starts. This can be achieved by forming a protective layer over the metal surface that prevents the dissolution and act as surface for electrodeposition of conducting polymer. This protective layer is known as passive layer. Typically, composition of passive layer is metal oxide or other compounds depending on type of acid used for electropolymerization. There are several factors such as electrolyte composition, concentration of monomer, electrochemical technique and potentials that affects passive layer formation (composition) which have directly

affects the integrity of conducting polymer coating. The important characteristics of a good coating is its adherence to the substrate, homogeneity and compactness. Adhesion of polymer coating varies along with roughness of the substrate; higher the substrate roughness better is the adhesion of the coating. Inadequate adhesion causes coating failure, which in turn is detrimental to the base metal as it gets exposed to the corrosive environment. Similarly, importance of homogeneity and compactness cannot be overstated; as, only a compact pore-free polymer coating can provide a better physical barrier for corrosion protection.

The ease of synthesis, control in physical properties, and multiple redox states make these polymers suitable for energy storage. Many researchers focused on pseudocapacitive behavior of these polymer. They have displayed excellent electrochemical performance with high specific capacitance (500-3400 $F \cdot g^{-1}$) which is significantly higher than carbon based materials. [29] The cycling process during charge-discharge involves ion doping and de-doping of conducting polymer that results in extra charge transferred to the reaction, thus enhanced the electrochemical performance. However, this charging and discharging require ion to moving in and out of the conducting polymer that results in swelling and shrinking of the material. This swelling and shrinking of polymer damages the integrity of conducting polymer thus decreases the cycling performance. To improve the mechanical stability and to reduce mechanical stress during charge-discharge, it can be used by compositing with other species that enhances the cyclability. For instance, supercapacitive properties of MnO_2 was greatly enhanced by wrapping it with conducting polymer to overcome the insulation feature of MnO_2. [30] The reversible faradaic redox reaction occurring at the surface of conducting polymer enhances the electrochemical performance of a device by improving the conductivity. However, this faradaic process makes ion transport more sluggish than electrostatic adsorption.

Conducting polymers can be used for transduction of ion-to-electron that makes them promising material for sensory electrodes. They have significant amount of porosity and delocalized charge centers that permit ions to diffuse and electron to migrate inside the polymer. They are preferred over other materials because: i) being electrical conducting, they can form an ohmic contact with materials such as carbon, gold and platinum, ii) ease of synthesis on variety of surfaces by electropolymerization of various monomers available, iii) they have both electronic and ionic conductivity, that can convert an ionic signal into an electronic one. These multifunctional properties help us to study ionic transport through conducting polymer film to improve the electrochemical performance of a device. These conjugated polymers can be used to intake specific ions from the bulk in a controlled way, this is known as ion inclusion. Depending on the oxidation state of a polymer they can intake either positively or negatively charged species into the matrix to attain electroneutrality. The ingress of positive charged ions can be seen if polymer is in reduced state and oxidized state can intake negative charged species. [31] Typically, with three electrodes system, current flows between working (WE) and counter electrode (CE) and voltage is measured with respect to the reference electrode (RE). There is a small potential difference between WE and CE that generates the positive charge centers inside the conducting polymer film. This created the concentration and potential gradient between CP film and the electrolyte solution. The negative ions start to move towards positively charged polymer film creating double layer at the interface. Few of these negative ions contributes in charging of double layer and few diffuses through the polymer film. The migration of negative ions continues till overall electroneutrality was attained, thus redox reaction. This is the ion intake process that migrates through CP film from one end to the other. The above discussion of ion transport is the motivation of this dissertation and study the performance of conducting polymer in various application areas.

1.4 Research objectives

The transport of ions through conducting polymer film can be measured electrochemically using commonly used electrochemical techniques such as cyclic voltammetry (CV), chronoamperometry, electrochemical impedance spectroscopy (EIS). When small pulse of current is passed through the film this creates the deficit or excess of ions on the surface of a film. This pushes ions towards equilibrium throughout the polymer and by following the relaxation of the surface potential. Considering all the factors discussed above, we electrosynthesized high performance conducting polymer coating on different substrate and study the ion transport through electrolyte to electrode in four different projects. There are various kinds of conducting polymers namely nitrogen (PAni, PPy) and sulfur (PTh, PEDOT) based and their derivative that were used to study in this dissertation. The first two project discussed the performance of nitrogen based conducting polymers while third focused on sulfur based because of high tendency of sulfur to interact with metal surfaces.

The first project discussed the effect of various acidic medium on passivation of steel and electropolymerization of polypyrrole. The coating morphology was comparing when coating produced using various doping agents. Further, the integrity of the coating was evaluated by testing their adhesion and was enhanced by the adding of adhesion promoters. Additionally, the harsh bleach treatment was performed multiple times and thermal stability of the produced coating was tested. The further bleach observations were included in different dissertation (Mingyu Qiao). Moreover, the corrosion performance of the coating was investigated in salt solution (marine environment).

The second project focuses on the electropolymerization of polyaniline on stainless steel. The reversible change in oxidation states of polyaniline was exploited to study the electrochemical exchange of anion from the produced coating. This study helped in understating the favorable and non-favorable condition for electropolymerization of polyaniline. The electrochemcial anion exchange enhanced the corrosion performance of polyaniline. Additionally, the coating adhesion was evaluated and was enhances using bio-adhesive as adhesive agent in the coating that improved the coating's electrochemical performance. Further, this study was applied to study the anion transport from the solution to the coating to understand the electrochemical activity of the polyaniline.

The third project discusses the use of poly (3,4-ethylenedioxythiophene) coating as anticorrosive agent. The electropolymerization potential was optimized using electron transfer mediator that promotes the electron transfer during the polymerization thus reducing the potential by significant value.

The fourth project focus on the effect of various dopant acids on electrochemical performance of polyaniline as electrode material for pseudocapacitors. The electrochemical testing involves charge storage, cycling stability that can be affected by size of the dopant used.

Chapter 2

High performance polypyrrole coating for corrosion protection and biocidal applications

Abstract: Polypyrrole (PPy) coating was electrochemically synthesized on carbon steel using sulfonic acids as dopants. The effect of acidic dopants on passivation of carbon steel was investigated by linear potentiodynamic and compared with morphology and corrosion protection performance of the coating produced. The types of the dopants used were significantly affecting the protection efficiency of the coating against chloride ion attack on the metal surface. The corrosion performance depends on size and alignment of dopant in the polymer backbone. Both p-TSA and SDBS have extra benzene ring that stack together to form a lamellar sheet like barrier to chloride ions thus making them appropriate dopants for PPy coating in suppressing the corrosion at significant level. Further, adhesion performance was enhanced by adding long chain carboxylic acid (decanoic acid) directly in the monomer solution. In addition, PPy coating doped with SDBS displayed excellent biocidal abilities against Staphylococcus aureus. The polypyrrole coatings on carbon steels with dual function of anti-corrosion and excellent biocidal properties shows great potential application in the industry for anti-corrosion/antimicrobial purposes.

Keywords: Conducting polymer coating, corrosion protection, polypyrrole, antimicrobial coating, microbially induced corrosion (MIC)

2.1 Introduction

Conducting polymers are used in many different areas of research such as energy storage [32], catalyst [33], sensors [34], membrane filters [35] etc. Another important area is corrosion, it is an electrochemical process that degrades the metal and its alloys by chemically reacts with its surrounding environment mainly oxygen and water. Technically, corrosion is prevented by eliminating oxygen or water to reach metal surface. It can be achieved by providing a *"perfect"* barrier layer by covering its surface with coating. However, most of the coating are not impermeable to oxygen of water, therefore barrier is broken. Most common chemical and electrochemical methods for corrosion prevention are chemical inhibitors, cathodic and anodic protection [36]. Therefore, it is necessary to develop a method and materials to control corrosion. The conducting polymer coating proved to be best choice for corrosion protection materials where many different types of conducting polymer coatings have been developed on different substrates. Their corrosion protection performance have been evaluated and found reduction in corrosion rate due to anodic protection given by conducting polymer [37–40]. It was first reported by Deberry, who prevents stainless steel degradation by conducting polyaniline coating [41]. Since then numerous work has been reported on corrosion protection performance of conducting polymer coating on various metals such as Al, Cu, etc. [21,42,43].

They can be used in different ways for corrosion protection such as blended with paints or used as primer for epoxy based paints [44], can be used as corrosion inhibitors by direct addition into corrosive media and electrodeposition of conducting polymer on the metal surface. However, the major issue with electrosynthesis of conducting polymer coating on metals such as carbon steel is the oxidation potential of monomer is high that lead to metal dissolution before the formation of

coating [45]. Therefore, it is necessary to form a protective layer over the metal surface before electropolymerization. Many metals can naturally form oxide film when in contact with air thus become passivated. However, for most of the active metals, passivating the surface and electropolymerization of the polymer become two-step process. To prevent this active dissolution of a metal, acidic electrolyte conditions were chosen using appropriate dopant for conducting polymer, e.g. sodium p-toluene sulfonate [46] and oxalic acid [47,48]. Therefore, this study was focused on the effect of type and size of dopants used for electropolymerization of polypyrrole. The effect of acidic dopants on passivating behavior of carbon steel was studied. The performance of polypyrrole coating was investigated as corrosion preventing material. Moreover, biologically corrosion is also known to cause the deterioration of metal surfaces by the action of metabolic activity of microorganisms, also known as microbially influenced corrosion (MIC) [49,50]. It was reported to account for 20% of the total cost of corrosion [51], some of which drastically accelerate the corrosion kinetics through the production of corrosive agents such as protons and electrons, or the formation of concentration cells, which triggers the corrosion process [44]. There are many bacteria known to induce corrosion of metals not limited to carbon steels, stainless steels or copper and aluminum alloys, categorized in to aerobic and anaerobic bacteria. Amongst them anaerobic sulfate-reducing bacteria (SRB) are responsible for accelerated corrosion damages to the offshore steel structures and ships, which was reviewed in detail by Dennis Enning and Julia Garrelfs [52]. In addition to anticorrosion properties, polypyrrole was reported to have antimicrobial activity [53]. Therefore, loading the anti-corrosion coating with biocidal activity will enhance the performance of the coating by preventing the ingress of chloride ions and killing the bacteria simultaneously, making it multifunctional. The other aim of this study was to investigate the biocidal activity of PPy coating using different dopants.

2.2 Experimental Section

2.2.1 Materials. Pyrrole (Mw = 67.09 g·mol^{-1}, ρ = 0.967 g·cm^{-3}), platinum (Pt) gauze (100 mesh, 99.9% metal basis), *p*-toluenesulfonic acid (p-TSA), (±) camphor 10-sulfonic acid (CSA) were obtained from Alfa Aesar, USA. Sulfuric acid (SA) was purchased from Anachemia, sodium dodecyl sulfate (SDS) was from IBI Scientific and sodium dodecylbenzene sulfonate (SDBS) was obtained from Spectrum Chemicals. Decanoic acid was purchased from Tokyo Chemical Industry. All chemicals were used without further treatment or purification. Low carbon steel plate (AISI Type C1018, 1mm thick) was used for electrodeposition surface.

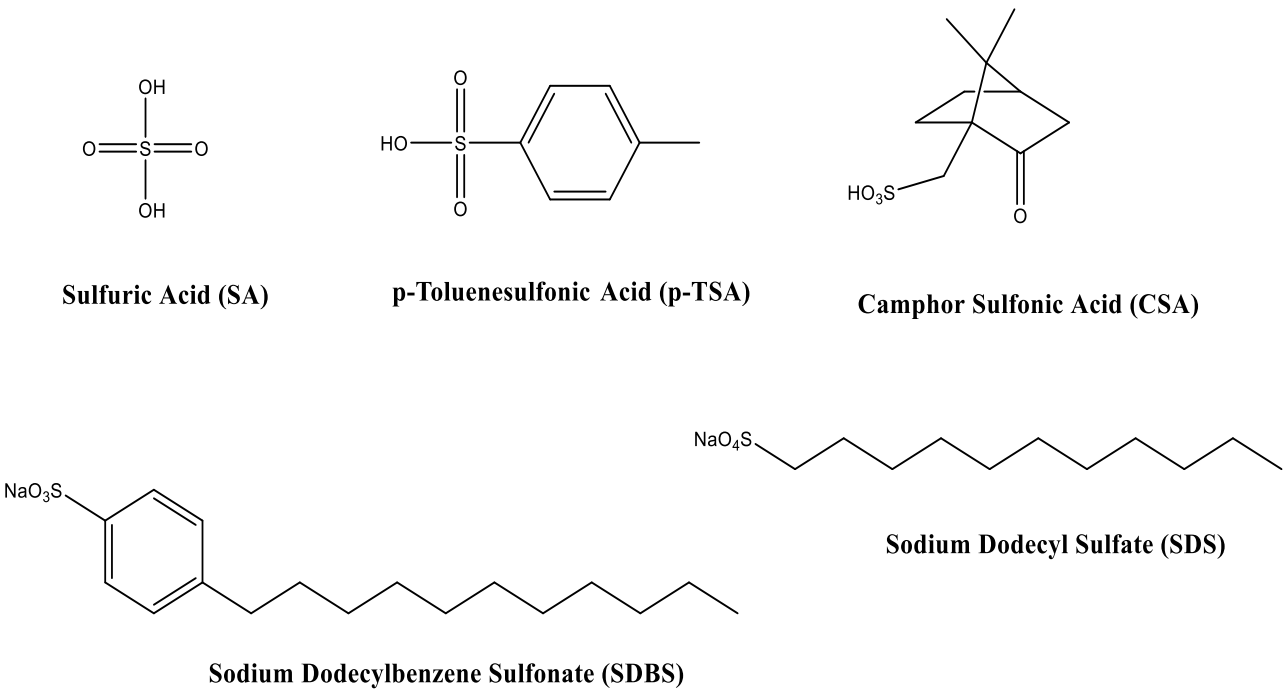

Figure 2.1 Chemical structure of doping agents used in this study.

2.2.2 Sample preparation. The steel samples of 1 cm × 0.5 cm were cut from 1mm thick plate and cold mounted into acrylic resin so that only one surface was exposed. The embedded sample was then polished by emery papers of different grit size starting from 800, 1000, and 1200 followed by ultrasonic cleaning in deionized water for 1 minute (DI water with ~18.2 Ω·cm resistivity).

2.2.3 Electrochemical synthesis. Polypyrrole (PPy) coating was electrochemically deposited using electrolyte containing monomer (pyrrole) along with the dopant. The dopants used in this work were divided in to two classifications according to the carbon chain length which were short chain dopants (SA, CSA, and p-TSA) and long chain dopants (SDS and SDBS) (Figure 2.1). The electrolyte solutions contain pyrrole (0.1M) with desired dopant concentrations varied from 0.1 to 1 M for short chain dopants, and 5 mM to 30 mM for long chain dopants. The electrochemical cell set-up used was a single compartment with three-electrode system, where carbon steel (1 cm x 0.5 cm) was used as a working electrode, Pt as a counter electrode, Silver/Silver chloride/KCl (3 M) (Ag/Ag^+, E° = +205 mV vs. SHE) and Mercury/Mercury Sulfate/K_2SO_4 (saturated) (MSE, E° = +650 mV vs. SHE) were used as reference electrodes. Potentiostatic deposition was carried out on CH Instrument (CHI 601D) potentiostat using Electrochemical Analyzer software (version 15.03) by applying 0.8 V/MSE for 5 min. All the potentials measured were mentioned on the plot wherever it was used.

2.2.4 Characterization. The surface morphology of the coating was recorded under Scanning Electron Microscope (SEM) on JEOL JSM-7000F at 20 keV with 10 mm working distance. The corrosion tests were performed in 3.5% NaCl with linear sweep voltammetry (LSV) at a scan rate of 1 $mV \cdot s^{-1}$, scanning ±150 mV from the open circuit potential (OCP). Fourier Transform Infrared (FTIR) analysis was conducted on a Thermo Nicolet 6700 FTIR. The crosshatch scotch tape

adhesion tester kit was used for testing adherence following the procedure mentioned in ASTM D3359 standard.

2.2.5 Biocidal efficacy test. Carbon steel coupons (1.5×1.5 cm^2) were prepared and coated with polypyrrole using SDBS and p-TSA as dopants following the same previously mentioned procedures. The PPy coated coupons were autoclaved at 121°C for 45 min and dried overnight at room temperature before use. The biocidal efficacies of PPy coated carbon steel samples were performed using a "sandwich" test method as described in previous report [54]. A gram-positive bacterium of *Staphylococcus aureus* (ATCC 6358) was used in this study. Briefly, a single colony of the bacteria was transferred into 15 mL of Trypticase soy broth (TSB, BD Co., MD) and incubated at 37 °C with 120 rpm of orbital shaking for 16 h. The culture was washed twice with Butterfield's phosphate buffer (BPB) through centrifugation and re-suspended in the BPB buffer. Bacterial population was estimated by the absorbance at $O.D._{640\ nm}$ and the inoculum with designated population was prepared. Then, an aliquot of 10 µL of the inoculum was added to the center of a PPy coated carbon steel coupon, and a second identical coupon was placed on the top. At the contact times of 1 min, 5 min, and 10 min, the coupons were transferred into 5 mL of BPB buffer solution and vortexed to detach bacteria from the coating. Ten-fold serial dilutions were made for all samples and each dilution was plated on trypticase agar plates. The plates were incubated at 37 °C for 48 h and bacterial colonies were enumerated and recorded for biocidal efficacy analysis. Bacterial reduction was calculated based on the equation: bacterial reduction $(Log) = (Log_{10}A) – (Log_{10}B)$, where A is the number of viable microorganisms inoculated on the surface before antimicrobial reaction, B is the number of viable microorganism recovered from tested materials after certain period of antimicrobial reaction time. Both A and B were calculated from the count of colonies on plates that 25 µL of solutions were plated. For A, viable bacteria

number inoculated (CFU) = count of colony on plate (CFU) x dilution factor/plated volume (0.025 mL) × inoculated volume (0.001 mL); for B, viable bacterial number recovered after reaction = count of colony on plate (CFU) × dilution factor/plated volume (0.025 mL) x total volume in washing solution (10 mL).

2.3 Results and Discussion

2.3.1 Passivation. The electrodeposition of conducting polymer on active metal like carbon steel (CS) is carried out in three different stages [55,56]: a) formation of passive film initiates and monomer adsorption occurs on the surface, b) growth of passive film, and c) polymerization of the monomer over the surface. It indicates the importance of passivation behavior for active metals like CS, as it starts corroding before monomer oxidizes (high potential oxidation). It implies that the faster the passive film forms, the faster the solvated monomer molecules adhere and polymerize on the surface to prevent metal dissolution at higher potential. To understand the effect of dopant concentration (p-TSA, sulfuric acid, and CSA), linear potentiodynamic scan was performed (Figure 2.2) on various concentrations of the dopants used. In case of p-TSA (Figure 2.2a), CSA (Figure 2.2b) and sulfuric acid (Figure 2.2c), typical feature of active-passive metal like CS was present. As potential scan starts from open circuit potential (OCP), -0.94 V/MSE, a clear passivation peak was observed, indicating the formation of Fe (II, III) oxide, further increase in potential leads to the oxidization of Fe (II, III) oxide to Fe (II) oxide, this can be seen by small peak at ca. -0.2 V/MSE [57,58]. As p-TSA concentration increase, the passivation potential gradually shifts more to negative until 0.8 M, and beyond this concentration it becomes insignificant for further increase to 0.9 and 1.0 M which have higher passivation potentials than it at 0.8 M p-TSA. This implies the formation of passive film becomes easier and forms faster at 0.8 M prior to the

formation of polypyrrole by lowering the passivation potential [28,59]. The high current density in 0.8 M p-TSA implies the extent of oxidation of the metal that forms thicker iron oxide passive film and there is a 1000 mV (approx.) negative shift in passivation potential from 0.2 to 0.8 M p-TSA. This large negative shift in passivation potential is beneficial for faster deposition of polypyrrole over the steel surface and forms uniform, and compact coating. Similarly, active-passive peaks were observed when electrolyte was changed to CSA (Figure 2.2b) where by increasing the potential from OCP the current density increase indicating the formation of iron oxide. However, with slight increase in potential this passive film breakdown and gives sudden increase in current density before it completely forms. Unstable passive films were observed for most of the concentrations of CSA used (Figure 2.2b), when potential was increased further from primary passivation potential (except 0.6 M) due to formation low strength of iron (II) oxide film. This is unlike iron (II) oxalate where oxalate salt of iron provides extra strength and adhesion to the coating [60]. In 0.2 M CSA, the passivation peak is much broader, and the corresponding potential is much more positive, which is closer to the formation of pyrrole radical-cation (+230 mV/MSE), that prevents the protective passive film formation. In Figure 2.2c, with sulfuric acid concentration higher than 0.2 M, it shows typical passivation peaks feature upon linear scan in various concentrations. At 0.2 M sulfuric acid, it started to form a passive film with much higher potential, which is beyond the potential at which pyrrole radical-cation formation occurs. This is due to the presence of strong oxidizing ions, that lowers the oxygen concentration at metal-electrolyte interface and prevents the oxidation of Fe (II, III) oxide to Fe (III) oxide (Figure 2.2c) [61]. This creates anode and cathode areas on the surface resulting in increased current, corrosion was accelerated and the probability of forming protective Fe (III) oxide film reduced [62].

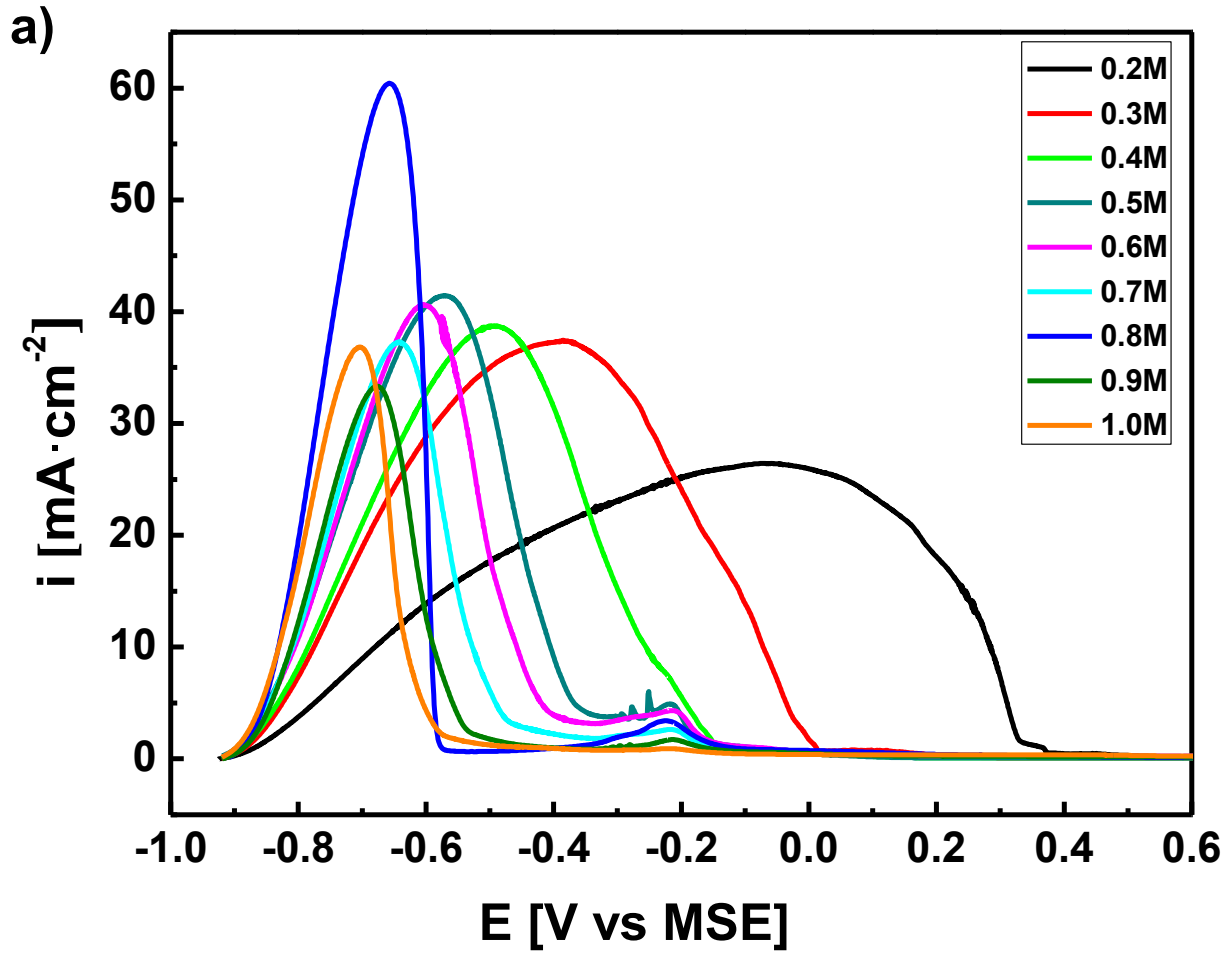
a)
i [mA·cm-2]
E [V vs MSE]
0.2M
0.3M
0.4M
0.5M
0.6M
0.7M
0.8M
0.9M
1.0M
60
50
40
30
20
10
0
-1.0
-0.8
-0.6
-0.4
-0.2
0.0
0.2
0.4
0.6

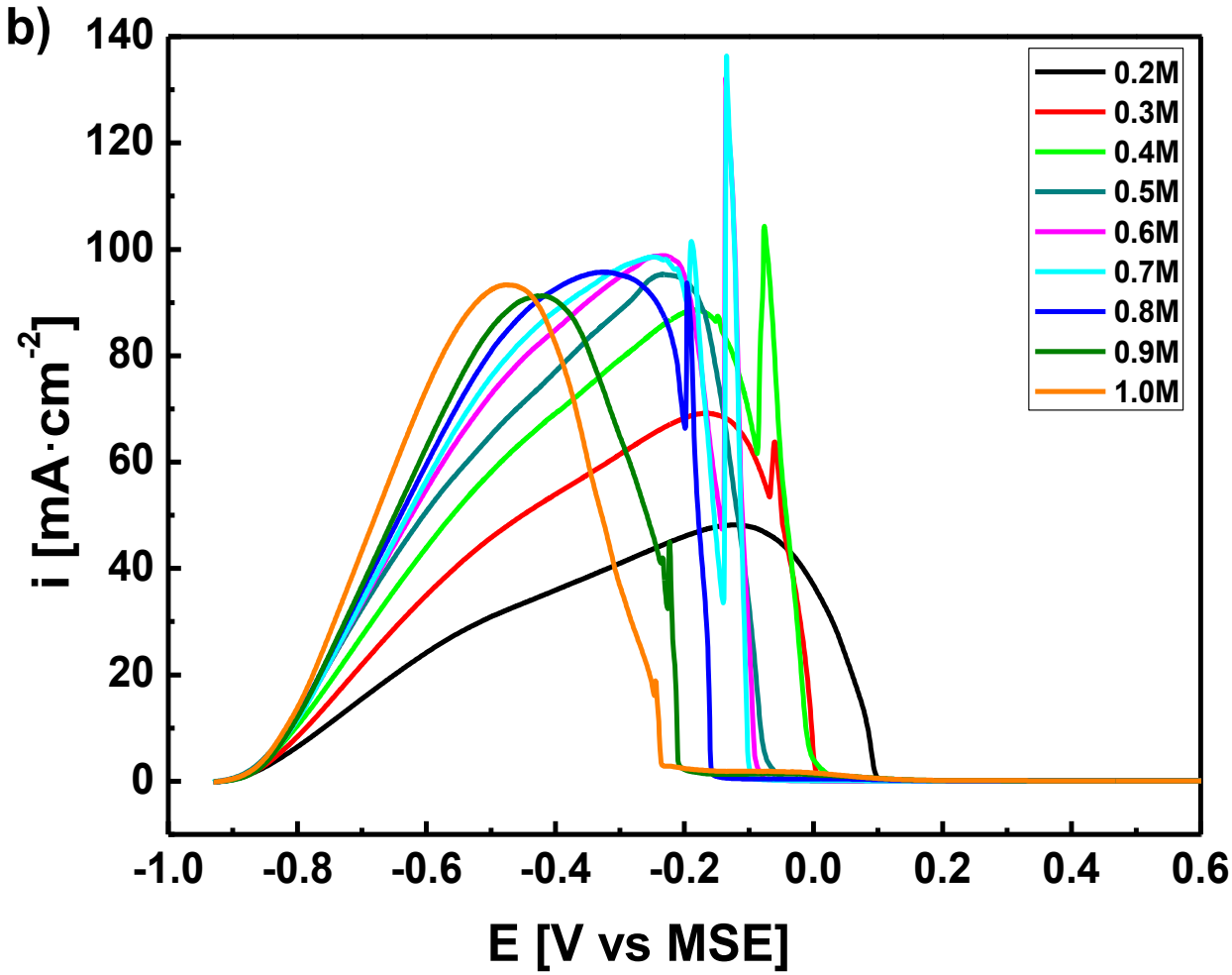
b)
140
120
100
80
60
40
20
0
i [mA·cm-2]
-1.0
-0.8
-0.6
-0.4
-0.2
0.0
0.2
0.4
0.6
E [V vs MSE]
0.2M
0.3M
0.4M
0.5M
0.6M
0.7M
0.8M
0.9M
1.0M

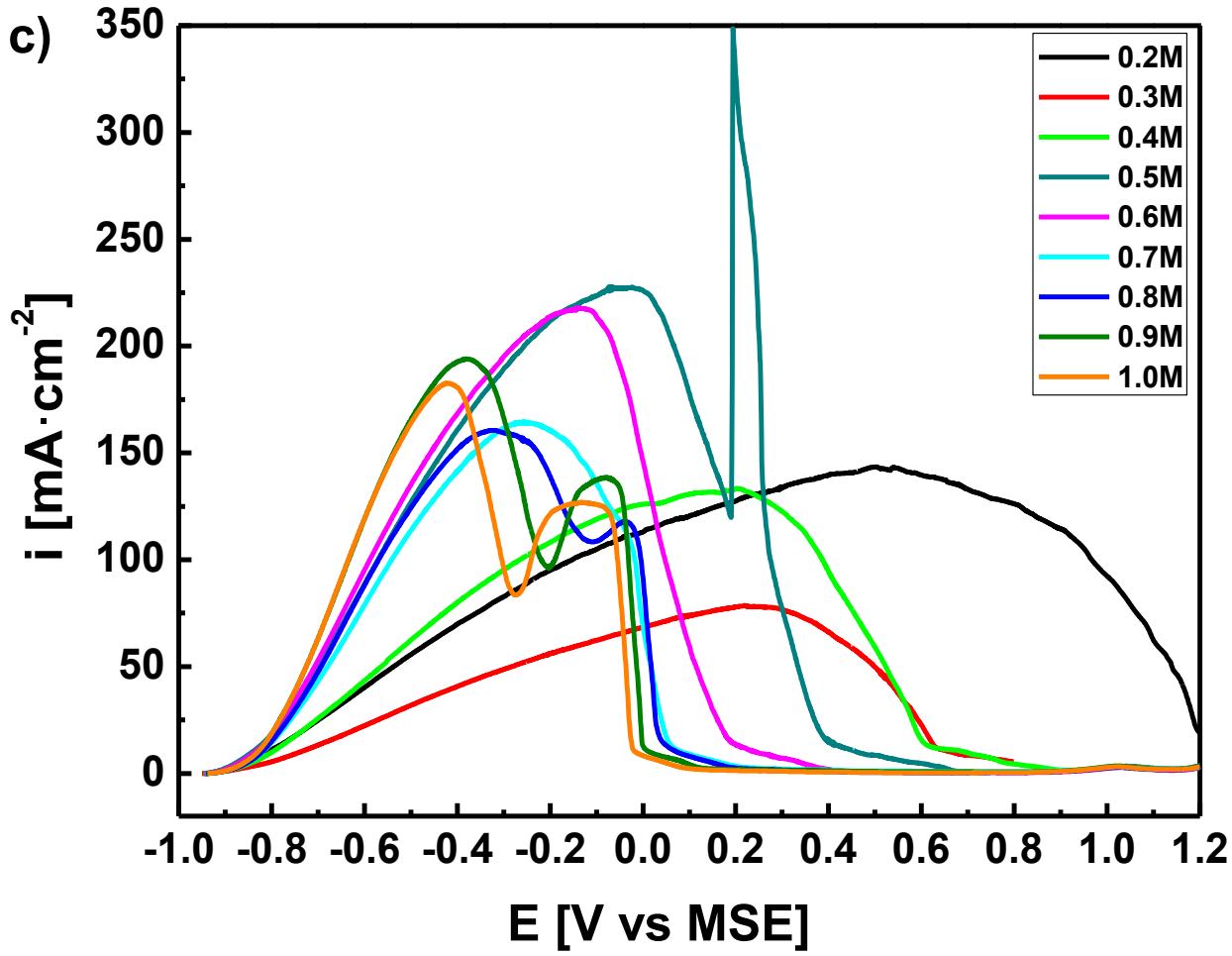

Figure 2.2 Linear potentiodynamic scan (10 mV·s^{-1}) of carbon steel in different concentration of: a) p-TSA, b) CSA, c) sulfuric acid, without monomer.

Only if the concentrations of sulfuric acid are at 0.7 M or higher, the passivation occurs potential lower than +200 mV (vs. MSE). But upon further increasing potential, semiconductive iron oxide passive film is formed, that limit the further growth thus breakdown of passive film occurred due to high acidic strength of sulfuric acid [2]. Therefore, concentrations for further investigation of adhesion and morphology of polypyrrole coating were chosen based on their lowest passivation potential i.e. 1 M for sulfuric acid, 0.6 and 1 M for CSA, and 0.8 M for p-TSA.

2.3.2 Coating morphology. Figure 2.3 shows SEM images of polypyrrole coating doped with different dopants using chosen concentration of dopants. Typical morphology of granular PPy can be seen in every dopant used. The morphology was not changed by dopants, but compactness and uniformity of the coating are enhanced in SDS and SDBS doped PPy. This is due the presence of long carbon chain in both dopant anions. When PPy was doped with p-TSA, more granular PPy was formed with no pores in the coating. Since both SDBS and p-TSA have benzene ring, their E_{corr} are close to each other which were 10mV apart approximately (Figure 2.11).

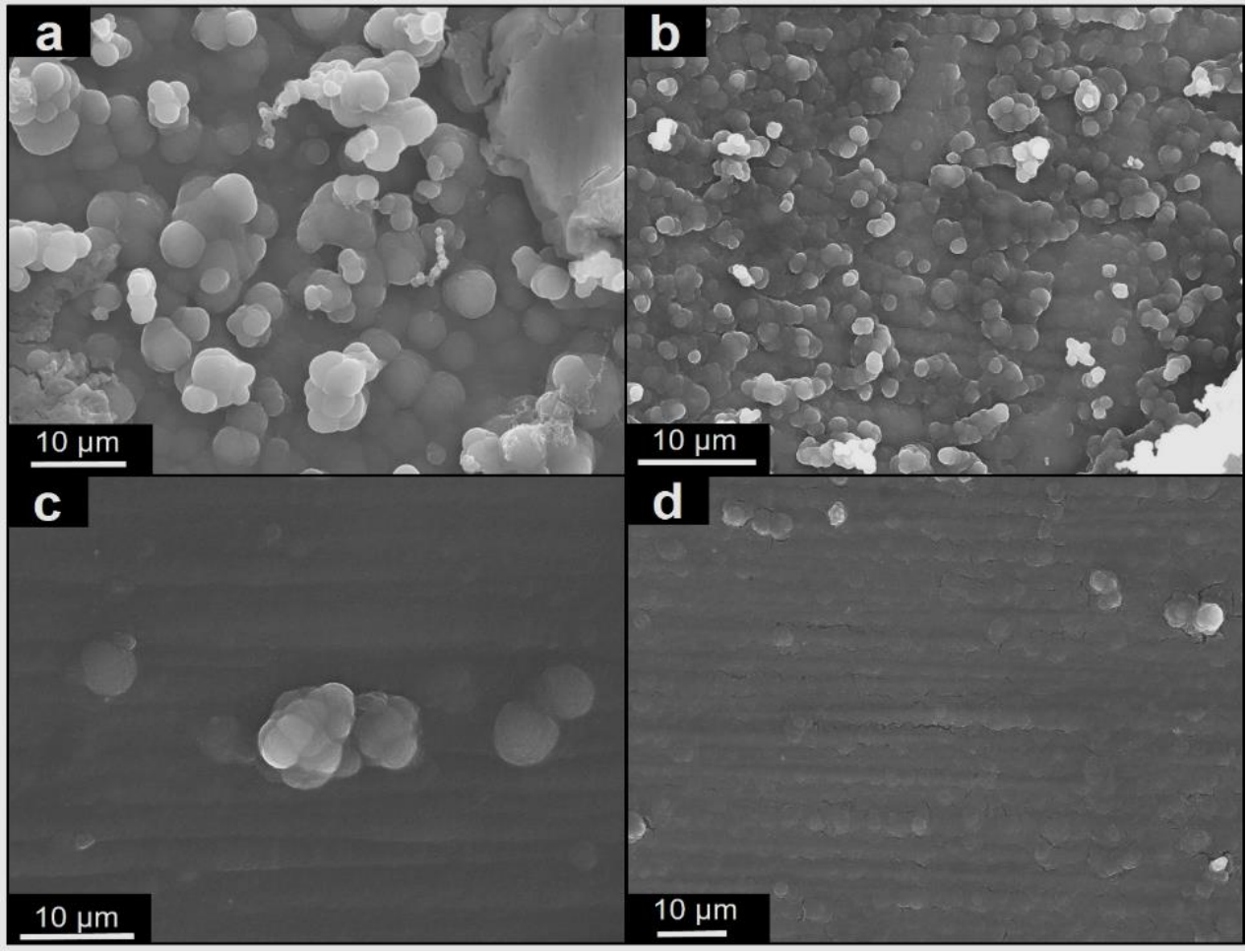

Figure 2.3 SEM images of the polypyrrole coating obtained from different dopants used: a) 0.8 M p-TSA, b) 1 M sulfuric acid, c) 25 mM SDBS, d) 25 mM SDS.

It makes both to be the best dopants if PPy coating is to be electrochemically synthesized on carbon steel. In SDS, although morphology looks uniform and compact, long carbon chains existed in anion have repulsion between the molecules creating small pores in the coating. This explains the lower E_{corr} than SDBS and p-TSA. A smooth and granular morphology can be seen in sulfuric acid doped PPy coating (Figure 2.3), but chloride can easily exchange sulfuric acid dopant anion making it vulnerable to chloride attack. This corroborates the lowest corrosion potential for sulfuric acid amongst other dopants used (Figure 2.11).

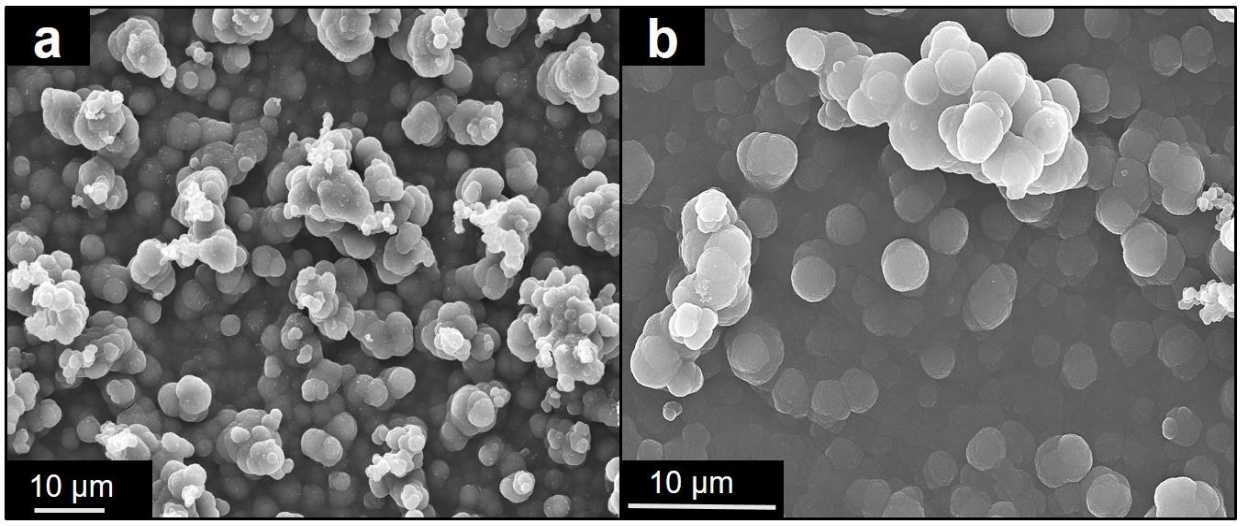

Figure 2.4 SEM images of the polypyrrole coating obtained by doping it with CSA: a) 0.6 M and b) 1 M.

For CSA, it has a cyclic structure occupies large volume in space. The relatively lower corrosion potential compared to p-TSA can be explained by its sterically hindered structure in which two methyl groups are bridged by one carbon that makes it difficult to arrange themselves in a lamellar packing like of p-TSA and SBDS. For CSA system, 0.6 M CSA shows stable protective metal oxide layer and 1 M CSA show lowest passivation potential of all (Figure 2.2b). While to compare

the morphologies of the PPy films made at different CSA concentration, there are no significant differences, typical granular morphology can be seen in both chosen concentrations of CSA (Figure 2.4).

2.3.3 Anticorrosion properties

2.3.3.1 Short chain dopants: The corrosion protection performance depends on the size of anions used because large size anions are difficult to exchange during redox process thus penetration of corrosive ions like chlorides are highly reduced. The large size anions along with polymer chain provide barrier protection to the metal. Therefore, for short chain dopants to have the same barrier protection as in long chain dopants it is necessary to form homogenous, strong, and adherent passive film prior to electrodeposition of the polymer. For all the dopants, polypyrrole coating was electrodeposited by applying constant potential of 0.8 V (MSE) for 5 min. The potentiodynamic scan at 1 $mV \cdot s^{-1}$ was further performed for corrosion test on selected concentrations of the dopants as shown (Figure 2.5). The p-TSA at 0.8 M forms the best compact coating, which is in accordance with our linear potentiodynamic scan (Figure 2.2a) that shows faster passive film formation. There are more solvated pyrroles over the surface and forms radical-cation easily to polymerize on the steel surface, forming uniform and compact black film of polypyrrole, this can be corroborated from SEM image (Figure 2.3). It can also be explained by the presence of benzene ring in p-TSA, which forms a π- π stacking within the p-TSA molecules by overlapping p-orbitals of the benzene ring, creating a lamellar sheet like structure that helps in forming uniform, compact barrier to prevent ingress of chloride ions.

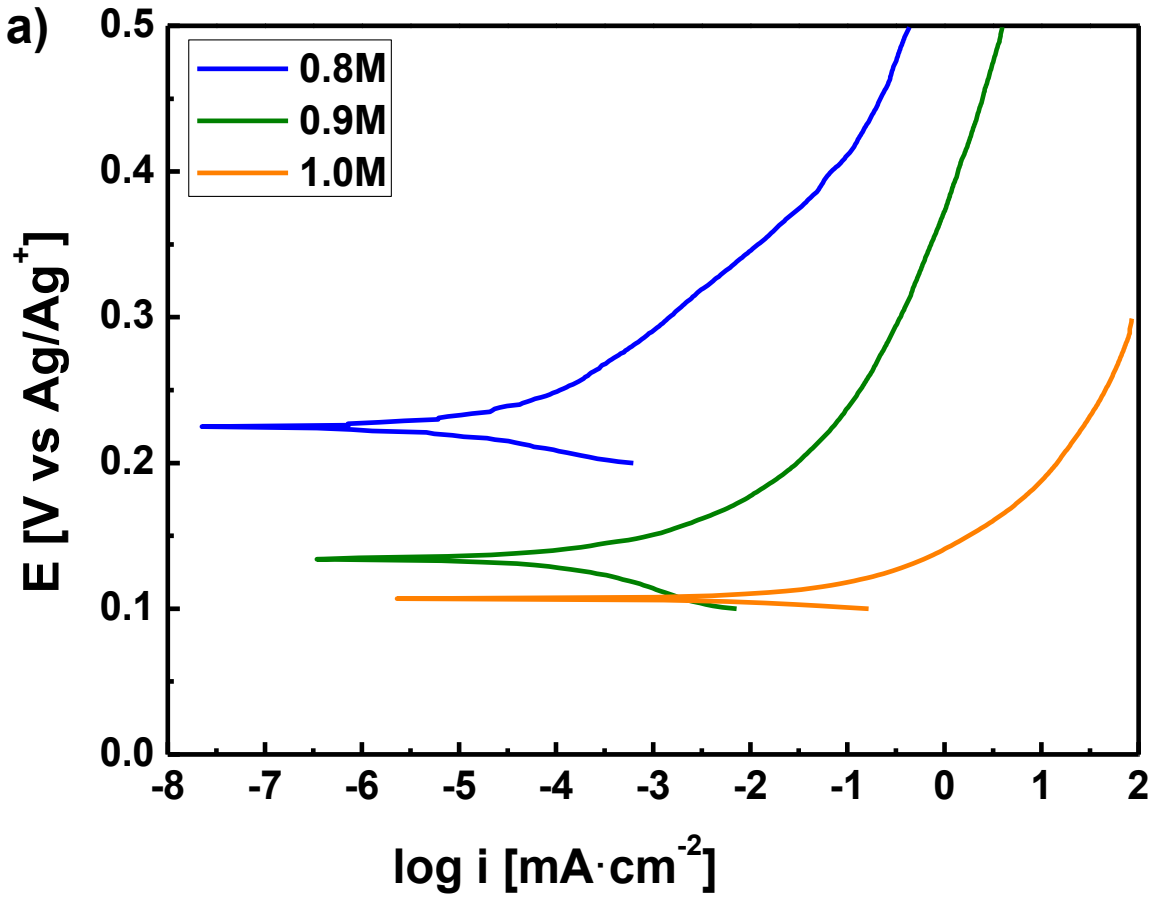
a)
0.8M
0.9M
1.0M
E [V vs Ag/Ag+]
log i [mA·cm-2]
0.0
0.1
0.2
0.3
0.4
0.5
-8
-7
-6
-5
-4
-3
-2
-1
0
1
2

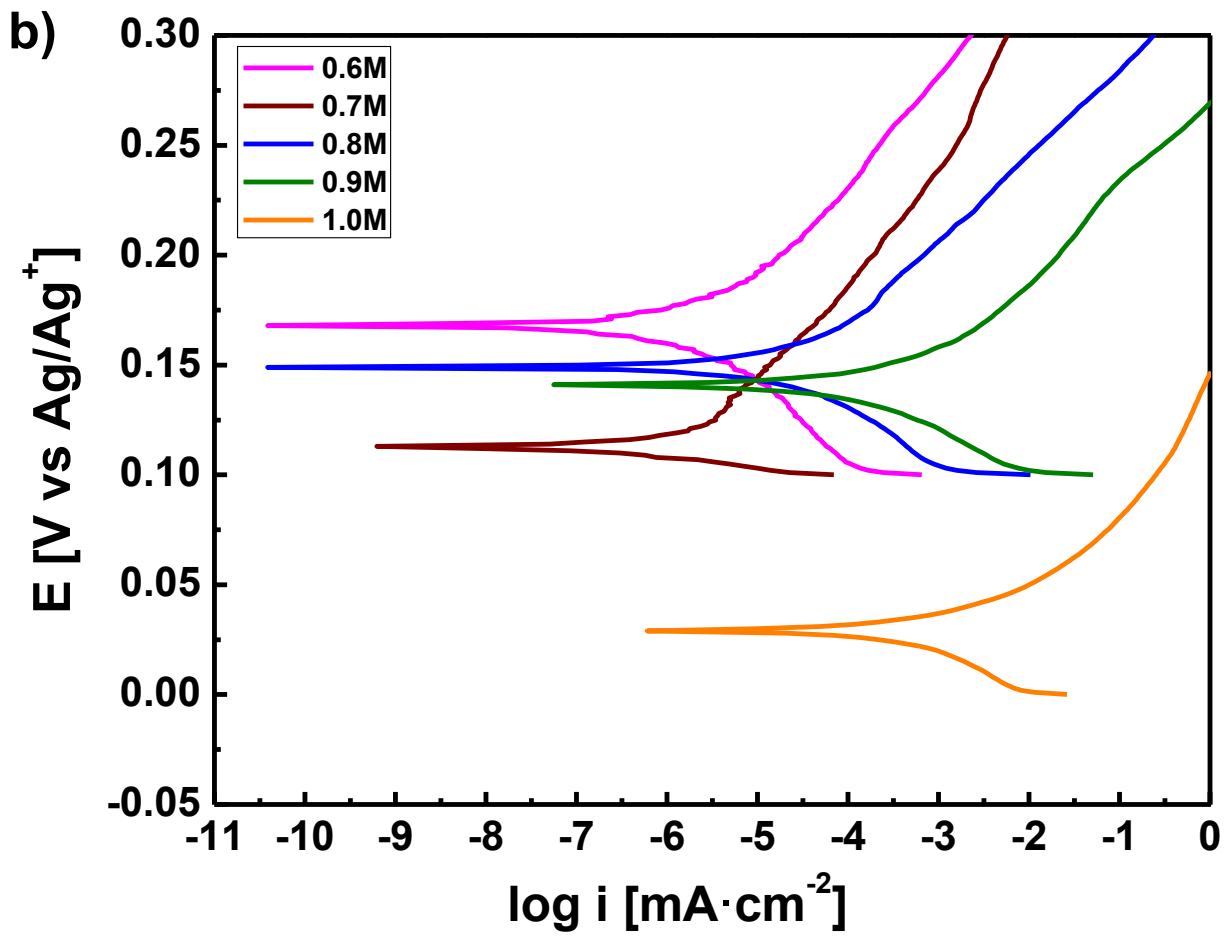
b)
0.6M
0.7M
0.8M
0.9M
1.0M
E [V vs Ag/Ag+]
0.30
0.25
0.20
0.15
0.10
0.05
0.00
-0.05
-11
-10
-9
-8
-7
-6
-5
-4
-3
-2
-1
0
log i [mA·cm-2]

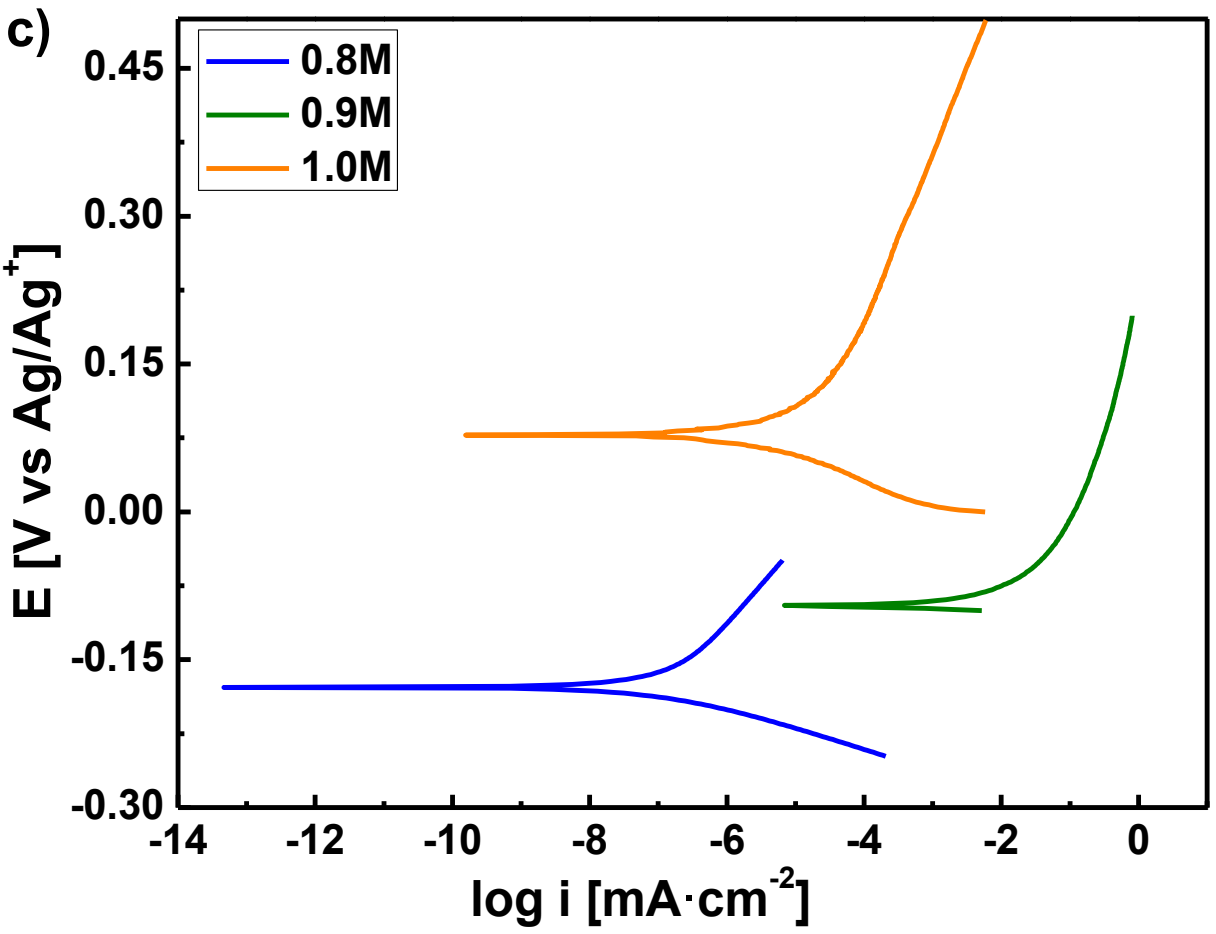

Figure 2.5 Potentiodynamic polarization curves scanned at 1 $mV.s^{-1}$ in 3.5% NaCl for PPy coating doped with: a) p-TSA, b) CSA and c) sulfuric acid.

Unlike p-TSA, despite of the cyclic structure in CSA, there is more chance of steric hindrance between two molecules due to the presence of extra methyl group bridged together in the middle, thus more repulsion between the molecules is expected resulting in creating more pores in the produced coating. This may be the reason for lower corrosion potential than in p-TSA, but more than that of sulfuric acid because CSA anion is larger and not easily replaced by chloride ion. When dopant was changed to sulfuric acid, only three concentrations were found to be suitable for further investigation due to their passivation potentials lower than what is required for the adherent

passive film and polypyrrole coating. Amongst selected concentrations, 1 M sulfuric acid achieved the best PPy coating performance against corrosion as observed with its passivation behavior (Figure 2.2c). Critical current density does not play a key role in forming better coating, but passivation potential does. The best results for all the short chains dopants used are presented in Figure 2.6.

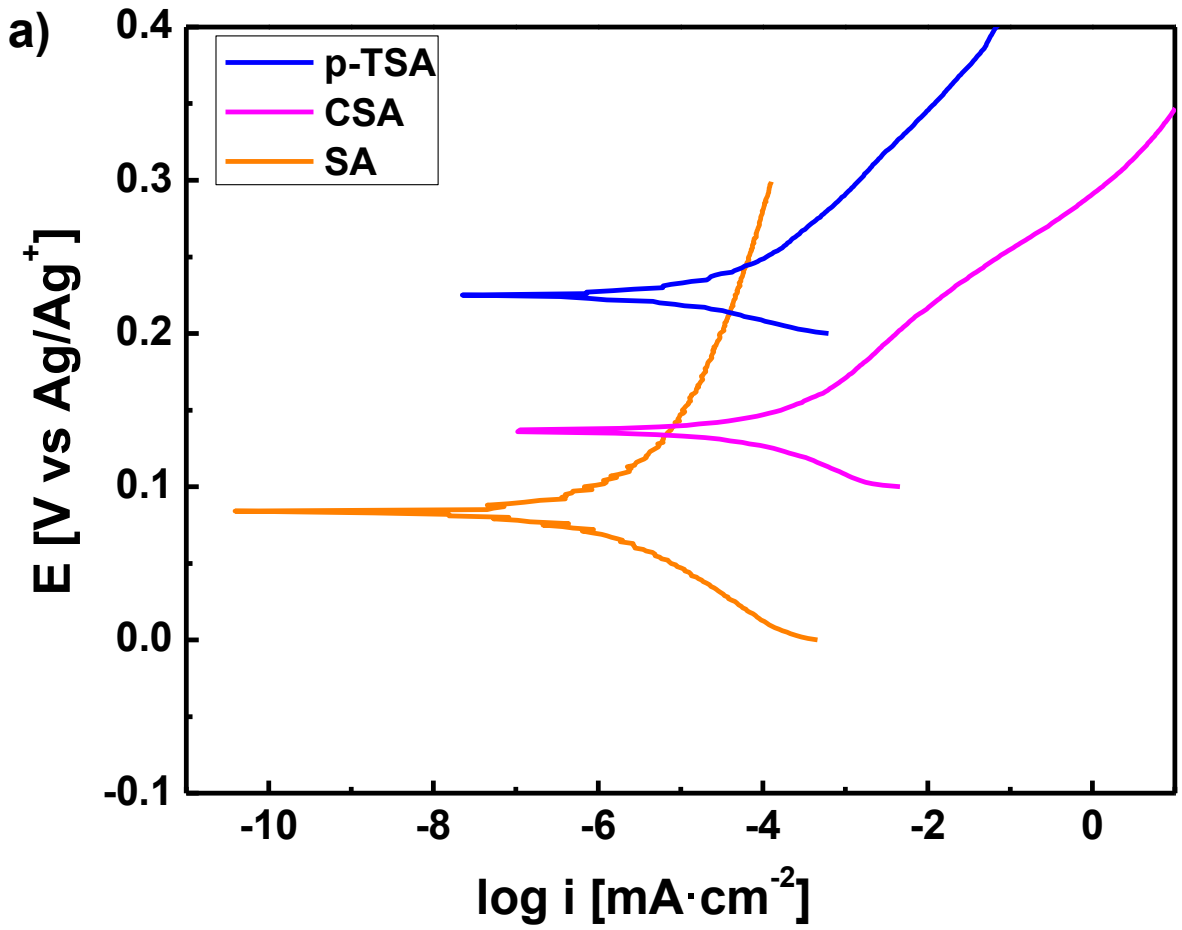

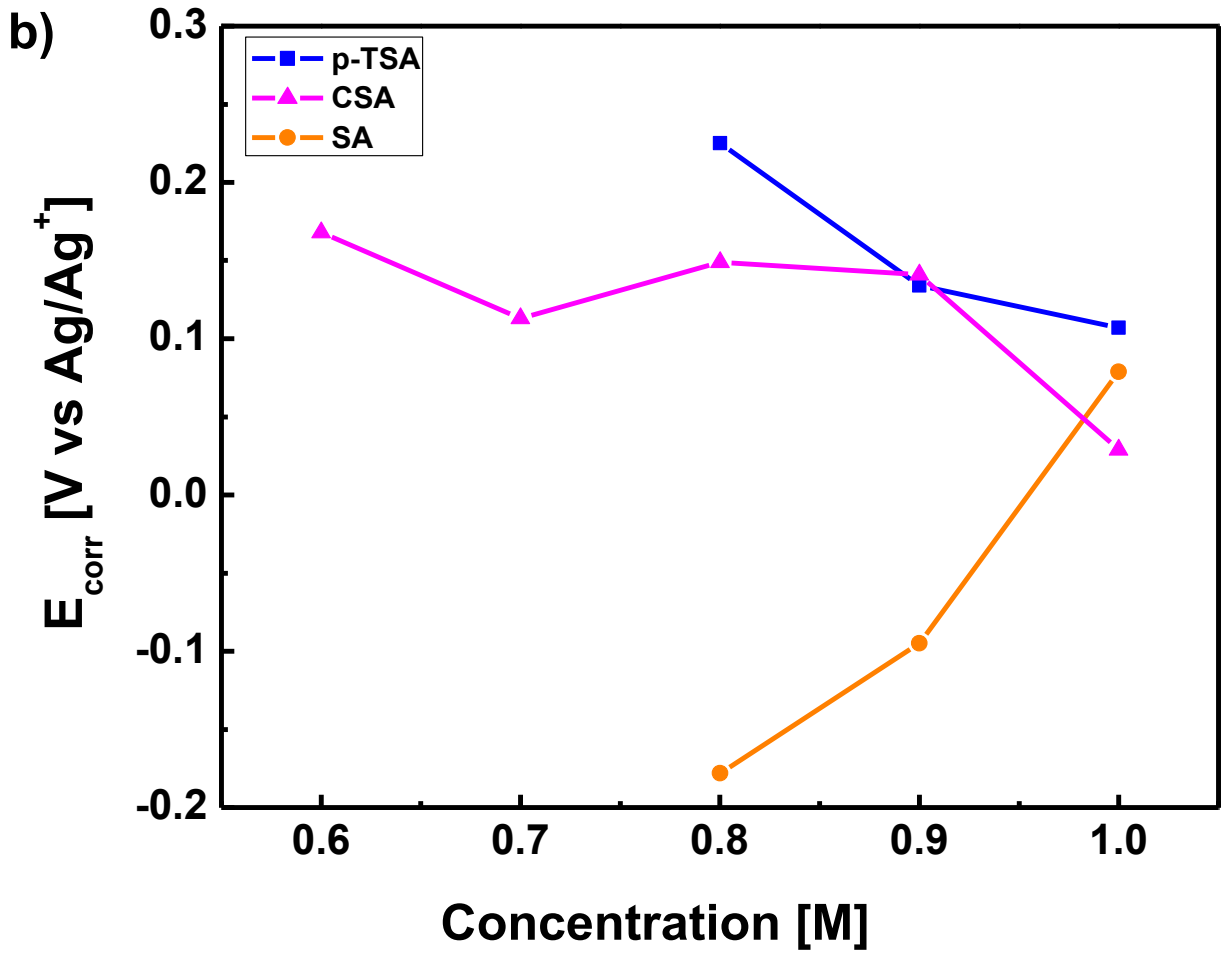

Figure 2.6 Potentiodynamic polarization curves scanned at 1 $mV.s^{-1}$ in 3.5% NaCl for PPy coating doped with short chain dopants at best concentration (a) and concentration vs. E_{corr} plot (b).

2.3.3.2 Long chain dopants: The long chain dopants chosen for this study were anionic sulfonic surfactants: sodium dodecyl sulfate (SDS) and sodium dodecylbenzene sulfonate (SDBS), because of their contribution in doping the conducting polymer and using as corrosion inhibitors, simultaneously.[63] The mechanism of inhibition is for functional groups to get adsorbed on the surface and form aggregates. The capability to form these aggregates is directly related to the micelle formation; therefore, critical micelle concentration (CMC) is a key indicator. For better understanding, surfactant concentration was increased from CMC (SDS=8.2 mM and SDBS=10

mM @25°C) to 30 mM and their corrosion inhibition efficiency was studied along with electropolymerized polypyrrole coating. In the SDS doped PPy coating, it clearly indicated that there were not enough micelles formed and adsorbed on the surface at concentration below CMC (Figure 2.7a).

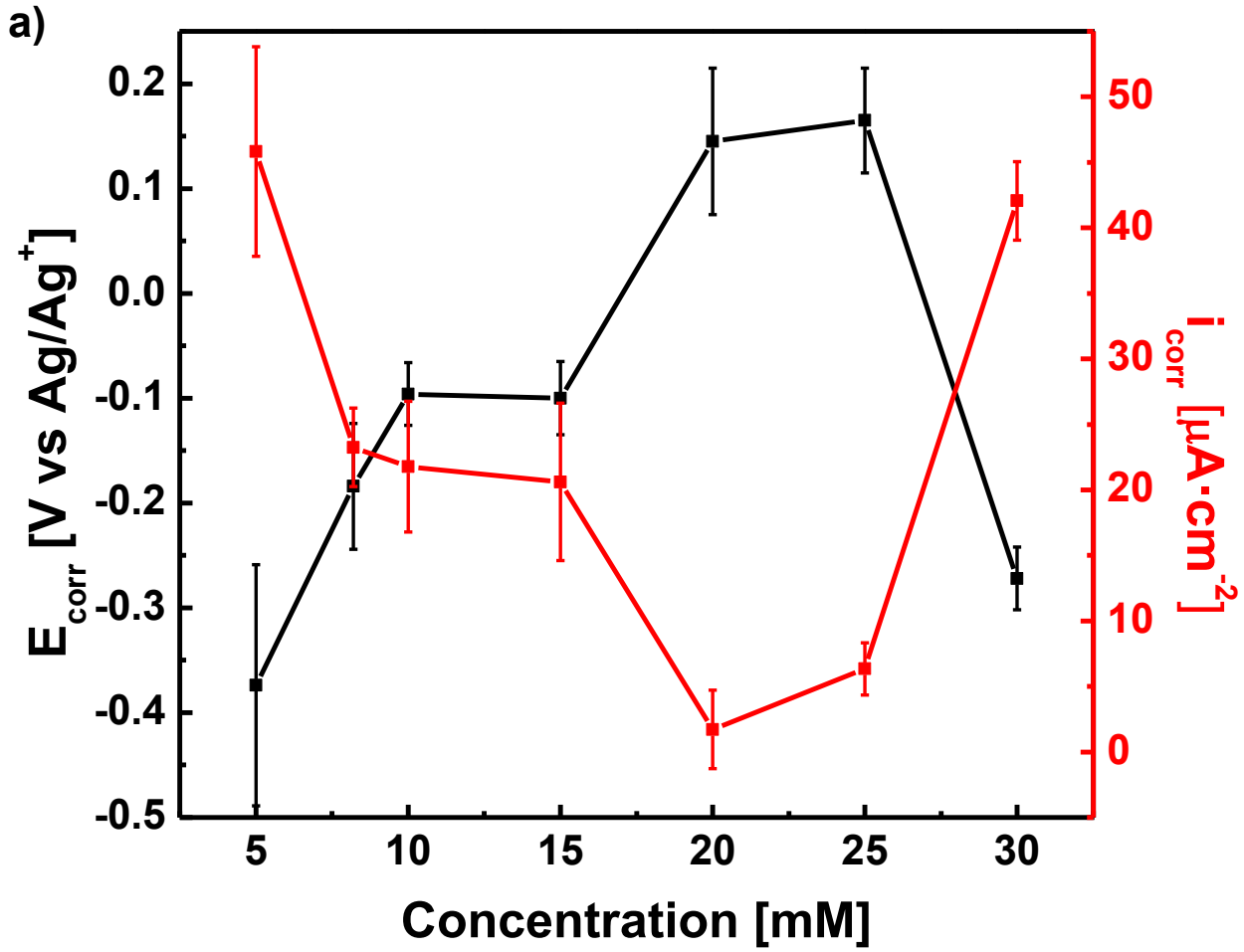

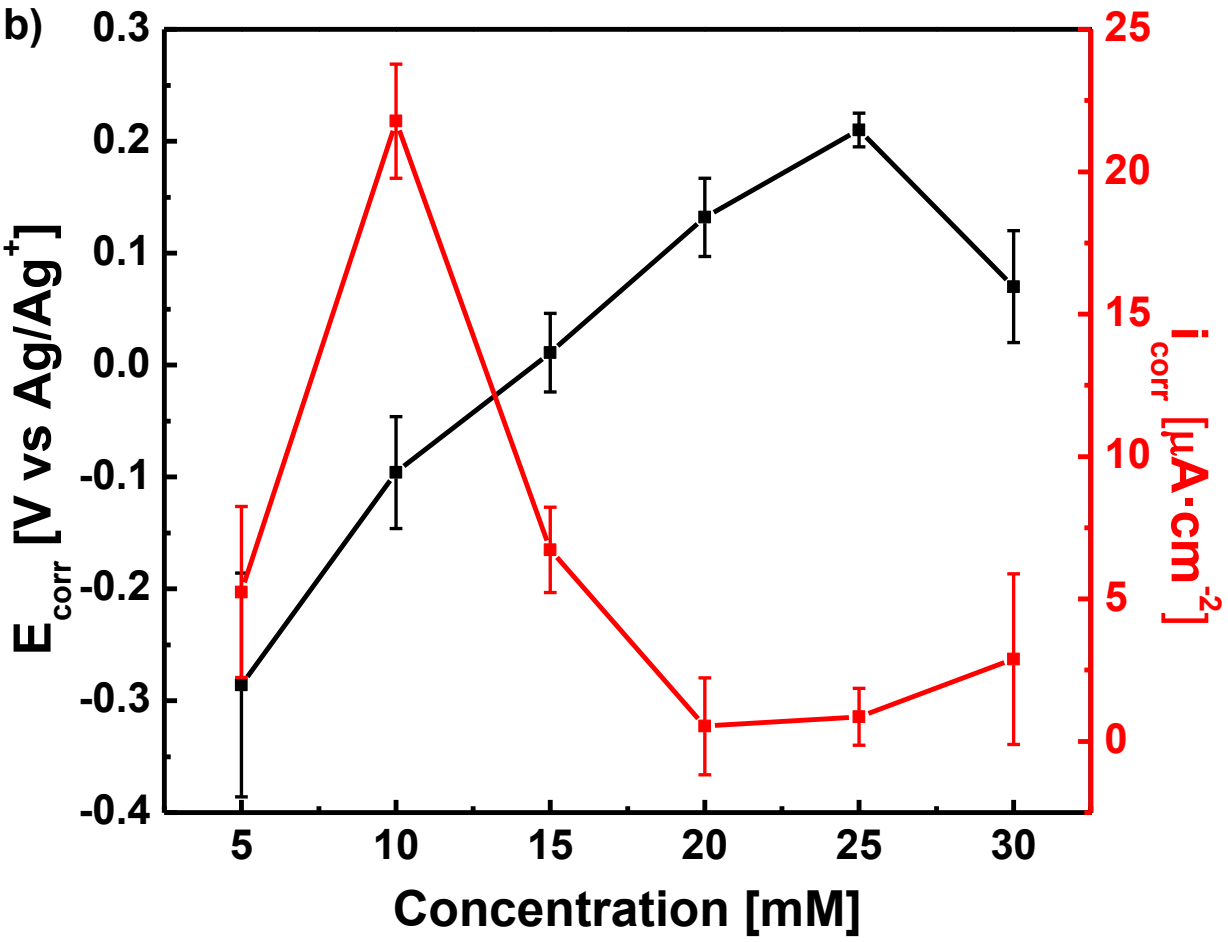

Figure 2.7 Variation of corrosion potential (E_{corr}) and corrosion current density (i_{corr}) with concentration of: a) SDS and b) SDBS.

On the other hand, if the concentration was increased to 8.2 mM (CMC for SDS), E_{corr} was significantly increased by approximately 200 mV in value. This indicates the presence of micelles on the surface of the metal is responsible for reducing the penetration of chloride ions. This provides three different protections all together in a single layer of PPy coating which are providing resistance to corrosive species and keeping the surface dry (barrier protection), keeping the potential of carbon steel in passive region (anodic protection), and covering the surface preventing access of corrosive substances to carbon steel (inhibition). Further increase in concentration leads

to more surfactant molecules adsorbed on the surface forming multiple layers of surfactant molecules to form an extra protective layer on the surface and it is evident from the shifts of E_{corr} value to more positive. Similarly, there is an anodic shift in E_{corr} when concentration was increased from 5 mM to 25 mM in SDBS (Figure 2.7b). However, if concentration was further increased to 30 mM there is a sudden drop in corrosion potential, this is perhaps due to more surfactant molecules were adsorbed on the surface thus prevents polypyrrole coating formation. Amongst the two, SDBS proved to be the better for anti-corrosion performance. This is due to when pyrrole is electropolymerized with SDBS as a dopant, it forms a barrier to chloride ion by having π-π interaction within the molecules. Also, having higher electron density in SDBS, the negatively charged chloride were repelled preventing any further contact to the metal.

Table 2.1 Comparison of corrosion potential, corrosion current with corrosion rate for both dopants SDS and SDBS.

Concentration (mM)	**E_{corr} (mV)**		**i_{corr} (μA·cm^{-2})**		**CR (meter per year)**	
	SDS	**SDBS**	**SDS**	**SDBS**	**SDS**	**SDBS**
5	-0.374	-0.285	45.8	5.2	0.00054	0.00006
8.2	-0.184	-	23.2	-	0.00027	-
10	-0.095	-0.095	21.6	21.6	0.00026	0.00026
15	-0.096	0.011	20.6	6.8	0.00024	0.00007
20	0.145	0.116	1.72	0.52	0.00002	0.00006
25	0.164	0.213	6.4	0.86	0.00007	0.00001
30	-0.272	0.071	42.2	2.8	0.00049	0.00003

The corrosion rate of both the dopants are in alignment with their corresponding E_{corr} shifts. This can be explained from Figure 2.7 that corrosion rate is higher when corrosion is more favorable having negative or lower corrosion potential. The corrosion rate was calculated using Faraday's Law (Table 2.1):

$$CR = 3.27 \times 10^{-6} \frac{\text{equivalent weight}}{\rho} i_{corr}$$

where CR is corrosion rate in (meter per year), equivalent weight of iron is 28 $g \cdot mol^{-1}$, ρ is density of iron (7.8 $g \cdot cm^{-3}$) and i_{corr} is in $\mu A \cdot cm^{-2}$.

2.3.4 Adhesion. The carbon steel was polished with 1200 grit size emery paper for studying the adhesion of electrochemically deposited polypyrrole coating with all the dopants. The test indicates the importance of surface roughness for adherent coating which rougher surface has more sites to hold the coating together on the surface making a strong coating. However, rougher surface is not necessarily good for corrosion protection, when compared to smoother surface. There is more non-uniformity in the rougher coating, which results in more cracks when attacked by aggressive corrosive ions, such as Cl^-. Therefore, adhesion was improved by adding 1 mM decanoic acid (DA) to pyrrole monomer solution acting as an adhesion promoter.[64,65]

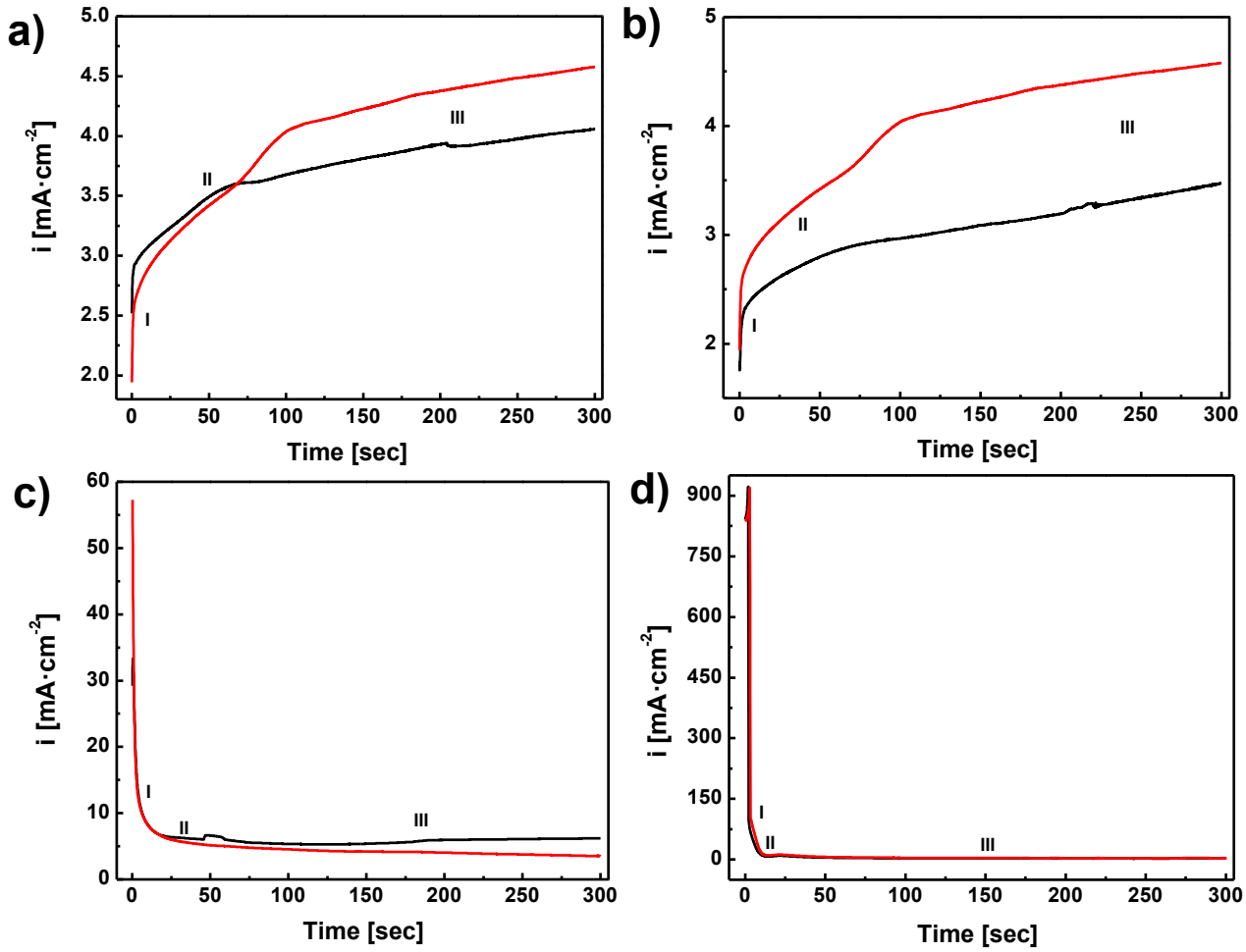

Figure 2.8 Chronoamperometric curves for electropolymerization of polypyrrole coating doped with: a) SDBS, b) SDS, c) p-TSA and d) sulfuric acid [black line – with no decanoic acid and red line – after addition of decanoic acid to monomer solution]

The electropolymerization of polypyrrole on the steel surface is characterized by three distinct regions: i) diffusion-controlled pyrrole oxidation (region I), ii) nucleation of polypyrrole takes place on the surface (region II) and iii) continuous growth of polypyrrole on the surface (region III). In Figure 2.8, the addition of decanoic acid does not interfere with electron transfer in electropolymerization of pyrrole. It enhances the adhesion significantly by forming an anchor between metal-coating interface.

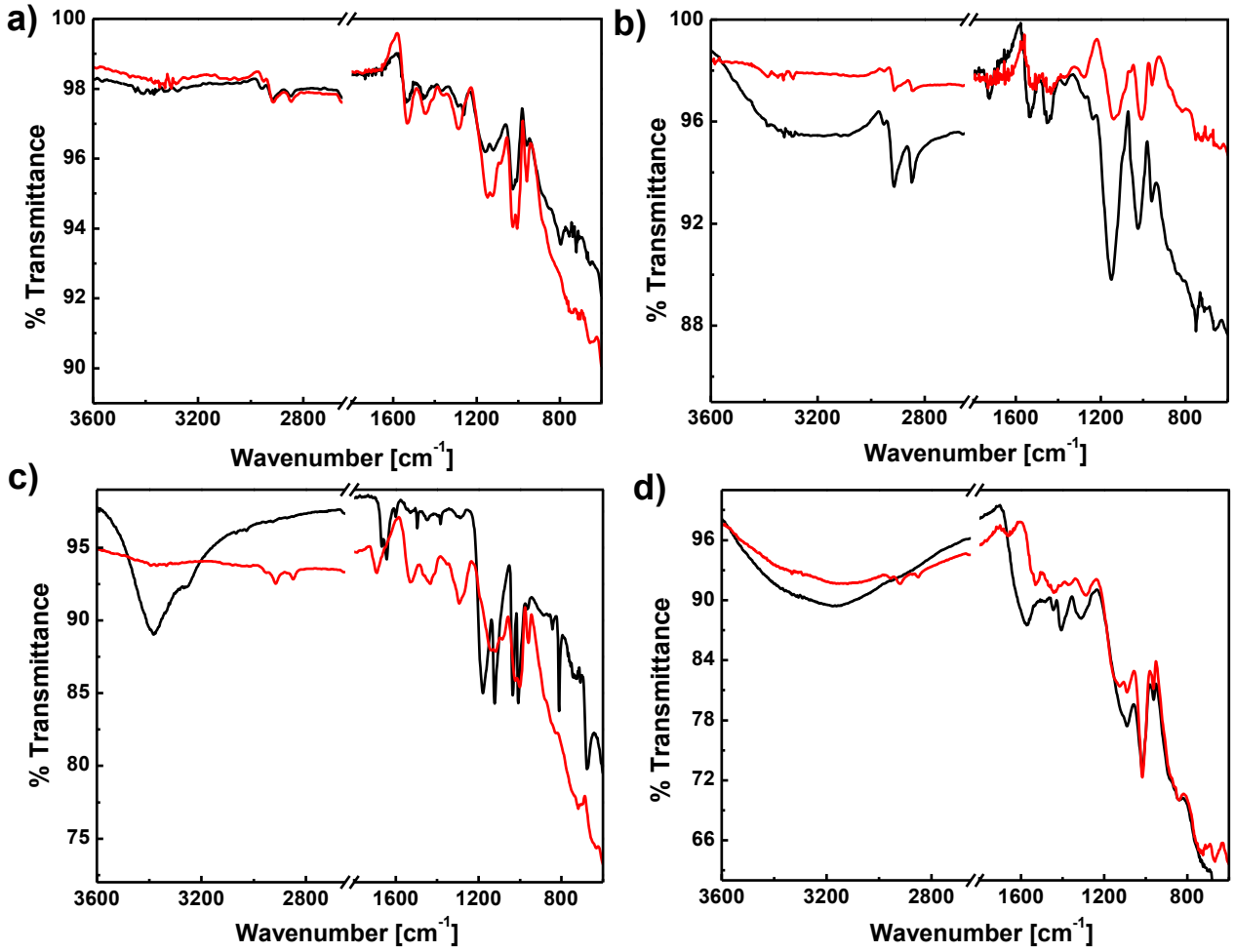

Figure 2.9 FT-IR spectra of polypyrrole coating doped with: a) SDBS, b) SDS, c) p-TSA and d) sulfuric acid [black line – with no decanoic acid and red line – with decanoic acid]

In Figure 2.9, the C-H stretching can be seen at 2850-2920 cm^{-1} in all spectra (red line) having decanoic acid in the coating system. This indicates the presence of long carbon chain of carboxylic acid within the polypyrrole coating. The absence of C=O nearly centered at 1700 cm^{-1} indicates the partial dissociation of carboxylic acid to carboxylate that form bidentate configuration to the metal surface.[31] This can be corroborated by the presence peaks at 1428 and 1530 cm^{-1} where COO^- stretching can be observed. However, in case of SDBS and SDS the C-H can be due to dodecyl (C_{10}) in the compound, hence it is difficult to distinguish between presence of decanoic acid or

dopant. Therefore, polypyrrole coating doped with p-TSA and SDBS were chosen for further biocidal efficacy test because of their good adhesion (Figure 2.10) and best corrosion protection property.

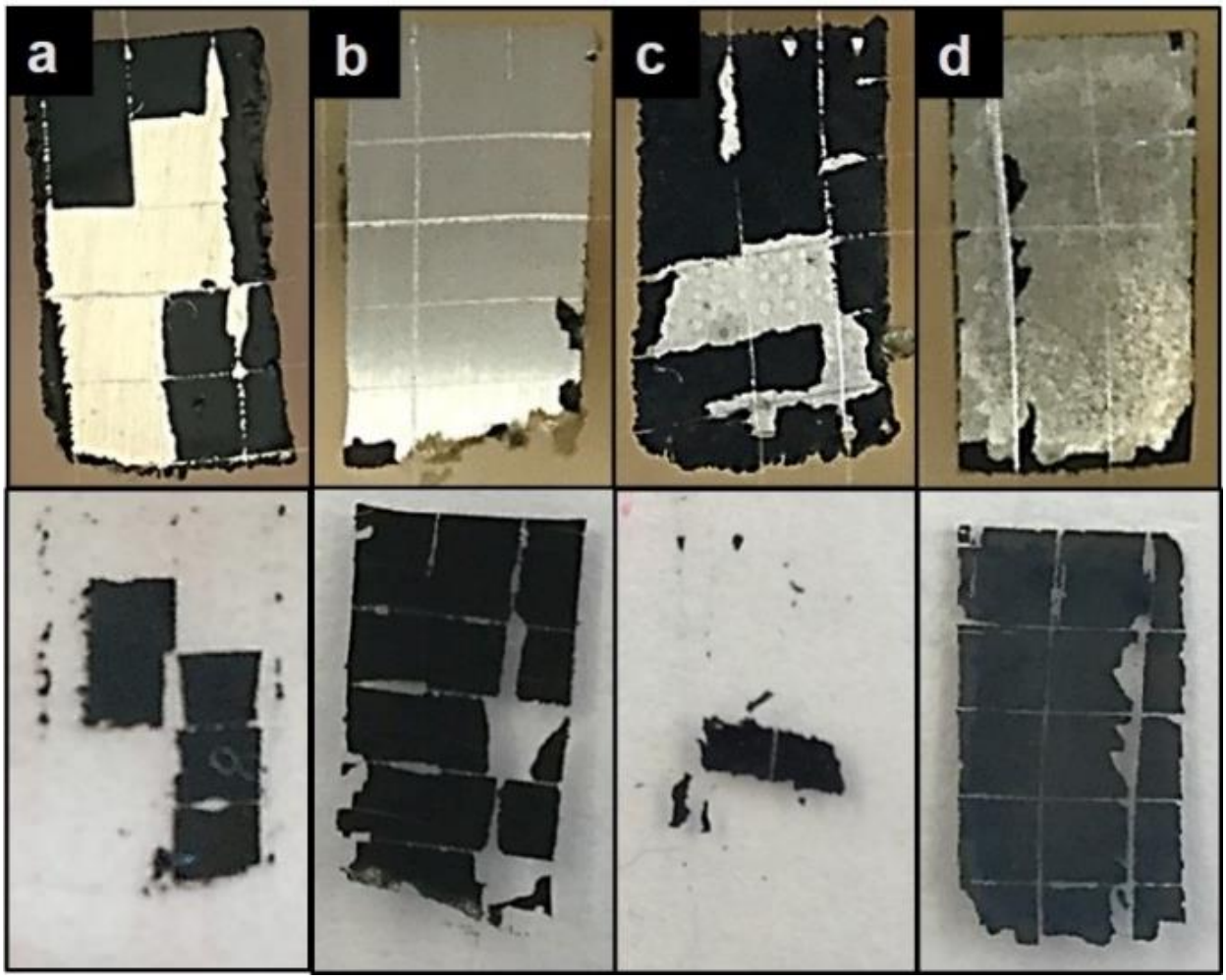

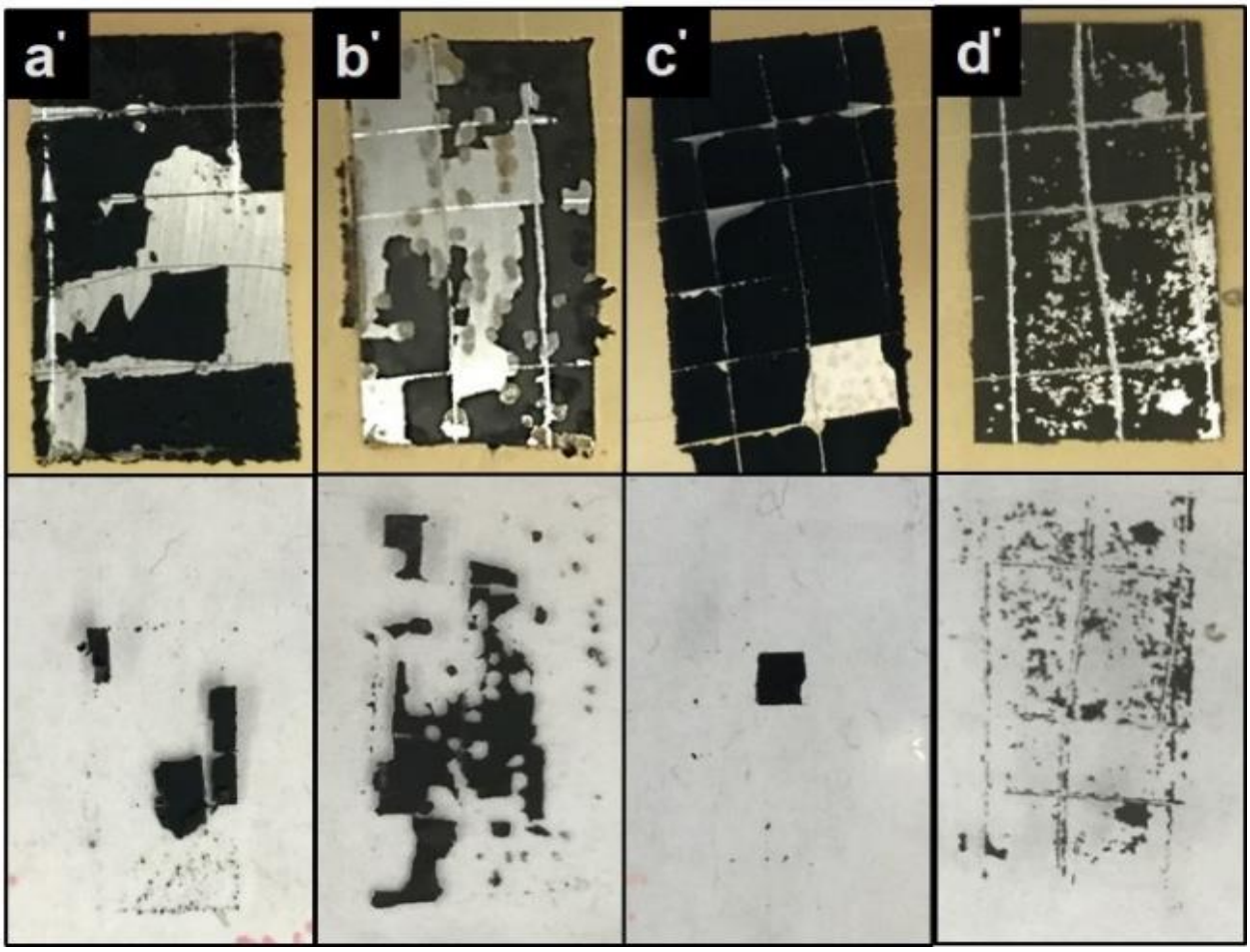

Figure 2.10 Cross hatch scotch tape tested samples for adhesion as per ASTM D3359, polypyrrole coating doped with: a) SDBS, b) SDS, c) p-TSA and d) sulfuric acid and a′) SDBS+DA, b′) SDS+DA, c′) p-TSA+DA and d′) sulfuric acid + DA, with their corresponding area removed after testing.

2.3.5 Biocidal effect. As shown in Table 2.2, uncoated carbon steel samples caused about 0.86 log reduction (86.32% kill) of bacteria after 10 min of contact. However, after being coated with polypyrrole, the biocidal activity increased significantly. For polypyrrole coating doped with SDBS, it caused 5.66 log reduction of bacteria within 10 min, which was considered as a 100%

killing of bacteria. This biocidal activity is better than the previously reported results with very limited killing rate of bacteria (26% of *S. aureus*) using polypyrrole.

Table 2.2 Biocidal activity of polypyrrole coating on carbon steel obtained from different dopants.

Samples	Contact Time	Bacteria reduction (log)	Bacteria kill (%)[i]
CS	10 min	0.86	86.32
CS-PPy-p-TSA	1 min	0.57	73.24
	5 min	0.96	89.12
	10 min	1.92	98.79
CS-PPy-SDBS	1 min	3.23	99.94
	5 min	3.53	99.97
	10 min	5.66	100

[i] Inoculum content: 4.5×10^5 CFU/sample of *Staphylococcus aureus*.

Additional tests were carried out to investigate dopant anion effects to polypyrrole biocidal efficacy. Our test confirmed that polypyrrole polymers doped with HCl caused about 1.5 log reduction of *S. aureus* within 10 min of contact. When p-TSA is used as dopant, with similar structure as SDBS but shorter carbon chain, it only caused 1.92 log reduction (98.79% kill) of bacteria with same contact time of 10 min, still better biocidal efficacy than previously reported result[53]. The antimicrobial function against bacteria was due to the presence of SDBS and p-TSA molecules embedded within the coating matrix. SDBS and p-TSA are both sulfonate antimicrobial molecules and the destruction mechanisms of sulfonate group were well studied before.

The destruction mechanism within this group was commonly hypothesized to be one of the three following mechanisms [66]: 1) protein denaturing, 2) essential enzyme inactivation, 3) membrane disruption and alteration of cell permeability. The length of chain attached to the sulfonate group also influences the antimicrobial function. Usually longer chain will enhance antimicrobial function of the molecule. This is in good alignment with results observed in this study that compared with p-TSA, SDBS with longer chain exhibited better antimicrobial activity. Consequently, the biocidal function of polypyrrole coating on carbon steel was found out to be synergetic effect of polypyrrole and dopants. Hence, it can be inferred that dopant with longer carbon chain proved to be suitable for electrochemically produced coating of polypyrrole since it enhances both the corrosion protection efficiency and biocidal effect of the coating.

2.3.6 Stability. The long-term stability of polypyrrole coating was evaluated by electrodepositing PPy on steel surface using SDBS as a dopant. The SDBS was chosen as a dopant because it has shown the maximum protection against corrosion and bacteria. The PPy coating was immersed in chlorine-based bleach solution (1% NaClO solution, pH=7.0/HCl, $[Cl^+]$ =414±8 ppm] for 10min. The chlorinated PPy coating was washed with copious amount of DI water followed by vacuum drying. The dried coating was then sterilized by autoclaving at 121 °C for 40min to transform PPy to PPy based N-halamine for antibacterial coating results were reported in Mingyu Qiao's dissertation. [67] As shown in figure 2.11, stainless surface is coated with black homogenous polypyrrole film. This coating showed excellent stability after treating it with 1% bleach and no significant damage was observed. Further, autoclaving process does not affect the homogeneity of polypyrrole coating, it showed the thermal stability of more than 100 °C for more than half an hour.

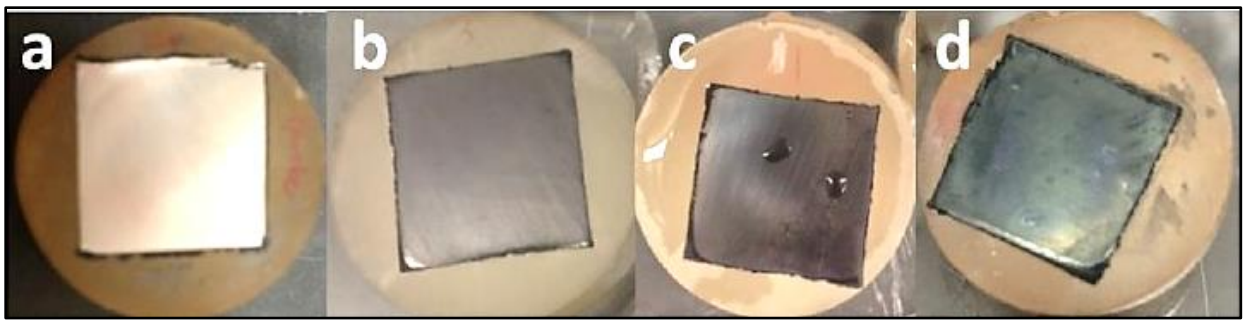

Figure 2.11 Appearance of (a) uncoated steel, (b) PPy coated steel, (c) PPy coated steel after chlorination treatment in 1% bleach for 10 min, and (d) PPy coated steel after autoclave at 121 °C for 40 min. [67]

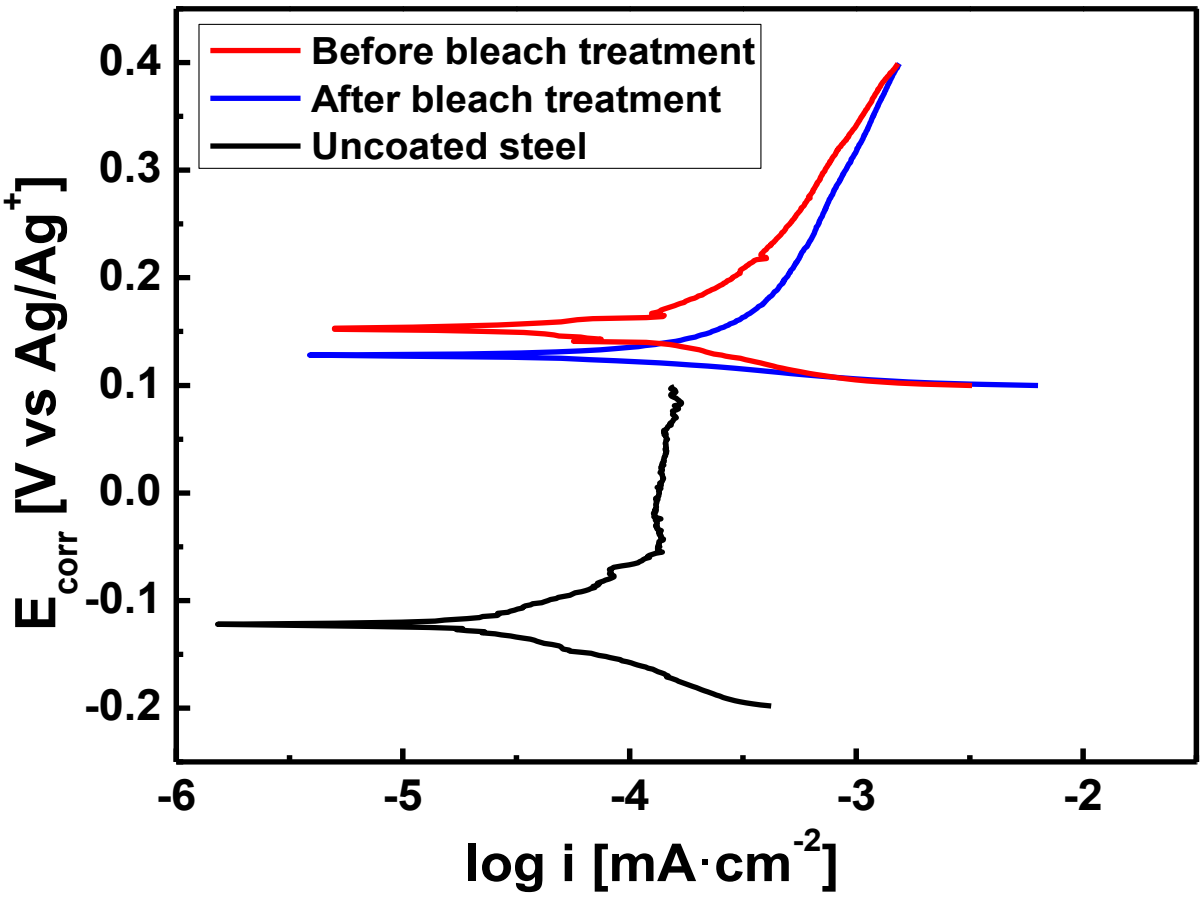

Figure 2.12 Tafel curves of polypyrrole (unchlorinated and chlorinated) coating compared with uncoated steel in 3.5% wt. NaCl.

The corrosion performance of polypyrrole was tested in 3.5% NaCl before and after bleach treatment. Figure 2.12 showed anticorrosive performance of polypyrrole coating and it ennobled the steel surface by shifting its corrosion potential (E_{corr}) from -0.12 to +0.15 V vs Ag/Ag^{+}. Although there was a slight decrease (30 mV) in corrosion potential after chlorination, the E_{corr} of +0.12 V vs Ag/Ag^{+} was still considered as good anticorrosion ability. The decrease in corrosion potential is due to the removal of SDBS from PPy while chlorination. SDBS was used both as dopant for the polymer and corrosion inhibitor simultaneously that protects the surface synergistically with PPy. The electrical resistances were 5 and 200 kΩ for unchlorinated and chlorinated polypyrrole coating, respectively. The conductivity was calculated to be dropped from 1.96 S/cm to 0.049 S/cm after chlorination which is still in semiconducting range. The formation of N-Cl bond to a certain extent blocked the electron transfer in the original conducting structure of oxidized PPy; however, this slight decrease in conductivity did not affect the function of PPy conducting polymer as anticorrosive coating.

It was evident that dopant size has an important role in suppression of metal corrosion and bacterial attack by providing barrier to corrosive ions and sulfate reducing bacteria from the coating system. Larger anions are difficult to exchange from polymer to electrolyte therefore it is better for providing barrier protection. As it can be seen in Figure 2.11, larger dopant ions have higher E_{corr}, i.e., p-TSA and SDBS have corrosion potentials very close to each other and are the highest. This is because of the presence of extra pendant group in the structure that helps in forming sheet like structure preventing chloride ions to enter the coating system. Between the two, p-TSA provided little extra anodic shift than that in SDBS because p-TSA does not have long carbon chain like SDBS has.

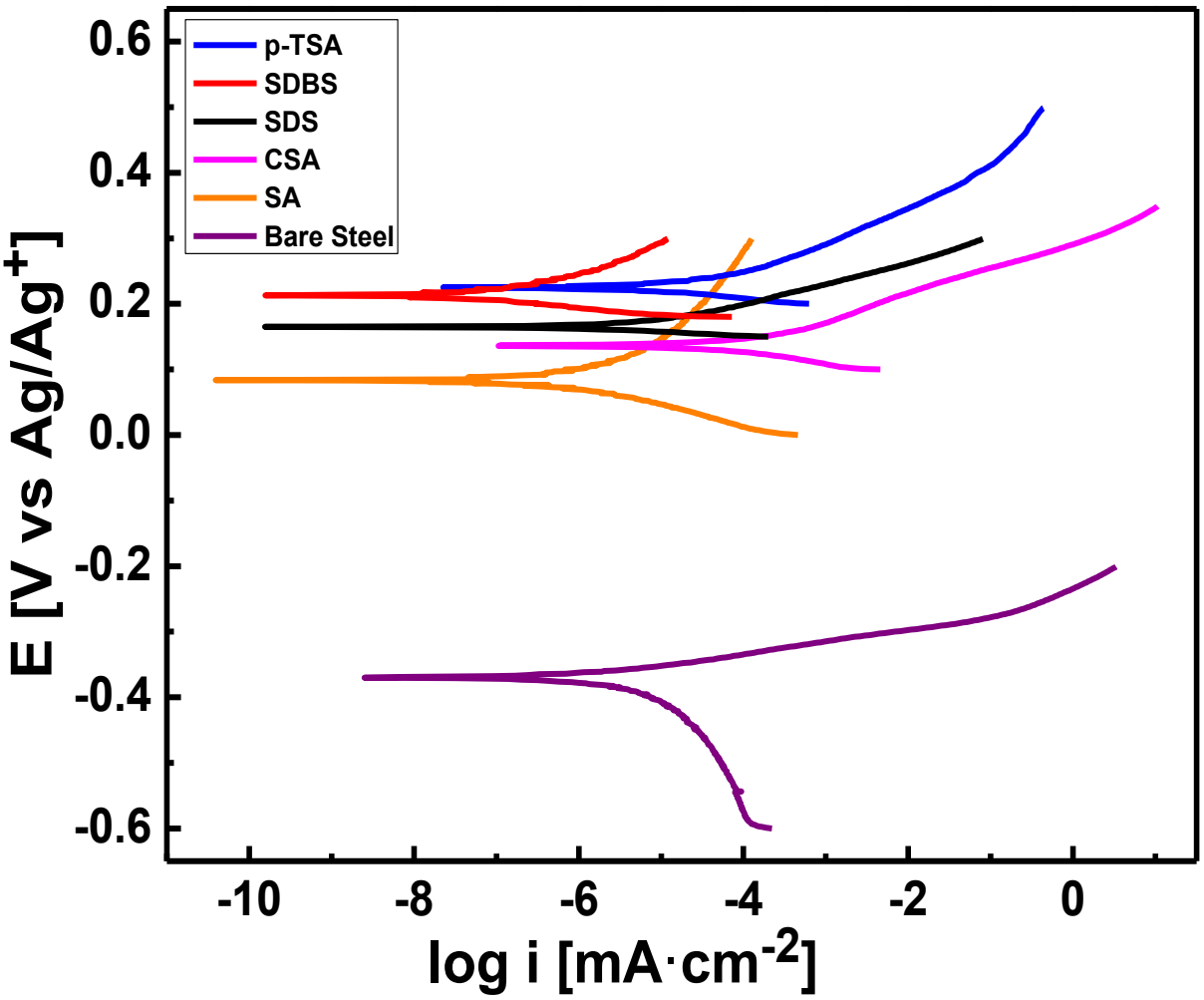

Figure 2.13 Tafel curves comparison of best result for all dopants used compared with uncoated steel.

Long carbon chains sometimes entangled with polymer chain or between each other creating amorphous like structure through which chloride ion can penetrate via tortuous path to corrode the sample. However, if SDS and SDBS are compared, it was evident that the presence of benzene is helping in the inhibition of chloride attack. Additionally, SDBS doped polypyrrole coating showed great potential to be used as antibacterial coating by swiftly killing 100% gram-positive bacteria (*S. aureus).*

2.4 Conclusion

Polypyrrole was synthesized electrochemically on carbon steel surface with five different dopants sub-categorized in short chain (p-TSA, CSA, and SA) and long chain dopants (SDS and SDBS). The potentiodynamic scan was performed on the bare steel sample to study the passivation behavior of steel in short chain dopant and it was found out the lowest passivation potential have better coating characteristics and better protection against corrosion. In CSA, it was observed that the stability of protective passive layer is of equally important for having better protection against corrosion. In this study, p-TSA and SDBS were found to be the best dopants for polypyrrole coating on carbon steel. This was due to the presence of aromatic rings from the dopant ions, which could result in π- π stacking to create lamellar structures, which prevent the ingress of chloride ions in the coating system. The study of enhancing adherence of coating showed improvement in adhesion that can be achieved by adding long chain carboxylic acid, such as decanoic acid acting as an adhesion promoter, directly in the monomer solution. In addition, the polypyrrole coating showed potent biocidal function, which it could contribute to reduce microbiologically influenced corrosion. Longer chain dopant (SDBS) was able to enhance the biocidal activity of PPy coating. The outcomes of this study can be further used in combination of commercially available organic paint topcoat to have longer life and higher corrosion potential with excellent biocidal properties. The polypyrrole coating has shown excellent stability in chlorine-based bleach solution and can withstand more than 100 °C for more than 30min. Our system can also be used as replacement of toxic metal primer, which is hazardous to many living organisms including human being and can be useful if used as an antibacterial or antifouling coating. Beyond in the anti-corrosion field, this work will benefit material interface related researches in general, and lead to in-depth studies of fundamental and applied sciences and technologies.

Acknowledgment

This work was supported by National Institute of Food and Agriculture, USDA.

Chapter 3

Enhanced electrochemical performance of polyaniline coating by facile anion exchange

Abstract: Polyaniline (PAni) was electropolymerized on stainless steel (SS) surface using sulfates (sulfuric acid, SA and p-toluene sulfonic acid, p-TSA) as doping anions. These dopant anions were electrochemically exchanged to phosphates (phosphoric acid, PhAc and phytic acid, PA) to enhance the corrosion performance of polyaniline. The dopants used for polyaniline were substantially affecting the anticorrosion performance of the coating depending on type of dopants, size and their alignment in polymeric chain. The protection efficiency was significantly improved when sulfates were exchanged to phosphates due to their inhibiting properties towards corrosion for stainless steel. The anion exchange was studied using electrochemical impedance spectroscopy (EIS) and was confirmed by Fourier Transform Infrared spectroscopy (FT-IR).

Keywords: polyaniline coating, dopant anion exchange, corrosion protection, corrosion inhibitors

3.1 Introduction

Polyaniline (PAni) is another nitrogen based conducting polymer that has been most widely studied like polypyrrole (PPy) because of its ease of synthesis, environmentally friendliness, and multiple redox states. In this project, we synthesized polyaniline-based coating that can be used as anticorrosive and anion exchange membrane simultaneously. Common practice used to protect stainless steel (SS) includes coatings, conversion films or to treat it with chromium to form

chromate (Cr_2O_3) film on the surface. This chromate film prevents the steel surface from degradation in aggressive medium [68]. However, chromate is toxic, hazardous to living being and is considered as carcinogenic agent [69]. Therefore, other materials must replace the use of toxic chromates to prevent its harmful effect. Conducting polymers are the class of material to be used in corrosion protection of metals and alloys to replace chromates and are considered to form green-coating. Many different types of conducting polymer coatings have been developed on different substrates. Their corrosion protection performance have been evaluated and found reduction in corrosion rate due to their anodic protection [38–40,70]. The conducting polymer coating can be deposited using either of depositing method i.e. chemically or electrochemically [56,71–75]. The electrochemical deposition is the most efficient way to synthesize conducting polymer coating due to their limited processability issues. Further, thickness and morphology of the coating can be adjusted by applied potential or current density. The problems with electrochemical deposition of conducting polymers is mainly associated with the nature of substrate such as each metal requires specific condition for conducting polymer deposition and depending on oxidation state, these polymers can be conducting or insulating. Barrier protection was provided by insulating form while active protection becomes easier when polymer is in conductive state where electrons were exchanged between polymer and metal substrate. This protection is provided by passivating (oxidation) the metal surface, making corrosion potential more positive. The protection performance of conducting polymer is significantly dependent on the type of dopant used, their size and alignment in polymer chain [27].

Polyaniline (PAni) is the most widely studied conducting polymers due to its facile synthesis, environmental friendliness, no toxicity, reversible redox behavior and acid/base doping/de-doping chemistry [76,77]. Many research areas have explored the advantages of conducting polyaniline such

as energy storage [32] catalyst [33], sensors [34] and membrane filters [35] etc. Moreover, it can be used for corrosion protection of metals and alloys. It was first reported by Deberry, who prevents stainless steel degradation by polyaniline coating [41]. Since then numerous work has been reported on corrosion protection performance of PAni on various metals such as Al, Cu, etc. [21,42,43] Deposition methods influences the protection efficiency of the coating, electrochemically deposited PAni provides better protection than that chemically deposited. This is due to direct deposition on the substrate and coating is free from oxidant contaminants.

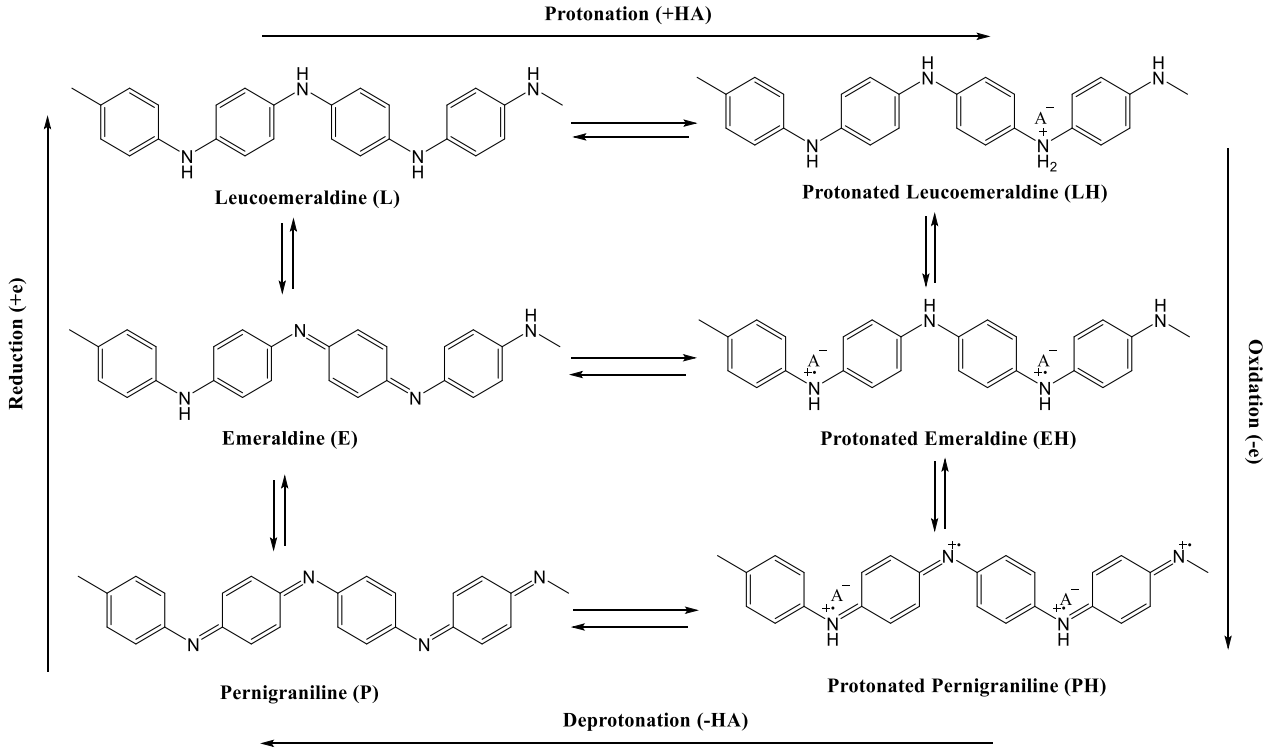

Figure 3.1 Different forms of polyaniline in its oxidation states.

PAni have three interchangeable oxidation states: leucoemarldine (L), emeraldine (E) and pernigraniline (P). The emeraldine form is widely used for various applications due to its easy transformation from non-conducting known as emeraldine base (EB) to conducting from known

as emeraldine salt (ES) by treating it with protonic acids. The unique property of reversible change between conducting and insulating form is doping and de-doping process. It is well known that cyclic voltammogram of PAni gives transformation of three different oxidation states (L, E, P) in strongly acidic electrolyte (figure 3.1). During positive potential scan, the first transformation occurs from LH (protonated leucoemeraldine) to EH (protonated emeraldine) that involves release of proton and anion from PAni with no insertion of anion. This is followed by conversion of EH to P which also involves release of protons and anions [78]. During negative potential scan, the reduction states of PAni were transformed by inserting anions and protons from the electrolyte, thus exchanging the anion. The level of doping is affected by pH of the solution and potential applied which depends on the degree of protonation. However, anion movement is of equal importance as degree of protonation when PAni film are used in electrolytes. This feature leads to the changes in redox behavior that alters the electrical and optical properties of PAni [79–81].

Various protonic acids have been studied to deposit protonated PAni ranging from smaller size (sulfuric acid, nitric acid, oxalic acid etc.) to larger size (dodecylbenzene sulfonic acid, camphor sulfonic acid, p-toluene sulfonic acid etc.) that plays a key role in protection mechanism. However, there are certain acids that does not provide favorable condition for electropolymerization of polyaniline (low deposition efficiency) such as phytic acid or phosphoric acid [82]. The deposition efficiency can be improved by the addition of sulfuric acid to the phosphoric acid solution. However, coating contains sulfate anions if only phosphate anions were desirable. This can be avoided by de-doping the polymer and re-doping it with preferred protonic acid where the electronic number of PAni does not change during the process of doping [83]. This doping-dedoping-redoping process involves several steps to achieve final coating and dedoping process involves treatment with aqueous base that may damage the coating. To reduce the number of steps involved

and avoid its treatment with base, dopant anions can be exchanged electrochemically [84]. In this work, we used this property of polyaniline of interchangeable oxidation states to exchange of dopant anion from electropolymerized polyaniline coating by cyclic voltammetry technique and evaluated their effect on anticorrosion performance of the coating on stainless steel. The dopant anions were exchanged from sulfates (SA and p-TSA) to phosphates (PhAc, PA) because of mild corrosion inhibiting properties of phosphates on stainless steel. By exchanging sulfates (Sf) to phosphates (Ph) have significantly enhanced the corrosion protection performance of polyaniline by providing anodic, barrier and inhibition protection all together with no influence on morphology of the coating. Further, active surface sites in coated PAni were calculated and number of sites accessible were calculated for each anion exchanged.

3.2 Experimental section

3.2.1 Materials. Aniline (M_w= 93.13 g·mol^{-1}, density = 1.02 g·cm^{-3}), platinum (Pt) gauze (100 mesh, 99.9% metal basis), p-toluenesulfonic acid (p-TSA) was obtained from Alfa Aesar, USA. Sulfuric acid (SA) was purchased from Anachemia. Phosphoric acid (PhAc) was purchased from EM Science, USA, Phytic acid (PA) was obtained from Tokyo Chemical Industry. All chemicals were used without further treatment or purification. Stainless steel sheet (SS316L, 1 mm thick) was used for electrodeposition surface.

3.2.2 Sample preparation. The steel samples of 1.5 cm × 0.5 cm were cut from 1 mm thick sheet and cold mounted into acrylic resin so that only one surface was exposed. The embedded sample was then polished by emery papers of different grit size starting from 800, 1000, and 1200. It was followed by ultrasonic cleaning in deionized (DI) water for 1 min (DI water with ∼18.2 Ω·cm resistivity).

3.2.3 Electrochemical synthesis. Polyaniline coating was electrochemically deposited using electrolyte containing 0.1M aniline and 0.5M dopant (SA, p-TSA). The electrochemical cell set-up used was a single compartment with three-electrode system, where SS (1.5 cm x 0.5 cm) was used as a working electrode, Pt as a counter electrode, Silver/Silver chloride/KCl (3 M) (Ag/Ag^{+}, E° = +205 mV vs. SHE) was used as reference electrodes. Electrodeposition was carried out on CH Instruments (CHI 760D) potentiostat using Electrochemical Analyzer software (version 17.06) by applying constant potential of 1V for 5 min when dopants used were SA, p-TSA. For comparison PhAc and PA doped PAni was deposited using constant potential of 1.2V for 60min for phytic acid and cyclic voltammetry (CV) for phosphoric acid (swept between -0.4 to 1.3V @10$mV \cdot s^{-1}$ for 20cycles).

3.2.4 Characterization. The surface morphology of the coating was recorded under Scanning Electron Microscope (SEM) on JEOL JSM-7000F at 20 keV with 10 mm working distance. The corrosion tests were performed in 3.5% NaCl with linear sweep voltammetry (LSV) at a scan rate of 1 $mV \cdot s^{-1}$, scanning ±150 mV from the open circuit potential (OCP). The corrosion test was performed on both as-produced and anion exchanged PAni coating. Anion exchange was studied by Electrochemical Impedance Spectroscopy (EIS) and confirmed by Fourier Transform Infrared (FTIR) analysis that was conducted on a Thermo Nicolet 6700 FTIR. The EIS was performed at open circuit potential (0.4V) in respective electrolyte solution (mentioned wherever plotted).

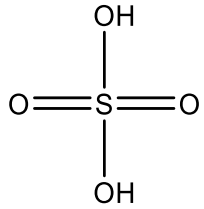

Sulfuric Acid (SA)

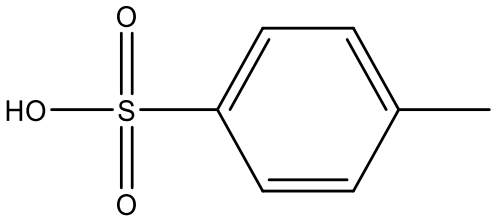

p-Toluenesulfonic Acid (p-TSA)

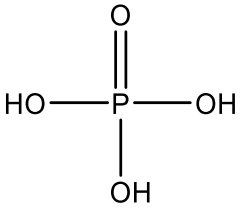

Phosphoric Acid (PhAc)

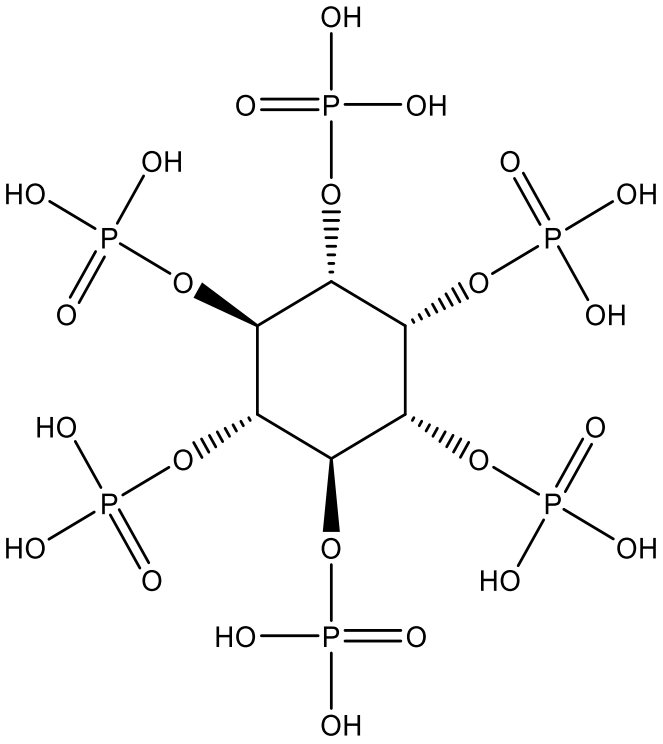

Phytic Acid (PA)

Figure 3.2 Chemical structure of doping agent for polyaniline used in this study

3.2.5 Anion exchange. The anion exchange of produced polyaniline coating was carried using cyclic voltammetry (CV) by sweeping potential between -0.3 to 1 V at 50 $mV \cdot s^{-1}$. The produced PAni coating (PAni/Sf) was rinsed with DI water and dried in air. Then dried PAni/Sf coating was transferred to phosphates solution (PhAc or PA) and impedance spectra was obtained at open circuit potential. Then cyclic voltammogram was recorded for 20 cycles for anion exchange followed by EIS. This procedure was repeated for another 20cycles and EIS was obtained. The full exchange cycle can be understood as: EIS-CV-EIS-CV-EIS. The anion exchanged PAni coating was then designated as PAni/Sf-Ph (Sf: sulfuric or p-toluene sulfonic acid and Ph: phosphoric or phytic acid). The size of anions of dopants used are arranged according to their ionic radii: phytic acid anion > tosylate (TsO^-) > hydrogen sulfate, HSO_4^- (0.221±0.019 nm) > dihydrogen phosphate, $H_2PO_4^-$ (0.213±0.019nm) [85].

3.3 Results

3.3.1 Electropolymerization. The electrodeposition of a PAni on SS surface was known to occur in three stages [55]: a) SS passivation and adsorption of aniline, b) aniline oxidation along with nucleation of PAni and c) PAni growth over the surface. These three stages are represented in chronoamperometric curves of electropolymerization of PAni on SS surface when doped with sulfuric acid and p-TSA, respectively, as shown in figure 3.3. There is a drop in current density in stage I that corresponds to the passivation of the surface. This passivation is necessary prior to electrodeposition of polyaniline on steel surface as metal dissolution starts before aniline oxidation occurs at higher potential [27,28]. The stages II start with increase in current due to aniline oxidation and nucleation process occurring at same time. This gives us green color coating over the steel

surface. This is followed by stage III where PAni film grows on the steel surface. The growth is more uniform when p-TSA was used as a dopant than when sulfuric acid was used. This uniform growth of PAni looks compact in SEM images (Fig. 3.9a&d).

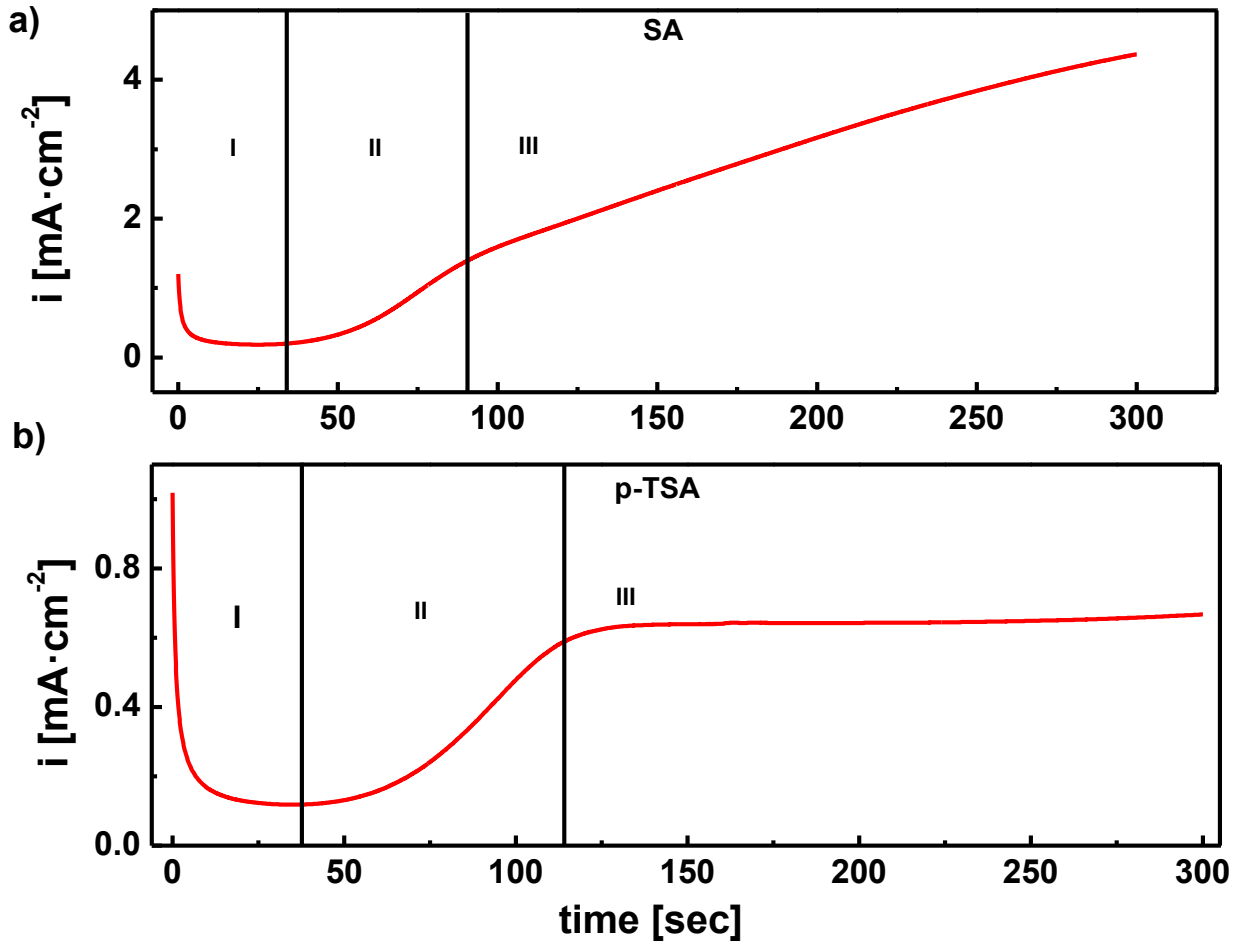

Figure 3.3 Chronoamperometric curves for electropolymerization of polyaniline coating on stainless steel using dopants: a) SA and b) p-TSA.

3.3.2 Anion exchange. It is well known that redox behavior of PAni can be studied electrochemically by cyclic voltammetry technique. The typical CV curve of PAni includes the oxidation and reduction peaks that explains the change in oxidation states of polyaniline in acidic

electrolyte. In Fig. 3.4, the CV shows the behavior of polyaniline in phytic acid (Fig. 3.4a & c) and phosphoric acid (Fig. 3.4b & d) solution for anion exchange. During first cycle, there is an increase in current density reaches its maxima that shows the transformation of emeraldine to pernigraniline form of PAni (visually observed the change in color of the coating from green to dark blue). This indicates the release of anions and protons from the polymer chain leaving PAni de-doped and leaves pore in the coating.

The peak current density decreases with increase in number of cycles due to degradation of PAni on continuing exchange of anion. This peak shift positive with increase in number of scan because of the increase in acidity of the solution due to release of sulfates anion into the phosphates electrolyte solution [76]. The positive peak shift was observed in all the CVs shown in Figure 3.4. The reduction peak was seen at 0-0.2 V on negative scan transforming the reduction states of PAni by inserting anion from electrolyte. The inserting anions were phosphates occupies the pores created by sulfates due to their higher charge and adsorption tendency over the steel surface [86,87]. The phosphates compensate the charge neutrality in PAni backbone chain and re-doped the polymer (color of the coating turns back to green). It was observed (visually) that the release of sulfate anion and insertion of phosphates anions attributes to de-doping and re-doping process. In case of PAni/pTSA, oxidation and reduction peaks were present even after 40 cycles this indicates the exchange was partial (Figure 3.4a & b). This is due to the size of phytic acid anion is much bigger than that of p-TSA (tosylate), therefore exchange is slow. However, in figure 3.4b, when TsO^- anion was exchanged to dihydrogen phosphate, the peak intensity significantly decreased with number of CV scans and get stable after 25 cycles. This indicates tosylate anion were exchanged at a faster rate in phosphoric acid than that in phytic acid [88]. The smaller size of $H_2PO_4^-$ makes them easy to exchange bigger size TsO^- anion in PAni chain. This is due the existence of

'size memory effect' of PAni chains. This makes doping efficiency variable for different anions, hence, different CV curves for both PAni/pTSA and PAni/SA. In figure 3c & d, the PAni/SA coating shows same characteristics peaks in both phytic and phosphoric acid, respectively, similar to that of PAni/pTSA. In many reports the dopant anion for sulfuric acid in PAni chain was proved to be HSO_4^- instead of SO_4^{2-} [89,90].

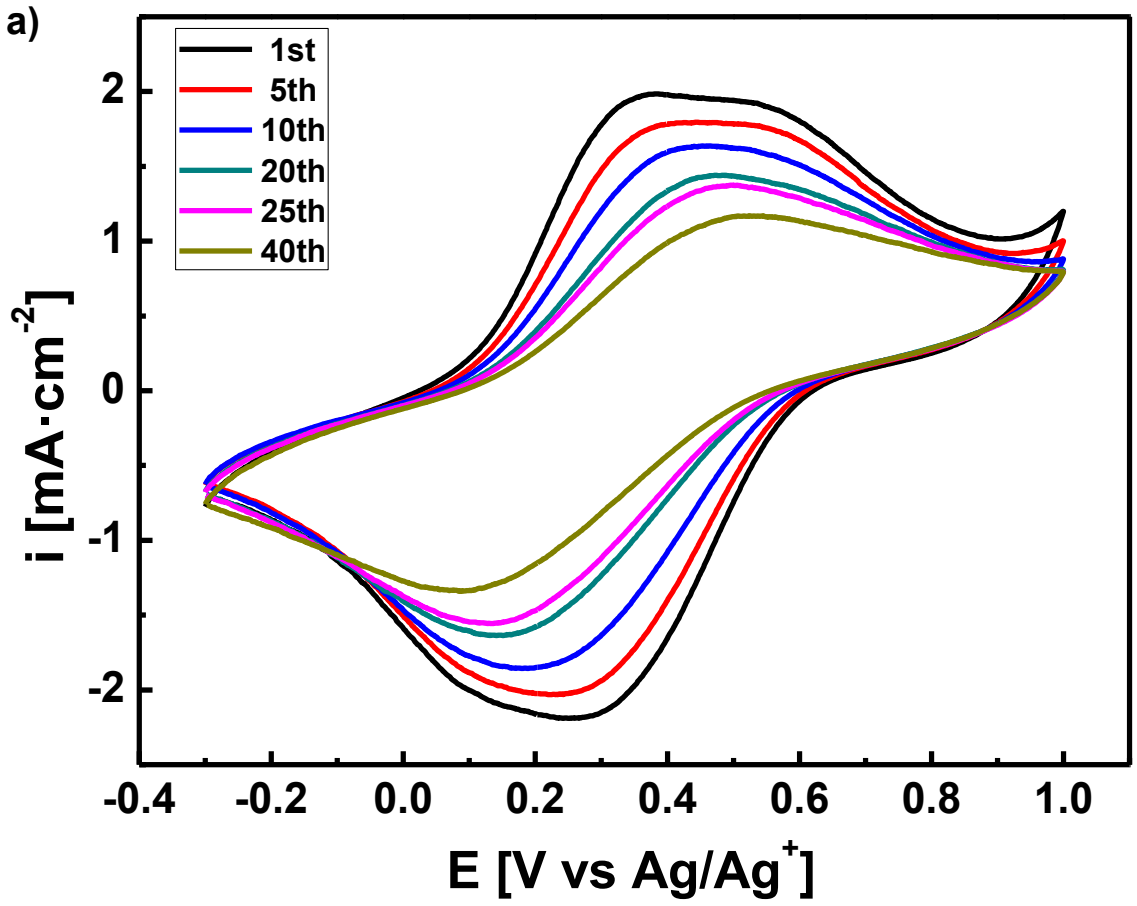

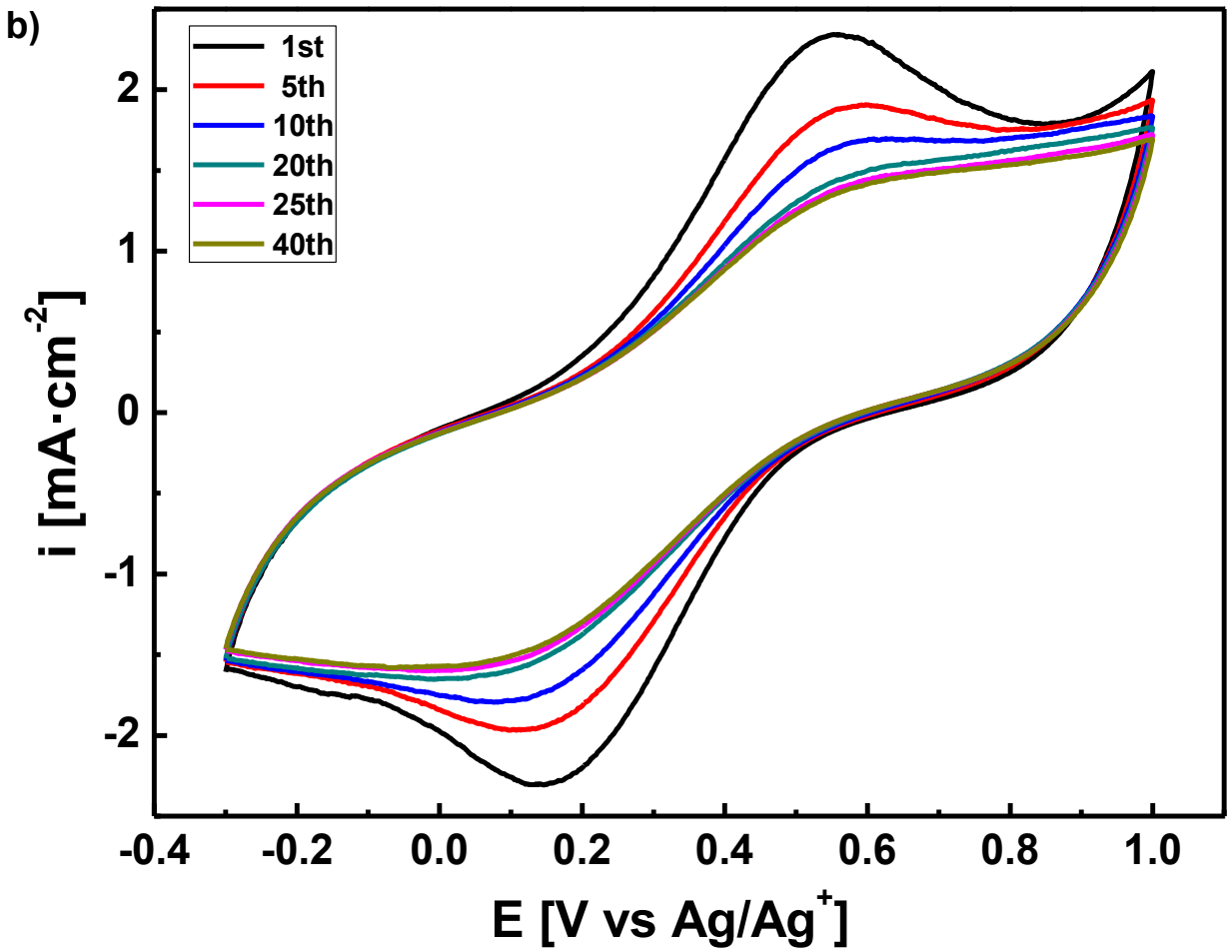
b)
1st
5th
10th
20th
25th
40th
i [mA·cm-2]
E [V vs Ag/Ag+]
2
1
0
-1
-2
-0.4
-0.2
0.0
0.2
0.4
0.6
0.8
1.0

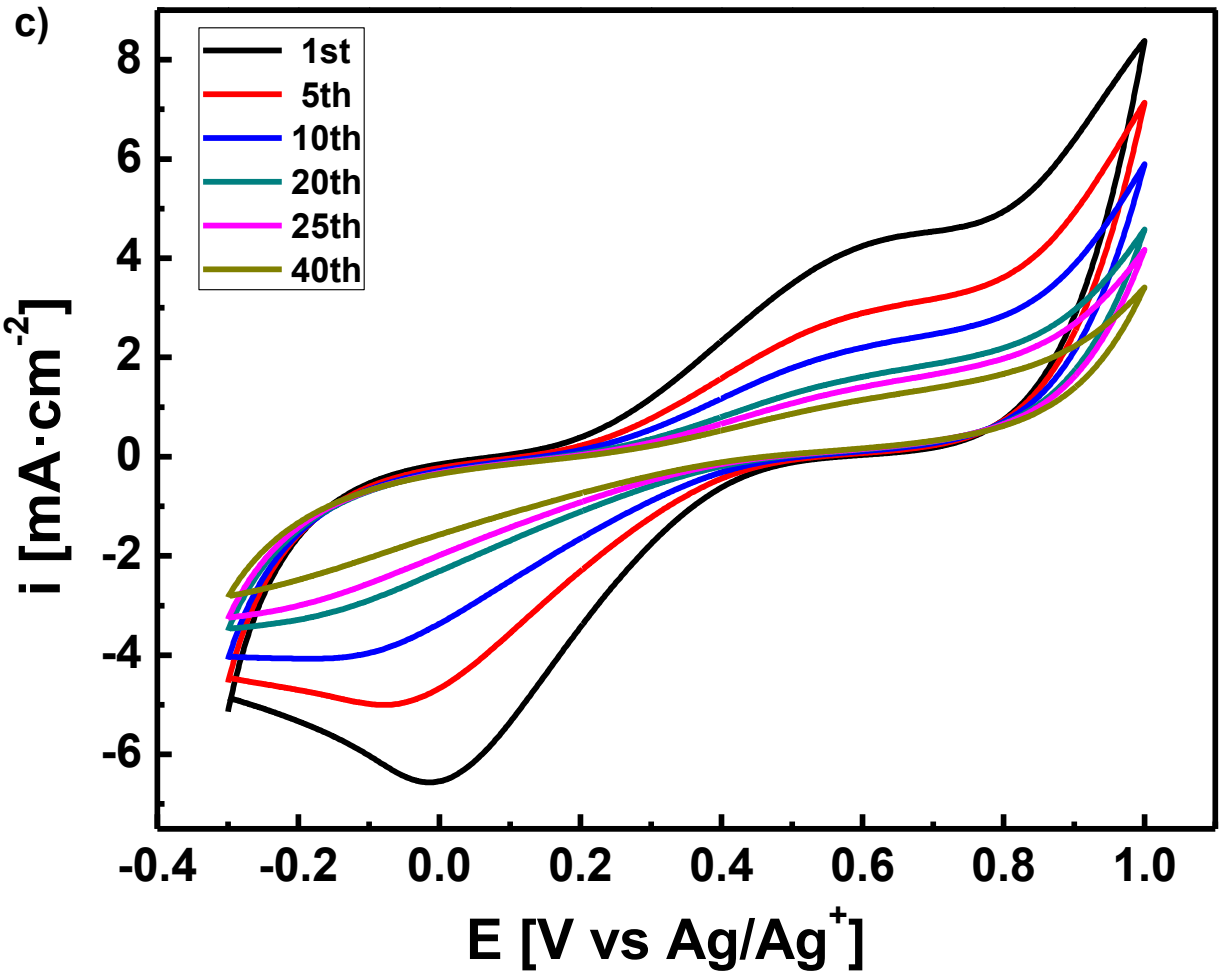
c)
1st
5th
10th
20th
25th
40th
i [mA·cm-2]
E [V vs Ag/Ag+]
8
6
4
2
0
-2
-4
-6
-0.4
-0.2
0.0
0.2
0.4
0.6
0.8
1.0

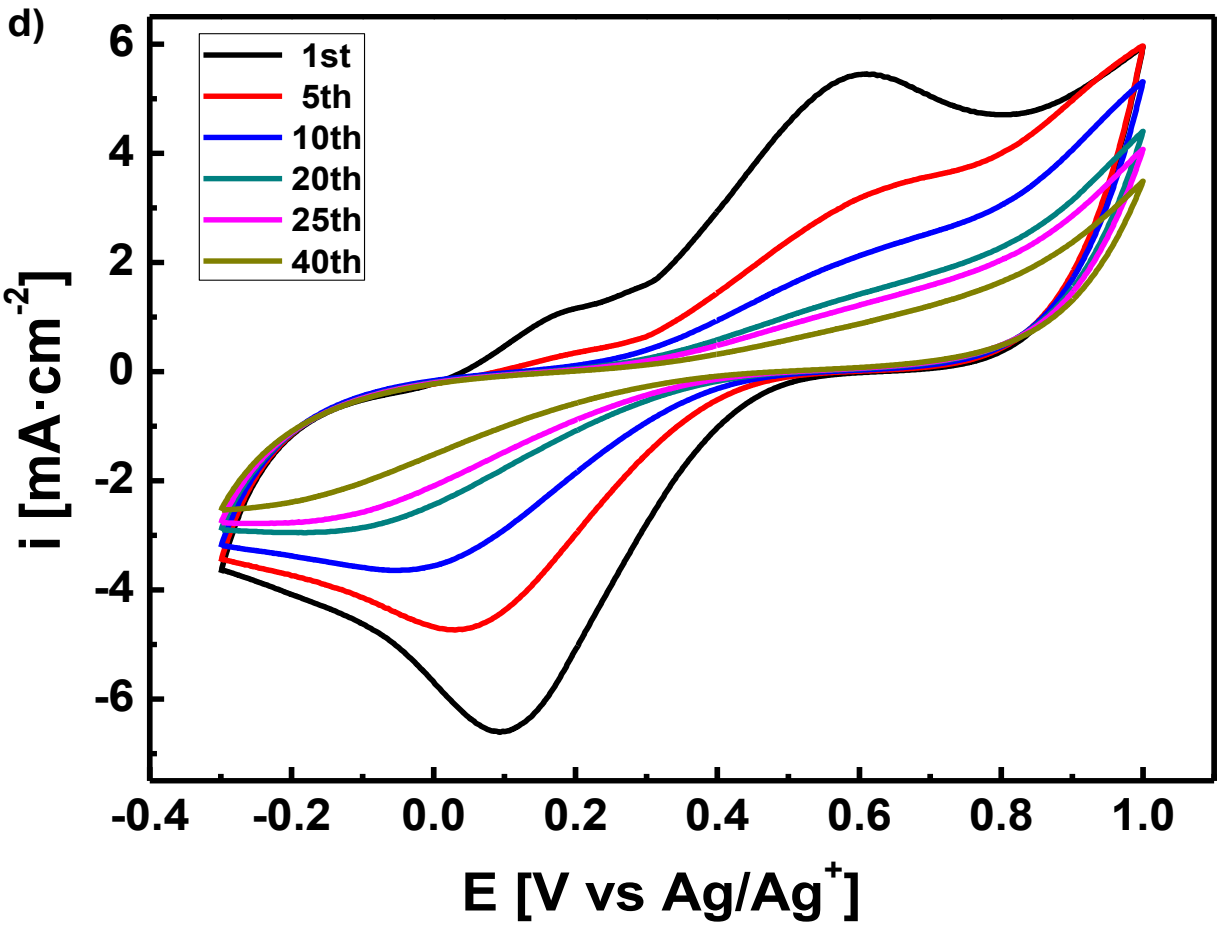

Figure 3.4 Cyclic voltammogram of PAni coating on SS for anion exchange from: a) p-TSA to PA, b) p-TSA to PhAc, c) SA to PA and d) SA to PhAc in their respective electrolyte solution.

On comparing phosphoric acid ($H_2PO_4^-$) and phytic acid anion, it was observed that peak current density at 0.6 V are highest in first cycle. This explains the easy release of hydrogen sulfate from PAni in phosphate solutions. The reduction peaks at 0-0.1V show the insertion of phosphates anion with intensity decreasing with increase in CV scans. In figure 3c, the reduction peaks diminish after 20^{th} scan, indicates exchange is slow and not complete after 20^{th} cycle in phytic acid. However, the exchange in phosphoric acid is noteworthy until 25^{th} cycle after which reduction

peak disappears. The explanation for this is the smallest size of dihydrogen phosphate ($H_2PO_4^-$) allows more phosphates to replace sulfate anions more easily due to size memory effect of PAni.

3.3.3 Electrochemical Impedance Spectroscopy (EIS). EIS is a useful technique to characterize conducting polymers electrodes in various application such as energy storage, sensors, corrosion protection etc. Based on impedance spectra obtained during exchange the equivalent circuit model was proposed as shown in figure 3.5. The ideal case capacitor (C) was replaced by constant phase element (Q) to obtain best fitting for the spectra with error of $1x10^{-12}$. The Q_1 is associated to electrical double layer forms at electrode/electrolyte interface, and Q_2 is due to pseudocapacitive behavior of redox PAni. The relation between Q and C can be understood as: $C=Q^n$ where values of n varies between 0 and 1 [91]. For ideal capacitor n=1 whereas for rough or porous electrodes such as conducting polymers, n<1.

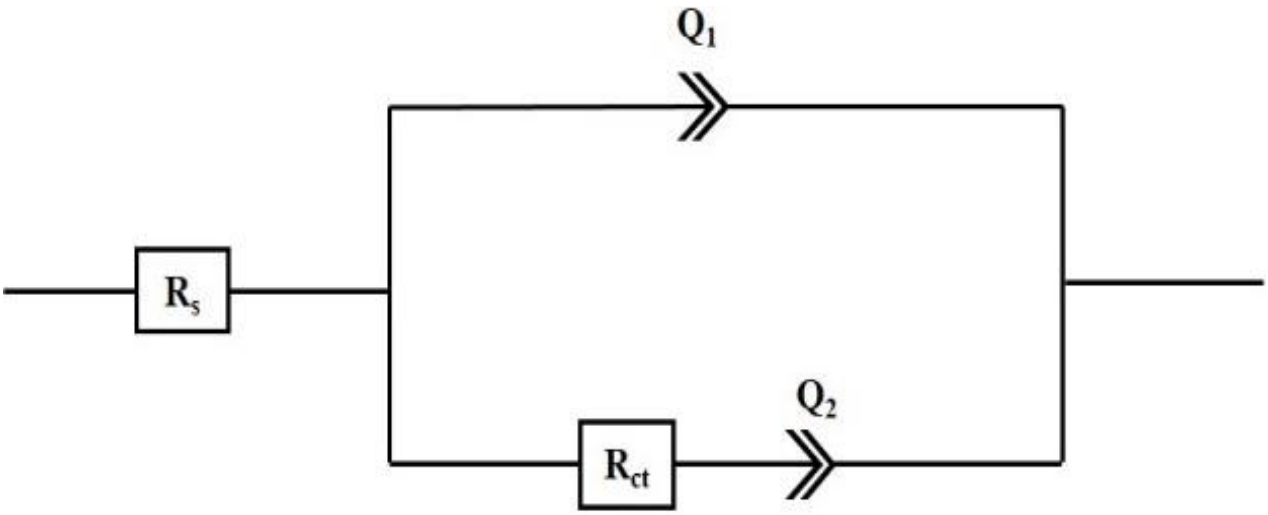

Figure 3.5 Equivalent circuit model for polyaniline coating on stainless steel for anion exchange

The impedance spectra of PAni coating on stainless steel to study anion exchange is shown in Figure 3.6. The charge transfer resistance has smallest value before anion exchange test, this shows PAni coating is in conductive state at the start and charge transfer is easier in phosphates solution. Further, this charge transfer resistance changes with CV scan indicating the different anion in PAni coating. This confirms the presence of phosphates in PAni. The large impedance value after exchange shows the increase in coating resistance. This indicates that exchange become difficult after every CV scan. Ideally, the vertical line at low frequency region indicates the capacitive behavior of the coating where it can store charge. However, small deviation from ideal capacitive line indicates the faradaic pseudocapacitive behavior of PAni.

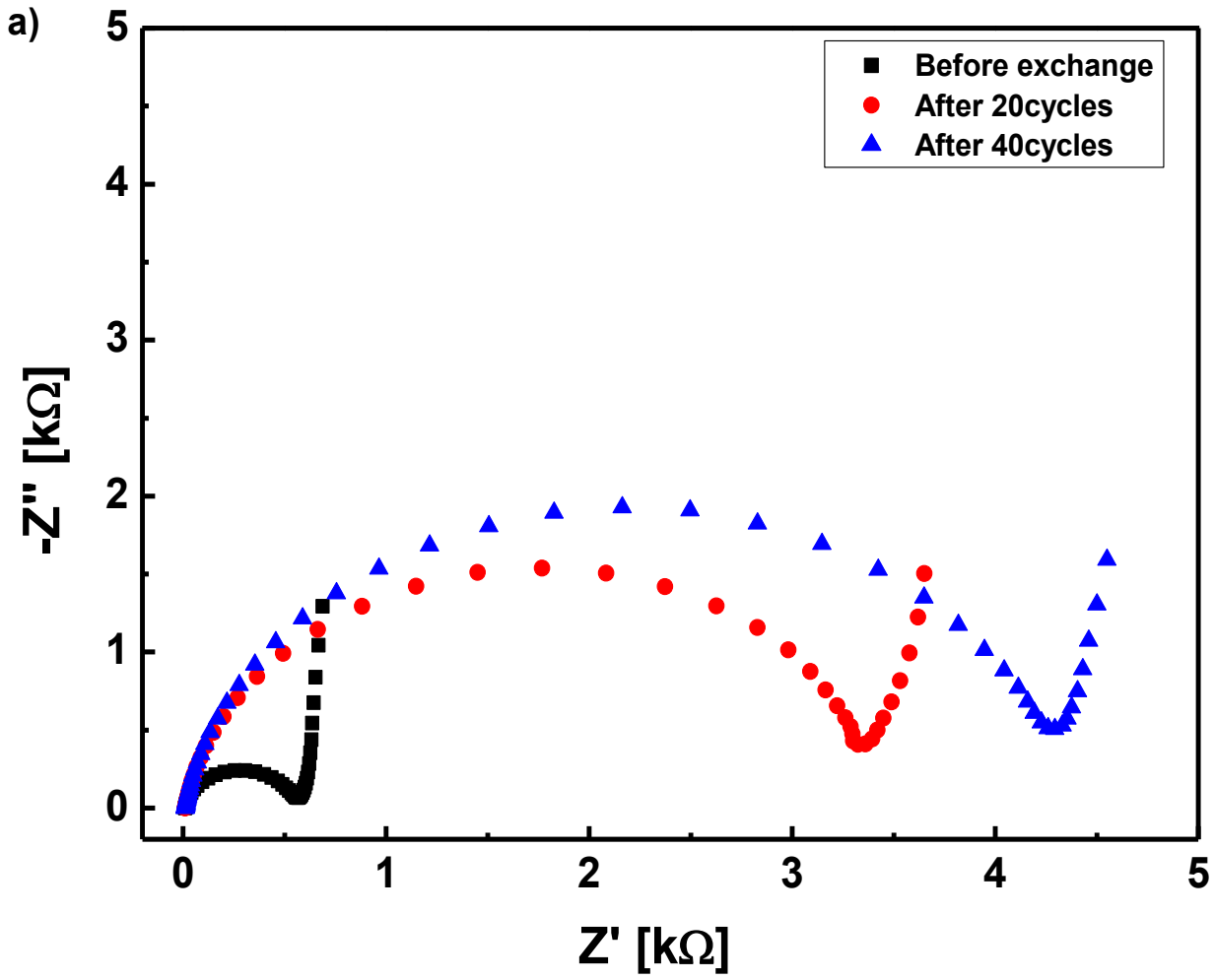

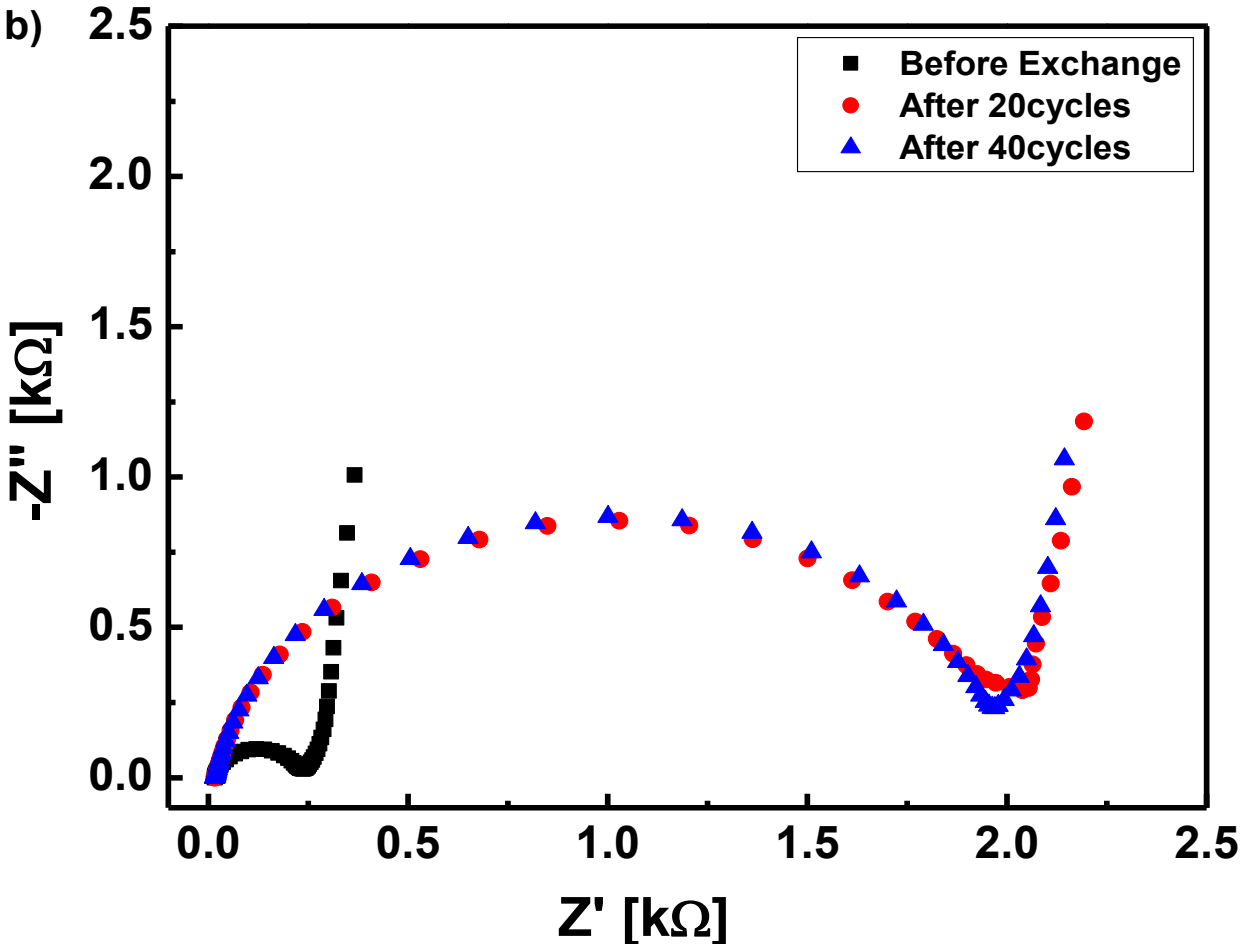
b)
Before Exchange
After 20cycles
After 40cycles
-Z'' [kΩ]
Z' [kΩ]
0.0
0.5
1.0
1.5
2.0
2.5

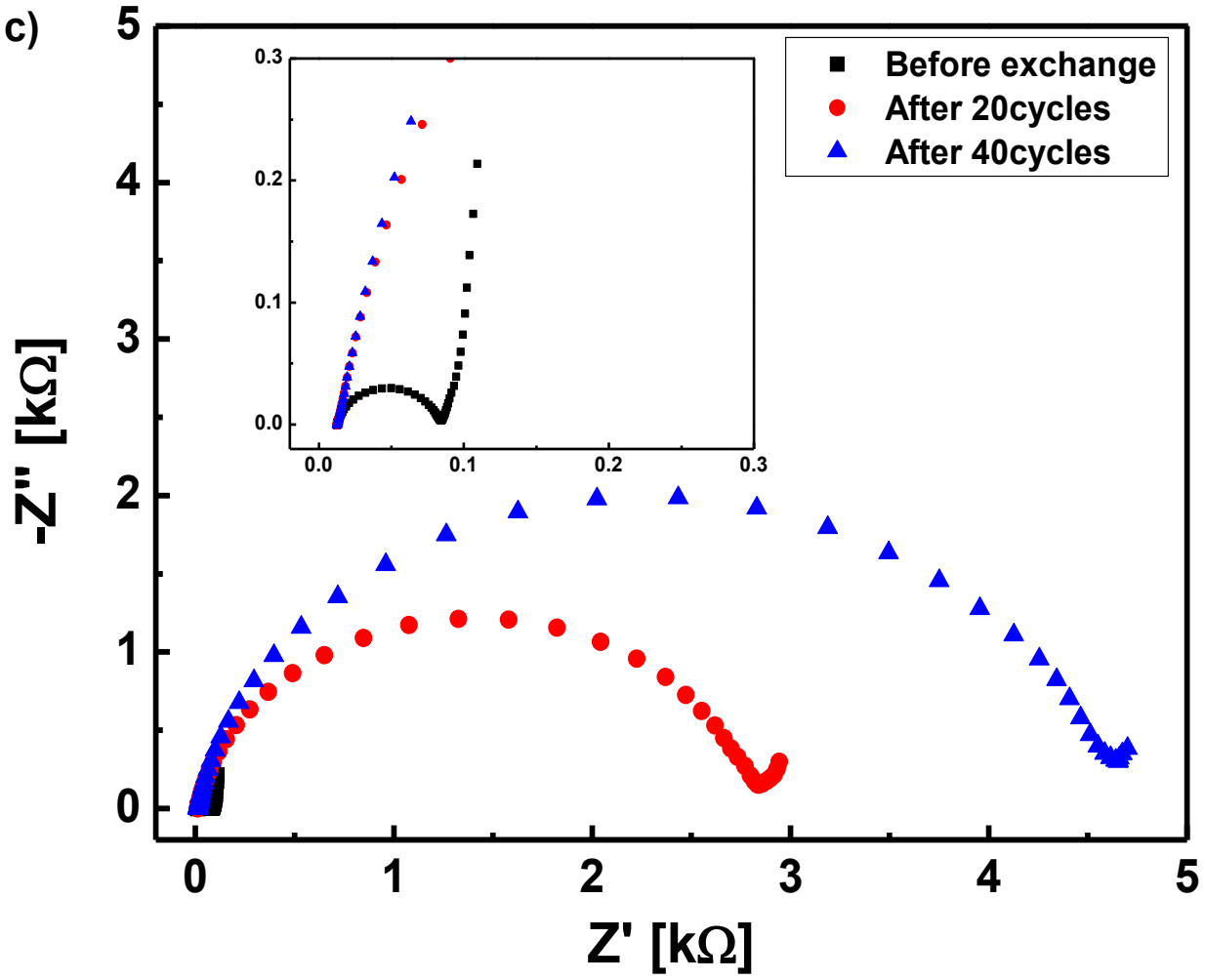
c)
-Z'' [kΩ]
Z' [kΩ]
Before exchange
After 20cycles
After 40cycles
0
1
2
3
4
5
0.0
0.1
0.2
0.3

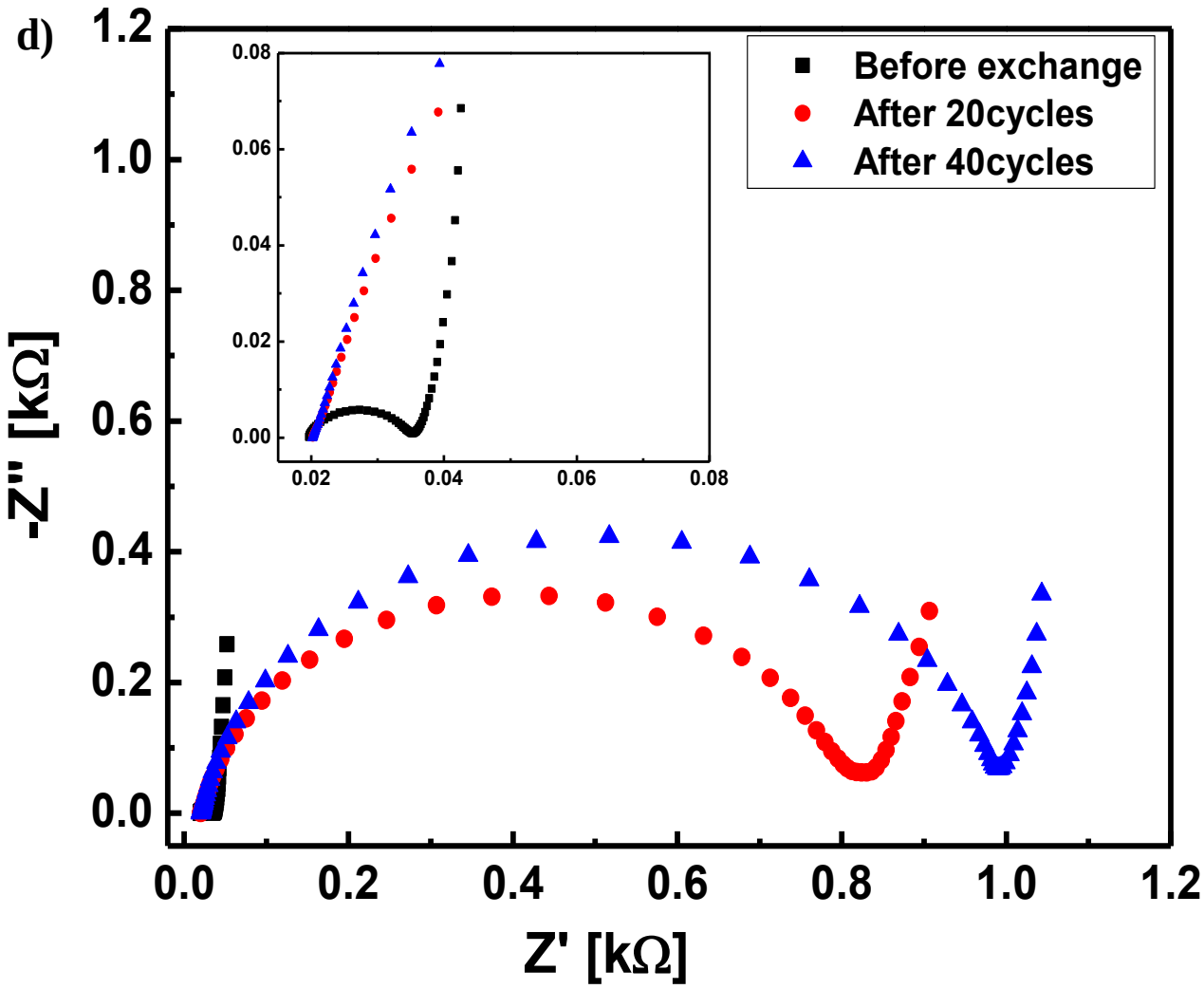

Figure 3.6 Impedance spectra of PAni coating on SS for anion exchange from: a) p-TSA to PA, b) p-TSA to PhAc, c) SA to PA and d) SA to PhAc in their respective electrolyte solution.

In Figure 3.6a & b, semi-circle is smaller in phosphoric acid electrolyte than in phytic acid. This is due to smaller size of dihydrogen phosphate ($H_2PO_4^-$) than phytic acid anion that can easily get transferred and exchange tosylate anions. Further, in figure 3.6a, after 40 cycles charge transfer resistance is larger than that after 20cycles. This shows that anion exchange was partial in phytic acid due to its bigger anion size. However, tosylate anions were easily exchanged to $H_2PO_4^-$ due

to its smaller anion size. The parameters obtained after simulation of PAni/pTSA coating are tabulated in table 3.1.

Table 3.1 Impedance parameters obtained after fitting of PAni/pTSA coating before and after exchange

	PAni/pTSA-PA						**PAni/pTSA-PhAc**					
	R_s (Ω)	Q_1 (μF)	n_1	R_{ct} (Ω)	Q_2 (mF)	n_2	R_s (Ω)	Q_1 (μF)	n_1	R_{ct} (Ω)	Q_2 (mF)	n_2
Before exchange	11.65	30.40	0.92	560.5	9.90	0.92	16.81	33.73	0.90	226.2	11.20	0.87
After 20cycles	11.75	35.19	0.92	3425	8.44	0.91	17.23	53.51	0.89	2015	10.12	0.89
After 40cycles	11.68	31.24	0.91	4352	8.21	0.92	17.16	34.88	0.90	1993	11.66	0.91

Similar behavior of anion exchange was observed when PAni/SA coating were used to exchange HSO_4^- to phytic acid and $H_2PO_4^-$ anion (Fig. 3.6c & d). The bigger semi-circle after exchange indicates the large coating resistance provided by PAni coating. This shows the exchange is difficult due to larger anion size of phytic acid, which is why there is very little capacitive behavior in low frequency region. The large coating resistance, phytic acid anion size and little or no capacitive behavior of the coating indicates the partial exchange of hydrogen sulfate to phytic acid. The EIS results agrees with our CV data where exchange is getting slower after each cycle. The parameters obtained after fitting of PAni/SA coating are tabulated in table 3.2.

Table 3.2 Impedance parameters obtained after fitting of PAni/SA before and after exchange

	PAni/SA-PA						PAni/SA-PhAc					
	R_s (Ω)	Q_1 (μF)	n_1	R_{ct} (Ω)	Q_2 (mF)	n_2	R_s (Ω)	Q_1 (μF)	n_1	R_{ct} (Ω)	Q_2 (mF)	n_2
Before exchange	12.67	45.65	0.88	72.23	56.57	0.89	19.44	104.9	0.78	16.58	52.26	0.94
After 20cycles	12.87	48.82	0.91	2812	29.46	0.72	20.62	55.31	0.89	799.1	30.73	0.81
After 40cycles	12.85	37.59	0.91	4542	37.52	0.94	20.53	36.89	0.90	980.8	37.07	0.91

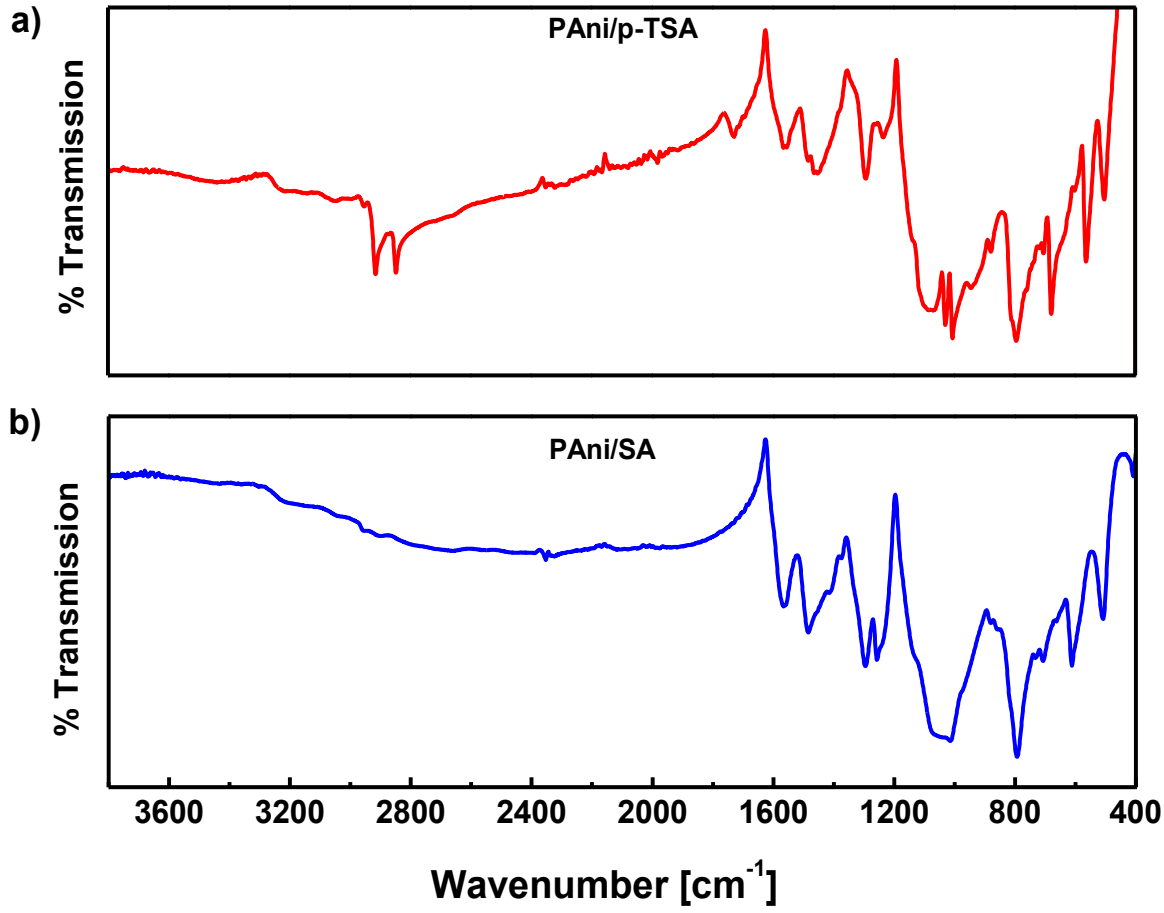

Figure 3.7 Comparison of FT-IR spectra of polyaniline coating on stainless steel doped with: a) p-TSA and b) SA.

3.3.4 FT-Infrared characterization. The FT-infrared spectra of p-TSA and SA doped polyaniline was recorded within frequency range of 4000-400 cm^{-1} and is shown in figure 3.7. The spectra showed all signature peaks for polyaniline with quinoid (Q), benzene (B) ring stretching and their combinations were observed (Table 3.3). The double peaks at 1225 and 1280 cm^{-1} corresponds to $-NH^{+}=$ and $C-N^{+\cdot}$ stretching that attributes to conductive polyaniline [92]. This was further corroborated by the presence of S=O stretching peaks around 1000-1100cm^{-1} that corresponds to tosylate and hydrogen sulfate (HSO_4^-) dopant anion in the polymer. Further, the broad peak at 1070cm^{-1} was observed that corresponds to C-H stretching of quinoid ring and stretching vibration of dopant anion. This peak is broader in PAni/p-TSA than that in PAni/SA this is due to the high density of delocalized electrons in p-TSA [93].

Table 3.3 FT-IR band assignment of PAni doped with p-TSA and SA

Peak assignment	**Peak positions (cm^{-1})**	
	PAni/pTSA	PAni/SA
C-H stretching	2916	-
	2846	-
C-H bending (aromatic from dopant)	1723	-
C=C stretching from quinoid-ring	1561	1567
C=N stretching with C-H bending of benzene ring	1489	1488
S=O from sulfate dopants	1074	1072
	1013	1009

Figure 3.8 shows comparison of FTIR spectra of polyaniline coating on stainless steel after anion exchanged from sulfates to phosphates. In figure 3.8a & b, all the peaks associated to polyaniline are present. The only peak differences were observed at 1000-1100cm^{-1} due to the presence of different dopant anion; phytic acid (figure 3.8a) and dihydrogen phosphate (figure 3.8b). The intensity and shape of the peak corroborates the exchange of anion from sulfates to phosphates. In figure 3.8a, the strong peak at 1150cm^{-1} with a shoulder at 1050cm^{-1} corresponds to asymmetric P-O stretching present in phytic acid [94]. The presence of phytic acid in PAni coating was further substantiated by doublet of C-H stretching from alkanes (Table 3.4). In figure 3.8a & b, the peak for sulfate in PAni/pTSA spectra changes from broad to sharp when anions were exchanged to phosphates indicating the change in anion due to different stretching vibration in IR signals for different anion present in PAni chain. The absence of C-H stretching peak in PAni/pTSA-PhAc (figure 3.8b) showed the exchange of tosylate by dihydrogen phosphate ($H_2PO_4^-$) anion.

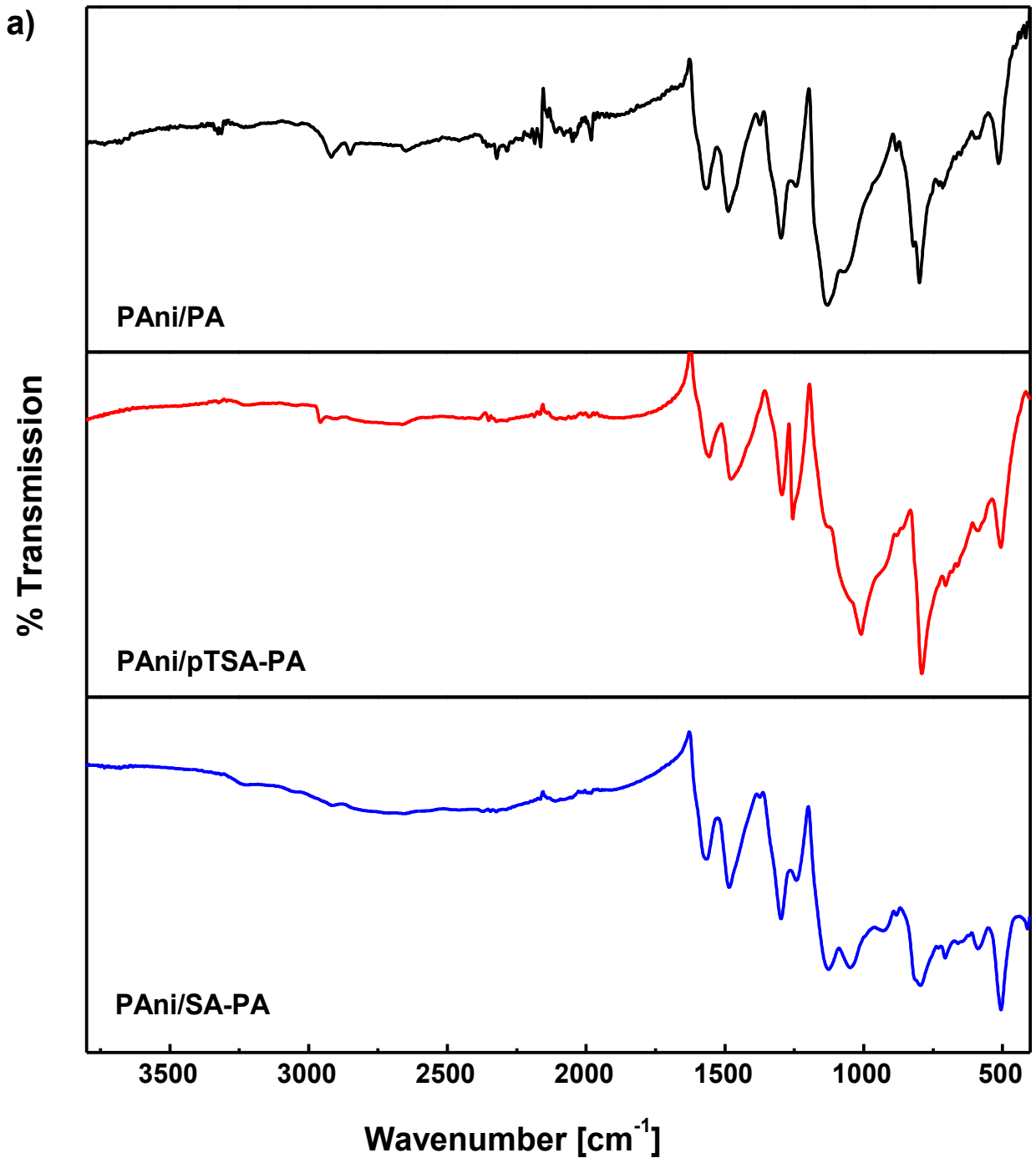
a)
PAni/PA
PAni/pTSA-PA
PAni/SA-PA
% Transmission
3500
3000
2500
2000
1500
1000
500
Wavenumber [cm-1]

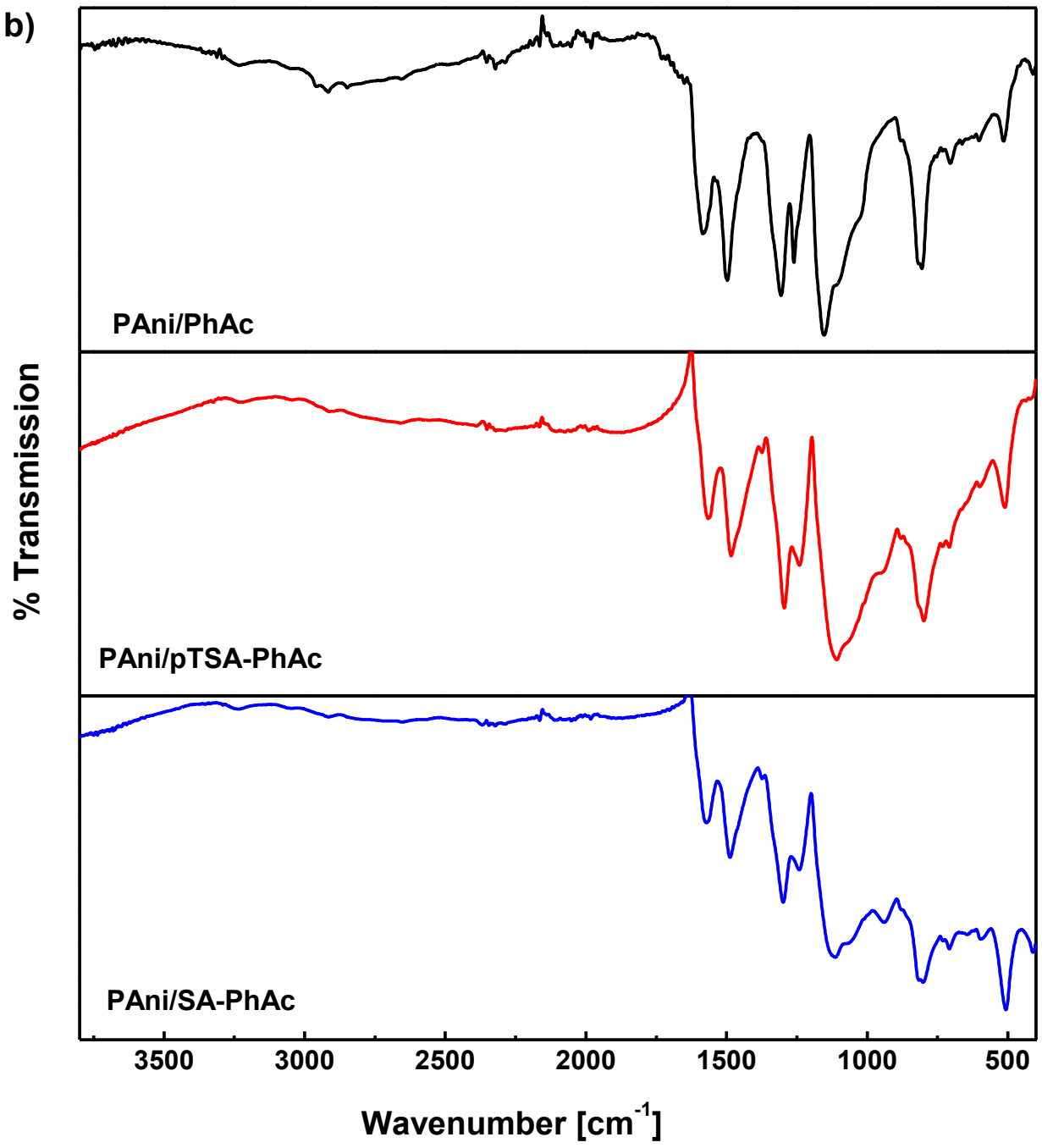

Figure 3.8 Comparison of FT-IR spectra of polyaniline coating on SS when dopants (p-TSA and SA) were exchanged to: a) PA and b) PhAc.

Similarly, for PAni/SA has broad sulfate peak ~1000cm^{-1}, this peak split into three peaks at 1100, 1050, 922cm^{-1} that corresponds to P-O stretching vibration from the phosphates indicating the exchange of sulfates in PAni (Figure 3.8a & b). Further, peaks in 400-600cm^{-1} region corresponding to O-P-O bending vibrations corroborated the presence of phosphate anion in the PAni coating.

Table 3.4 FT-IR band assignment of PAni with anion exchanged to phosphates

Peak assignment	**Peak position (cm^{-1})**					
	PAni/PA	**PAni/pTSA-PA**	**PAni/SA-PA**	**PAni/PhAc**	**PAni/pTSA-PhAc**	**PAni/SA-PhAc**
C-H stretching	2929	2959	-	-	-	-
	2840	2900	2915	-	-	-
C=C stretching (Q)	1569	1563	1569	1586	1570	1576
C=N stretching (Q) with C-H bending (B)	1483	1472	1483	1495	1490	1490
P-O stretching	1127	1143	1127	1153	1110	1115
	1057	1008	1041	1089	1046	1051
		922	922	1008	938	938
O-P-O bending	583	583	583	596	591	602
	513	503	502	511	511	506

3.3.5 Coating Morphology. Figure 3.9 showed the SEM images of polyaniline coating doped with sulfuric acid and HSO_4^- anion exchanged to phytic acid and $H_2PO_4^-$ anion. The sulfuric acid doped PAni have fibrillar and porous morphology (Fig. 3.9a) whereas p-TSA doped polyaniline has more uniform and compact coating with little granules on steel (Fig. 3.9d). This is due to benzene ring present in p-TSA that creates a lamellar structure by π-π stacking within the molecule. As shown

in figure 3.9b & c, when hydrogen sulfate anion was exchanged to phosphates anion, there is little or no effect on morphology of PAni coating. The porous structure of PAni/SA was slightly reduced when phytic acid was used to exchange sulfate (Fig. 3.9b). This is due to bigger size of phytic acid anion and its tendency to adsorb on steel surface. However, coating looks more porous when HSO_4^- was exchanged to $H_2PO_4^-$ due to smaller anion size of phosphoric acid anions. This porous coating does not affect anticorrosion performance of PAni because of inhibiting property of phosphoric acid. In case of PAni/p-TSA, coating morphology changed from uniform and compact to non-uniform and less compact. This is due to absence of benzene ring in phosphate dopants that result in more irregular morphology (Fig 3.9e & f). The lines in coating are steel ridges resulting from sanding (Fig 3.9 d-f).

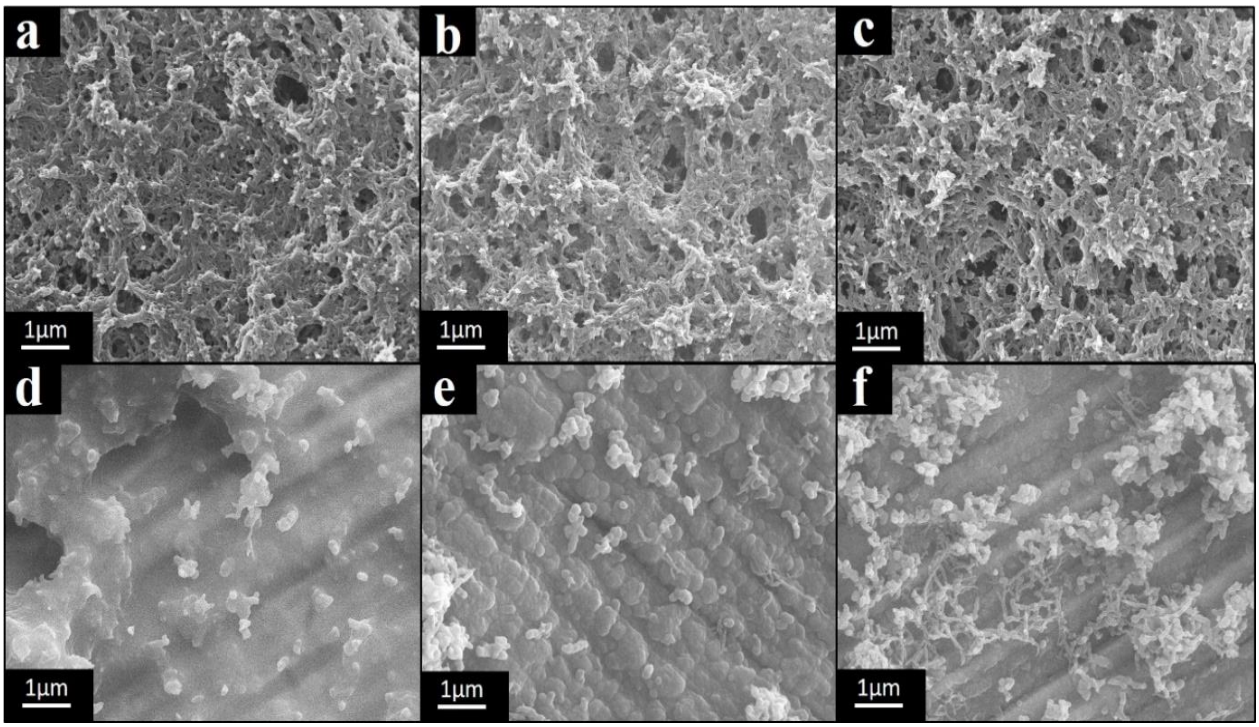

Figure 3.9 SEM images of PAni coating on stainless steel: a) PAni/SA, b) PAni/SA-PA, c) PAni/SA-PhAc, d) PAni/pTSA, e) PAni/pTSA-PA and f) PAni/pTSA-PhAc.

3.3.6 Anticorrosive properties. The corrosion protection performance of PAni coating depends on the type of dopants used and its size because large size anions along with polymer chain provide barrier protection to the metal. Figure 3.10 showed the anticorrosion performance of polyaniline coating when sulfate anions were exchanged to phytic acid (Fig. 3.10a) and phosphoric acid (Fig. 3.10b). On comparing sulfates, the corrosion potential of polyaniline coating has increased by 100mV when doped with p-TSA than that of SA. This is due to compact and uniform coating was produced when p-TSA was used as a dopant for polyaniline. Additionally, lamellar structure was formed by π-π stacking of benzene ring in p-TSA molecule preventing ingress of chloride ions in the coating. The presence of benzene ring also increases the electron density in coating thus repelling negatively charged chloride ion. However, the corrosion potential of polyaniline coating showed significant increase when sulfate anion from PAni were exchanged to phosphates. In figure 3.10a, hydrogen sulfate and tosylate from PAni were exchange to phytic acid anion, both coatings (PAni/pTSA-PA and PAni/SA-PA) showed equal corrosion potential of 0.23 V. This corrosion potential after exchange is 80mV and 200mV more positive than PAni/pTSA and PAni/SA, respectively. Nevertheless, the corrosion potential of PAni coating after exchanging sulfate anion to phytic acid anion is lower than PAni/PA by 70mV. The possible explanation is phytic acid anion is bigger than tosylate and HSO_4^-, the anion exchange in this case is considered as partial. Figure 3.10b shows corrosion test performed on PAni coating with anions (SA and p-TSA) were exchange to phosphoric acid. The corrosion potential of coating after sulfates were exchange to $H_2PO_4^-$ is 0.19V. The E_{corr} after exchange equals the corrosion potential of PAni/PhAc this is because of smallest anion size of $H_2PO_4^-$ of all the dopants used. This showed the complete exchange of sulfates from PAni to dihydrogen phosphates. The corrosion potential showed significant increase when sulfate anions were exchanged because phosphates have tendency to inhibiting corrosion by

forming chemical conversion film on steel. This film comprises of various oxide and iron phosphate that prevent corrosive attack on steel.

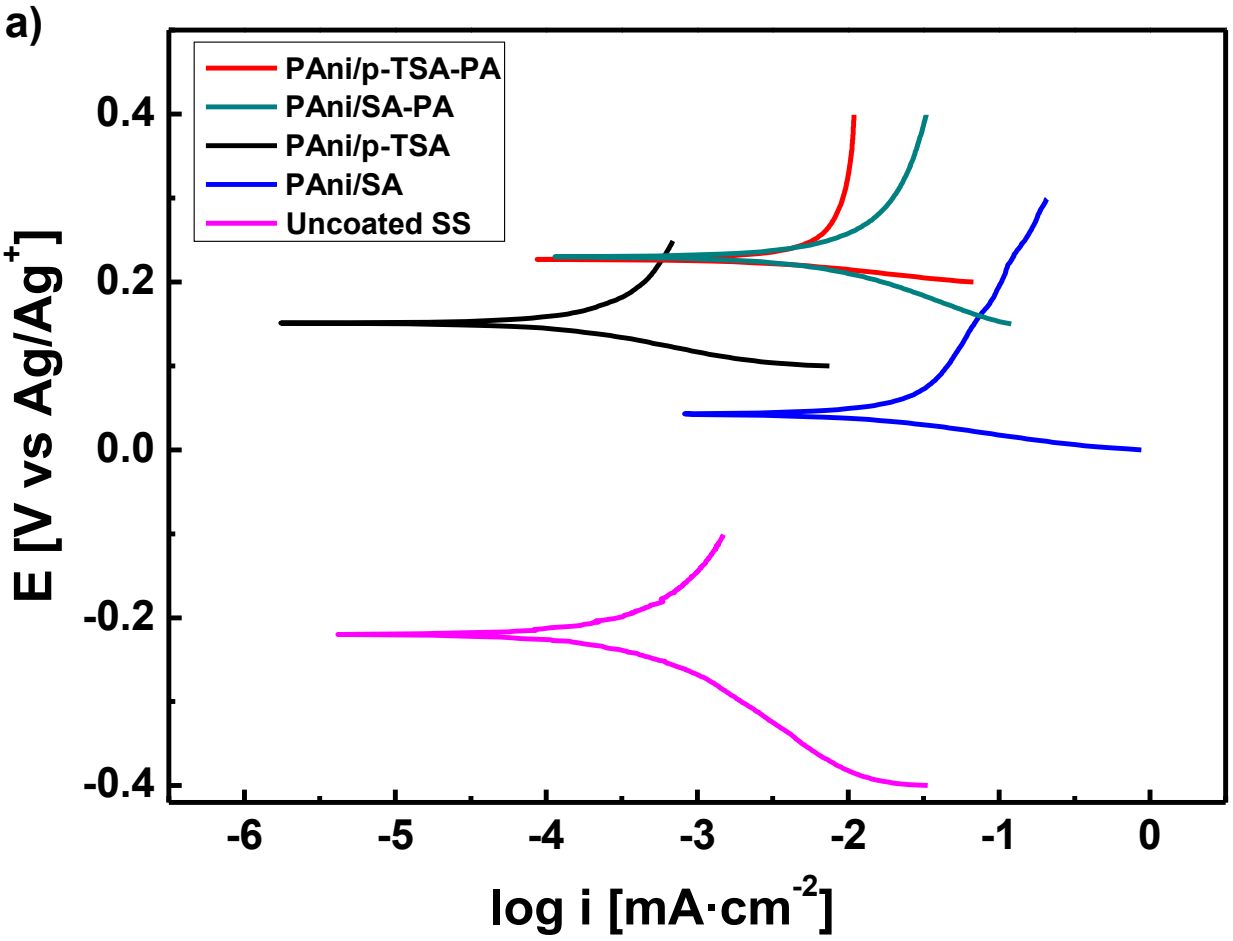

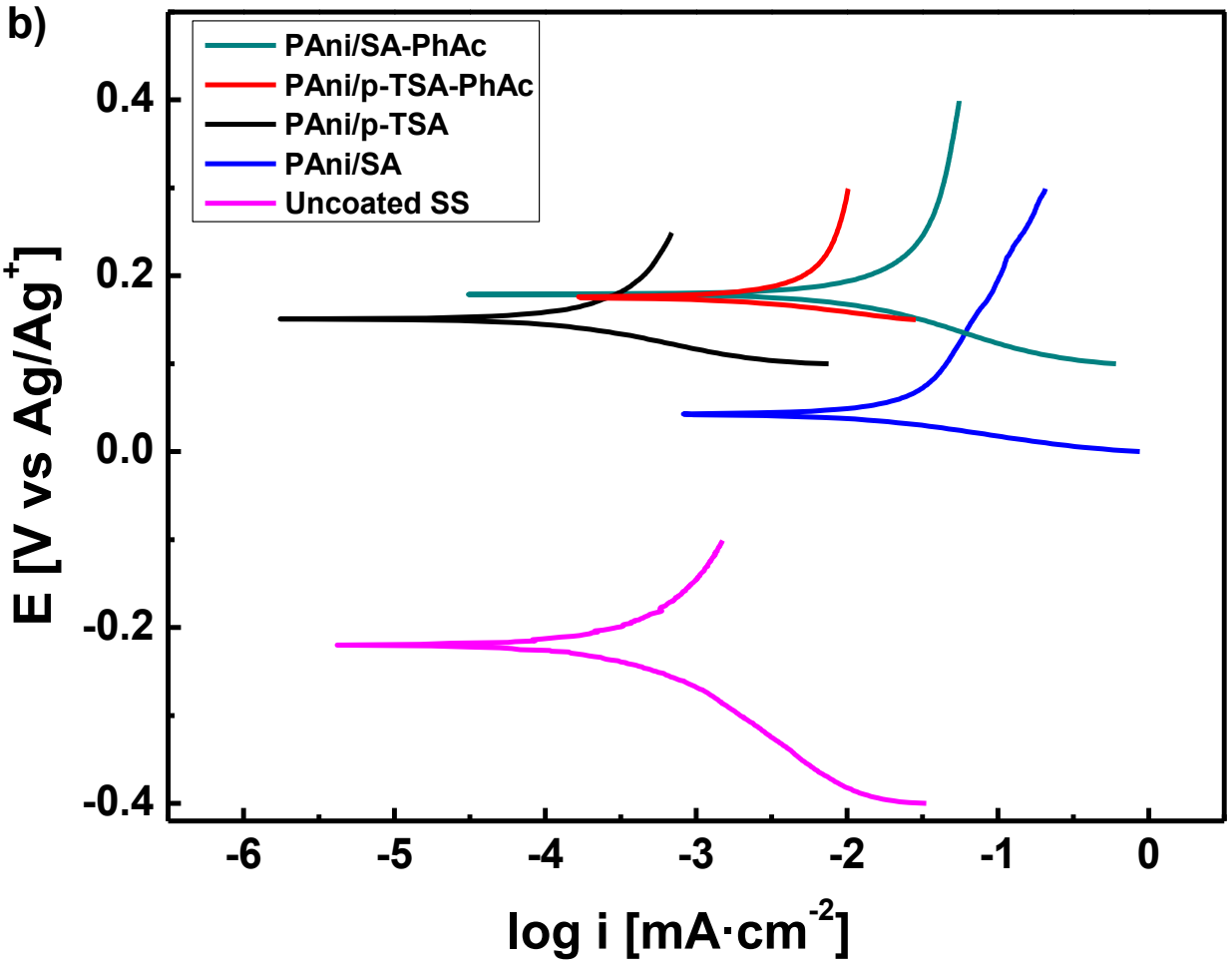
b)
PAni/SA-PhAc
PAni/p-TSA-PhAc
PAni/p-TSA
PAni/SA
Uncoated SS
E [V vs Ag/Ag+]
0.4
0.2
0.0
-0.2
-0.4
-6
-5
-4
-3
-2
-1
0
log i [mA·cm-2]

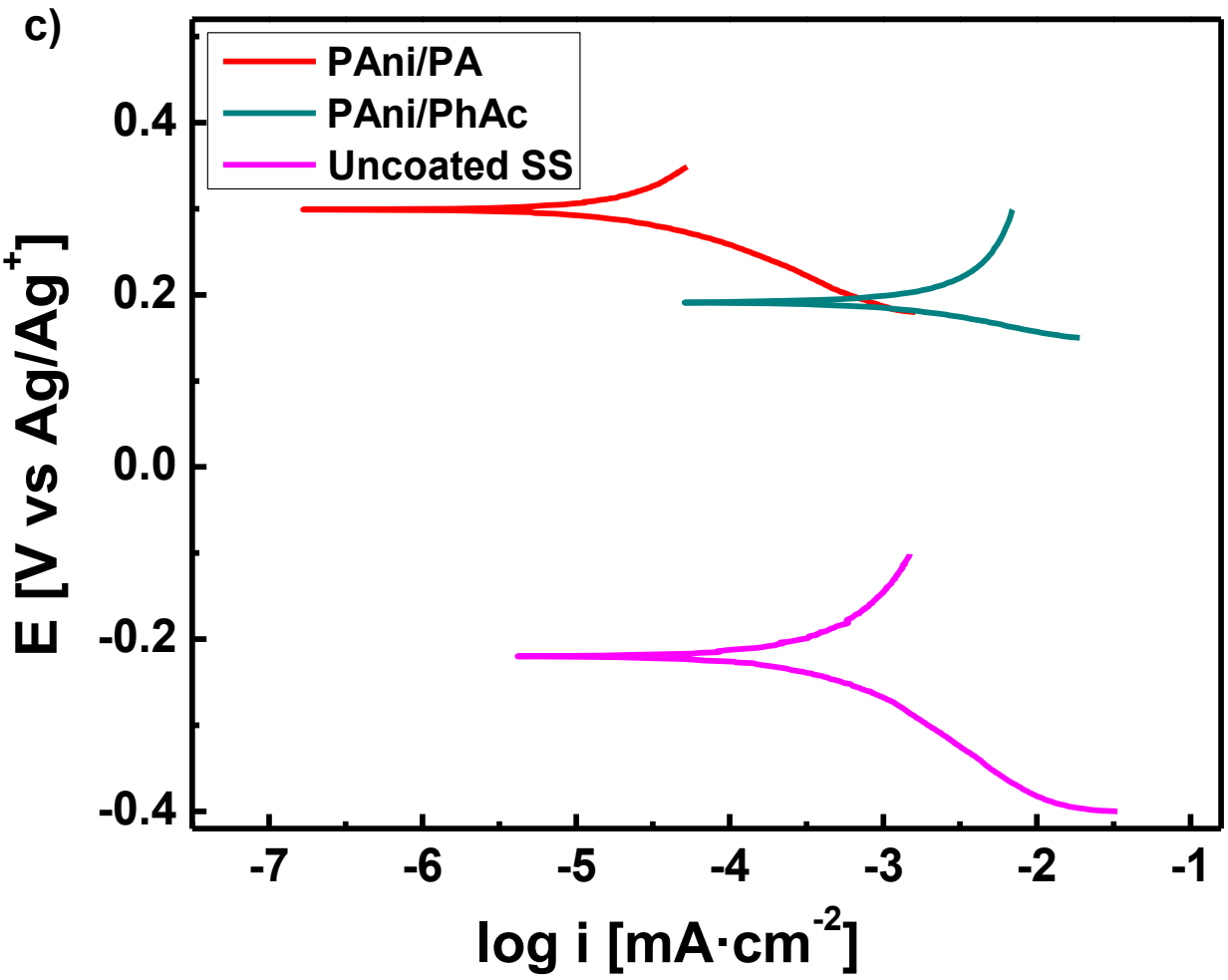

Figure 3.10 Tafel curves of PAni coating in 3.5% NaCl before and after exchange of anions to: a) phytic acid, b) phosphoric acid and c) comparison of PAni coating doped with phosphoric and phytic acid.

3.3.7 Quantifying Anion exchange. The charge accumulated in the polymer during the electropolymerization can be calculated from chronoamperometric curves. This charge can be used to calculate the number of redox sites in polyaniline coating using equation [95]:

$$N_r = \frac{Q_t}{n\,F}$$

Where N_r is number of redox sites (mol) in the polymer, Q_t is total charge consumed during electropolymerization of the polymer (510mC for PAni/SA and 114mC for PAni/pTSA), n (=2.3) is number of electron transferred per aniline monomer [96,97] and F is faraday constant. The maximum charge (Q_{max}) that was produced during anion exchange can be calculated by:

$$Q_{max} = \frac{Q_t\,(z)}{n}$$

Where z (=1) is the number of electron produced during anion exchange.

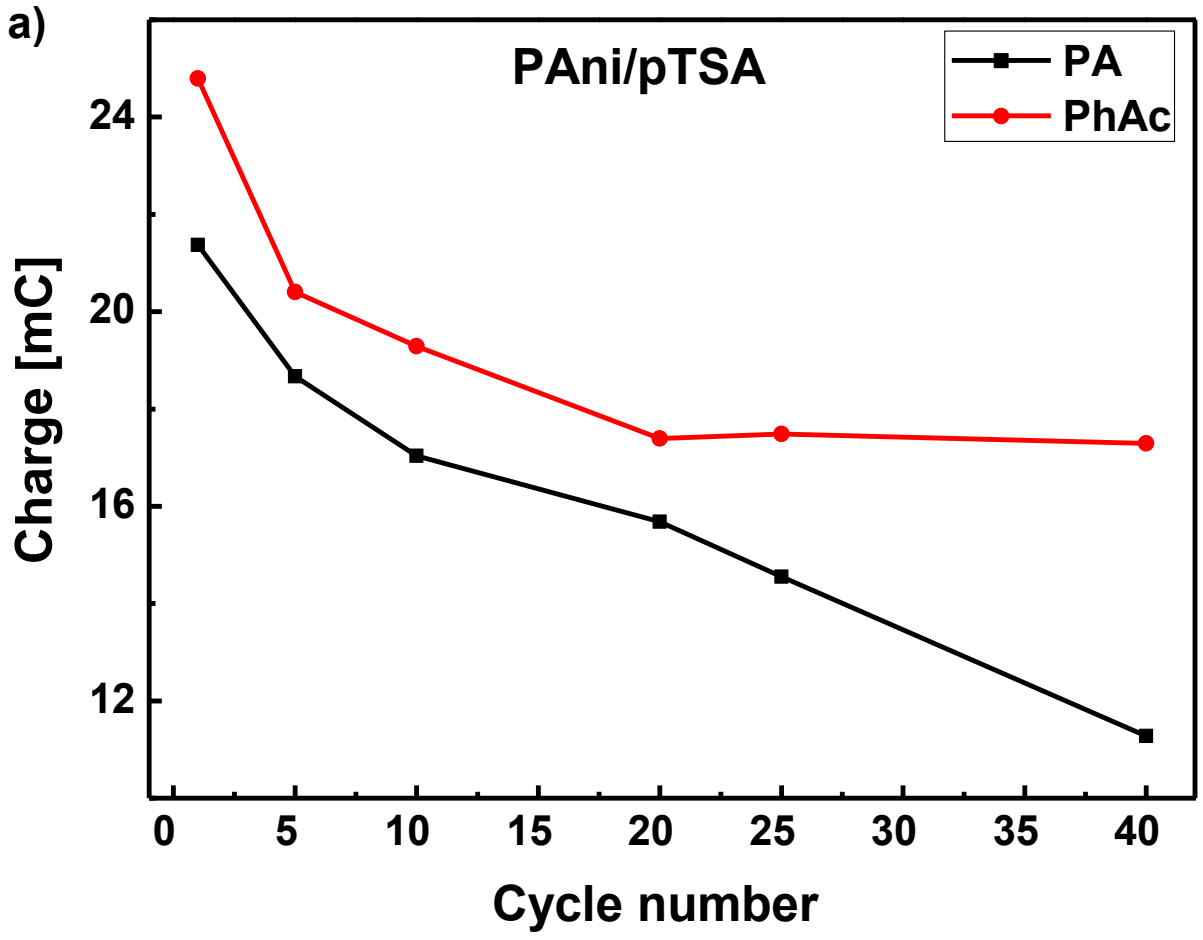

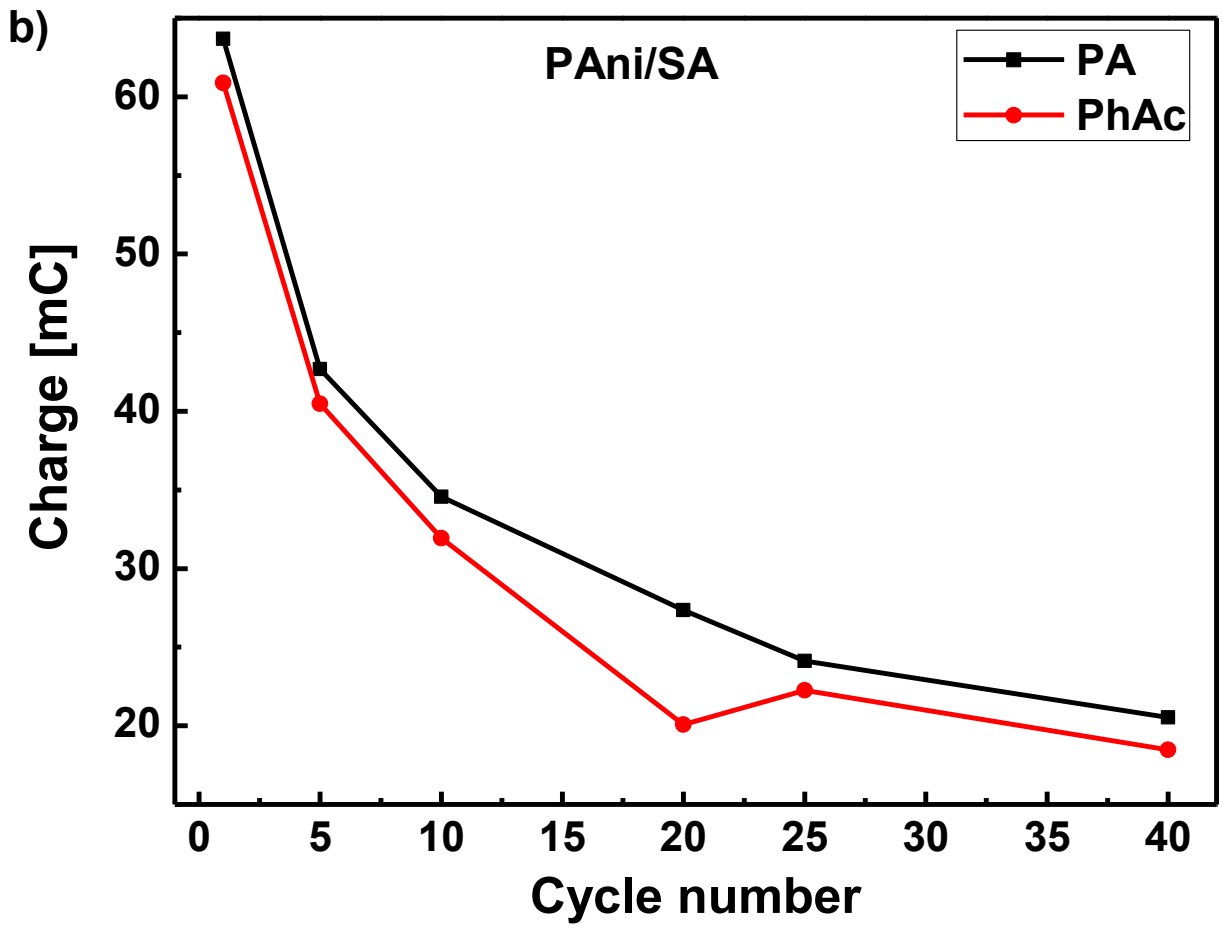

Figure 3.11. Maximum charge accumulated in PAni coating during the process of anion exchange in their respective electrolyte solutions

This maximum charge can be used to calculate the accessibility coefficient (A) that tells the number redox sites that were accessible during the exchange, given by:

$$A = \frac{Q_c}{Q_{max}}$$

Q_c is the maximum charge accumulated in the polymer during process of anion exchange.

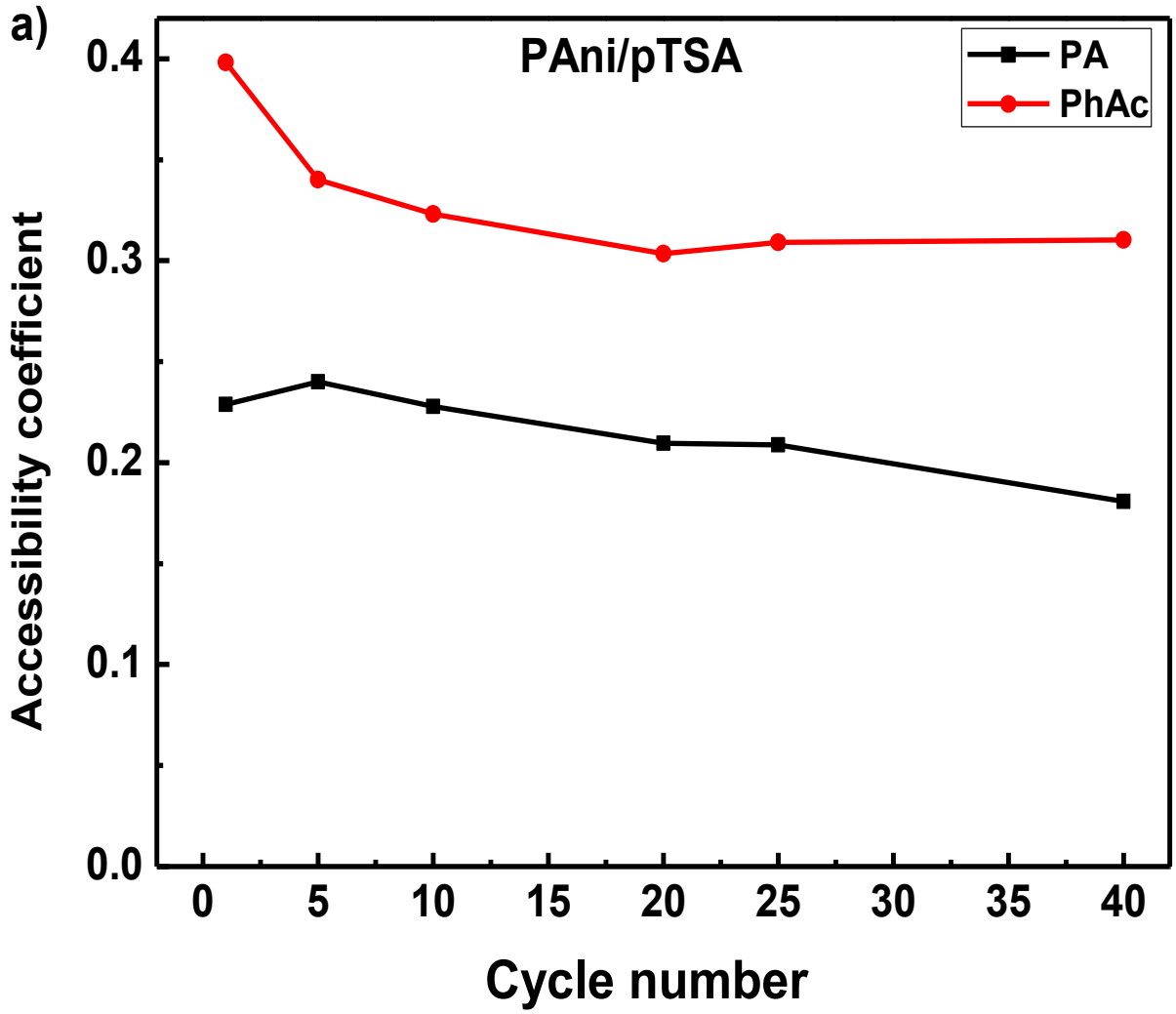
a)
PAni/pTSA
PA
PhAc
Accessibility coefficient
0.0
0.1
0.2
0.3
0.4
0
5
10
15
20
25
30
35
40
Cycle number

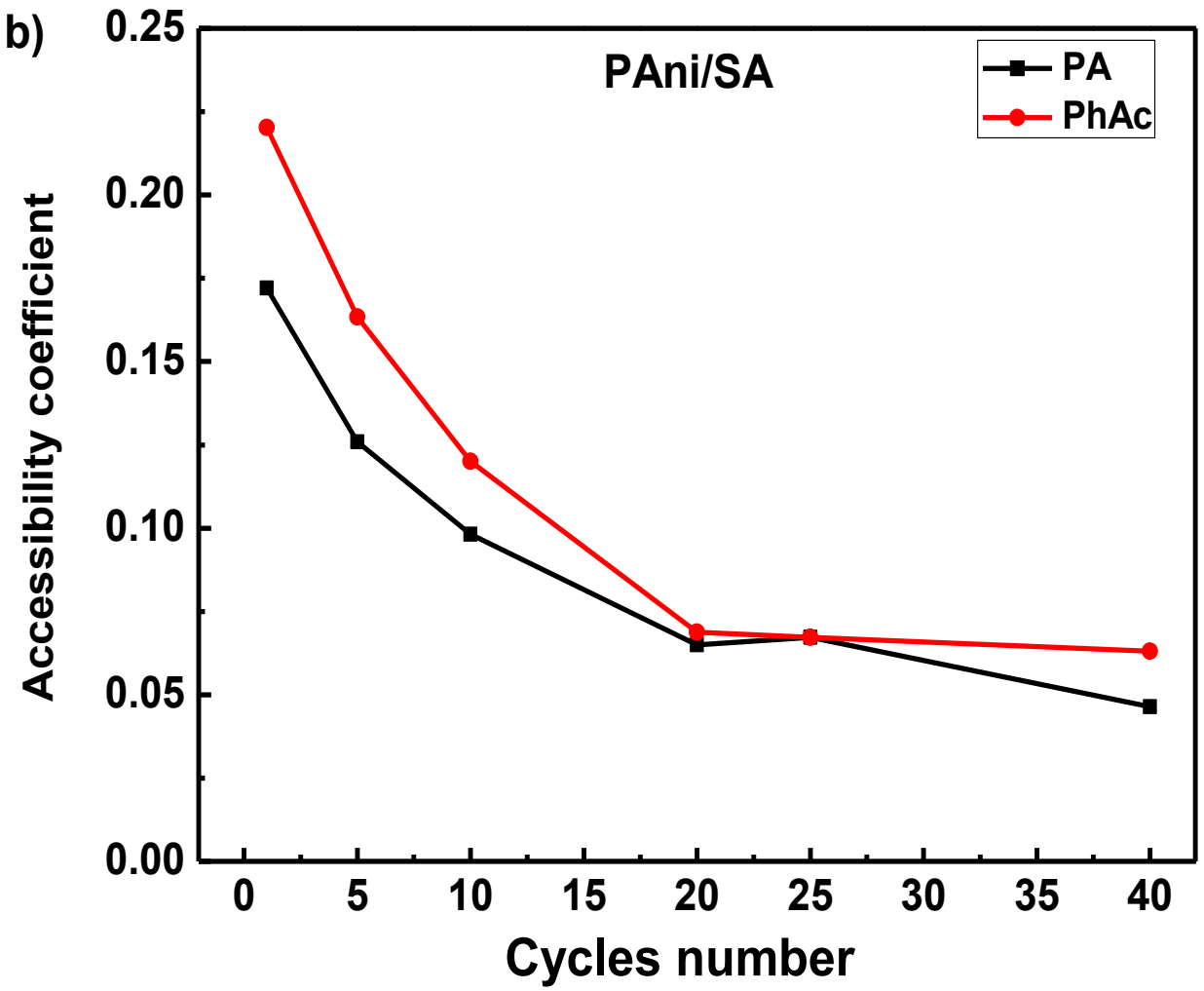

Figure 3.12 Number of redox sites accessible in PAni coating during the exchange in their respective electrolyte solution.

In figure 3.11, the maximum charge accumulated during the anion exchange is more in PAni/SA than that of PAni/pTSA and decreases with increase in number of CV scans. This indicates the slow exchange in PAni/pTSA with increasing cycling, hence more redox sites are accessible for phosphates anion to fill. On the other hand, the smaller HSO_4^- anion than TsO^- makes PAni/SA more compact thus reducing the accessible sites. This can be observed in figure 3.12 that shows the accessibility coefficient (A) is much smaller for PAni/SA than that of PAni/pTSA.

3.3.8 Adhesion. Adhesion is the major challenge when developing conducting polymer coating over steel surfaces. This is due to hydrophobic organic films and hydrophilic metal surfaces have inadequate adhesion between them for commercial purposes. The adhesion can be improved by treating steel by medium chain length fatty acid prior/during electrodeposition. It was demonstrated that n-alkanoic acids modify the steel surface by forming self-assembled monolayer (SAM). The SAM modified steel surface has shown good adherence of polypyrrole coating. It was believed that SAM do not interfere with electron transfer during electrodeposition instead derives the reaction at monolayer/solution interface, acting as anchor between coating and meta surface [27,65].

Additionally, dopamine (DAm) is bio-adhesive that mimics the adhesive behavior of biological moieties of marine mussels [98]. This molecule is amine functionalized catechol that can be used modify the surface to enhance coating adhesion. It can be self-polymerized on variety of surfaces such as metals, polymer, glass etc. by increasing the pH to alkaline. Its strong interaction with surface is substrate independent [99,100]. Several studies has been reported on electrochemical deposition of polydopamine on conductive surfaces such as platinum, gold, SS etc. [101–104] However, coating produced is not conductive. Therefore, depositing conducting polymer and polydopamine together may enhance adhesion and meet electrical conductivity property. The results showed positive corrosion potential of polyaniline coated steel. In addition to reduction in the rate of corrosion, the primer coating provides good adhesion to the metal. The main aim of this study is to enhance the adhesion of electropolymerized polyaniline coating keeping corrosion potential in positive range. For adhesion, 1mM dopamine hydrochloric acid was added to the 0.1M aniline and 0.5M sulfuric acid as a dopant and coating was produced by following same procedure as described in experimental section 3.2.3. The corrosion tests were performed in 3.5% NaCl with

linear sweep voltammetry (LSV) at a scan rate of 1 $mV \cdot s^{-1}$, scanning ±150 mV from the open circuit potential (OCP). The crosshatch scotch tape adhesion tester kit was used for testing adherence following the procedure mentioned in ASTM D3359 standard.

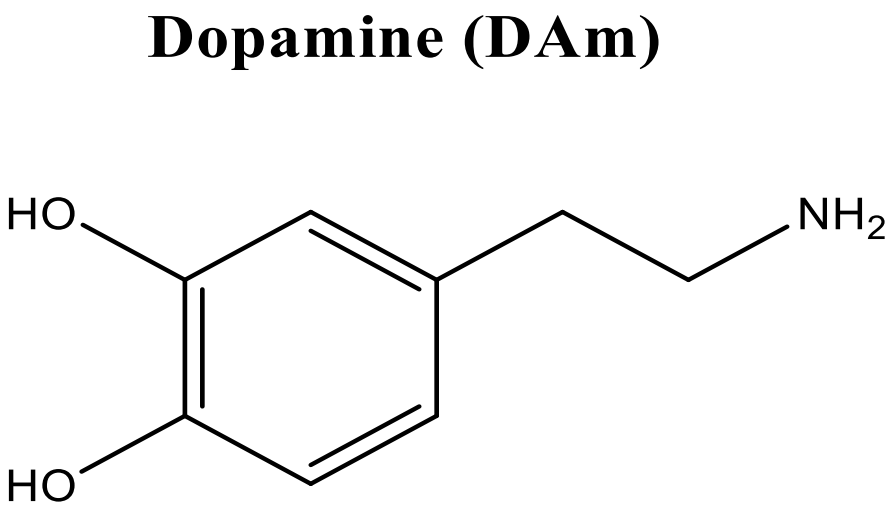

Figure 3.13 Chemical structure of dopamine used in this study

The electrodeposition of a PAni on SS surface was known to occur in three stages [55]: a) SS passivation and adsorption of aniline, b) aniline oxidation along with nucleation of PAni and c) PAni growth over the surface. These three stages are represented in chronoamperometric curves of electropolymerization of PAni on SS surface when doped with sulfuric acid before and after addition of dopamine as shown in figure 3.14. There is a drop in current density in stage I that corresponds to the passivation of the surface. This passivation is necessary prior to electrodeposition of polyaniline on steel surface as metal dissolution starts before aniline oxidation occurs at higher potential [27,28]. The stages II start with increase in current due to aniline oxidation and nucleation process occurring at same time. This gives us green color coating over the steel surface. This is followed by stage III where PAni film grows on the steel surface. The chronoamperometric curves shows no difference after addition of dopamine, this indicates that dopamine does not interfere with electron transfer in electropolymerization of aniline.

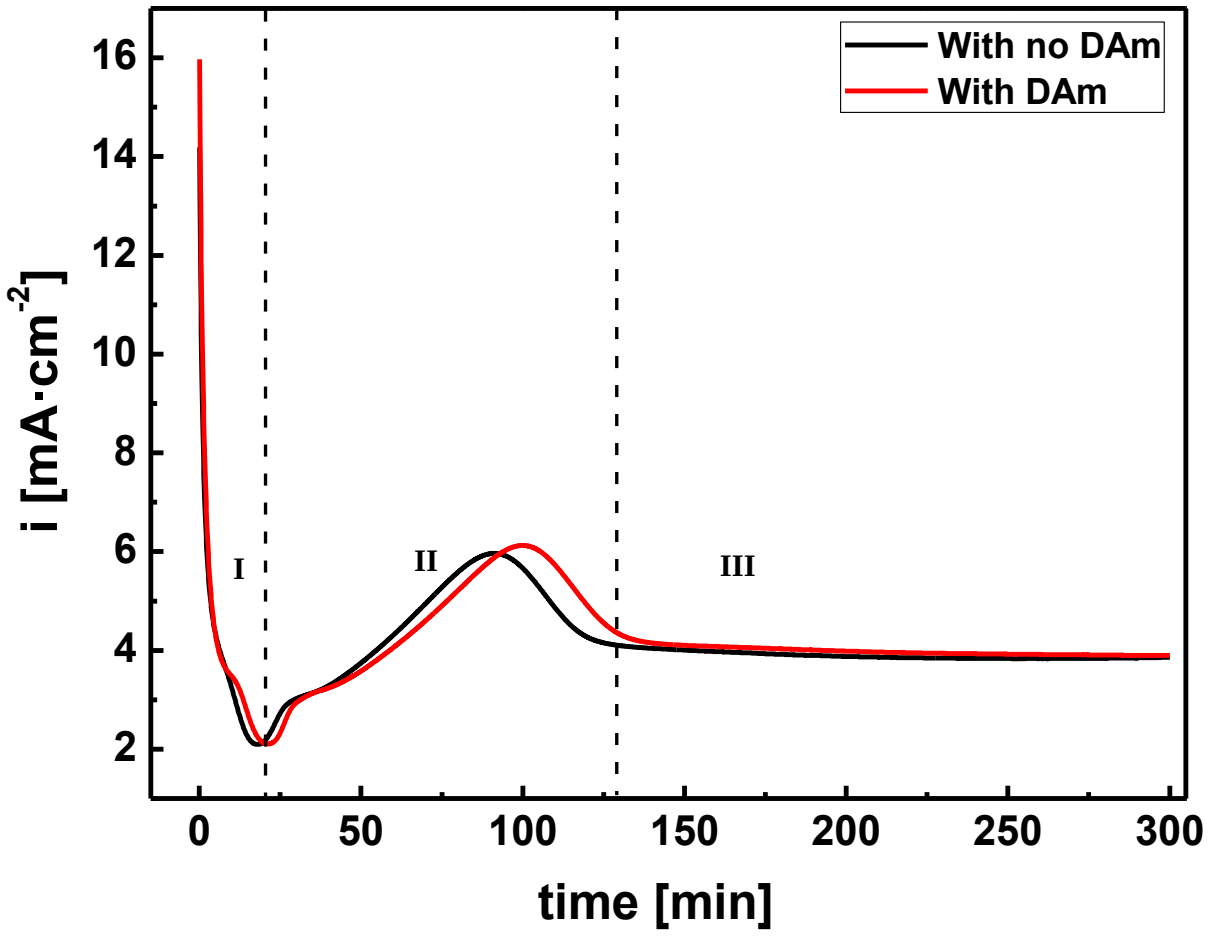

Figure 3.14 Chronoamperometric curves for electropolymerization of polyaniline coating on stainless steel using sulfuric acid as a dopant before and after addition of dopamine to the electrolyte.

The corrosion protection performance of PAni coating depends on the type of dopants used and its size because large size anions along with polymer chain provide barrier protection to the metal. Figure 3.15 showed the anticorrosion performance of polyaniline doped with sulfuric acid. Comparing with uncoated SS, the corrosion potential of PAni/SA increased by +210mV indicating the anodic protection. On adding dopamine, the corrosion potential of coating further increased by +220mV. This is due the presence of benzene ring in dopamine that forms lamellar structure by π-

π stacking within the molecule preventing ingress of chloride ions in the coating. Moreover, the presence of benzene ring increases the electron density in coating thus repelling negatively charged chloride ion. The scotch tape peel-off test was performed according to ASTM D3359 on 0.5in. x 0.5in. as shown in figure 3.16. The coating after the addition of dopamine during electropolymerization showed excellent adhesion on steel surface.

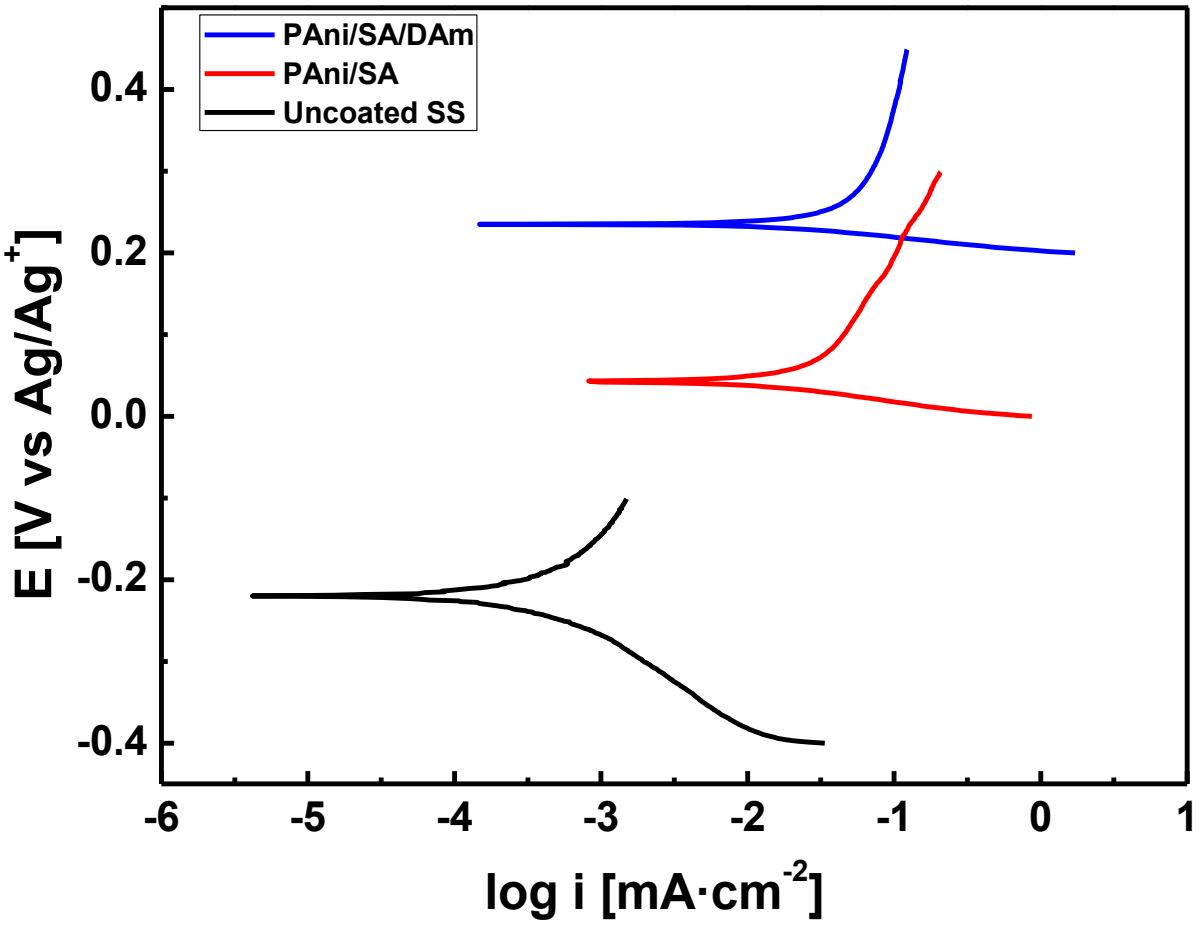

Figure 3.15 Tafel curves of PAni coating in 3.5% NaCl before and after addition of dopamine compared to uncoated steel.

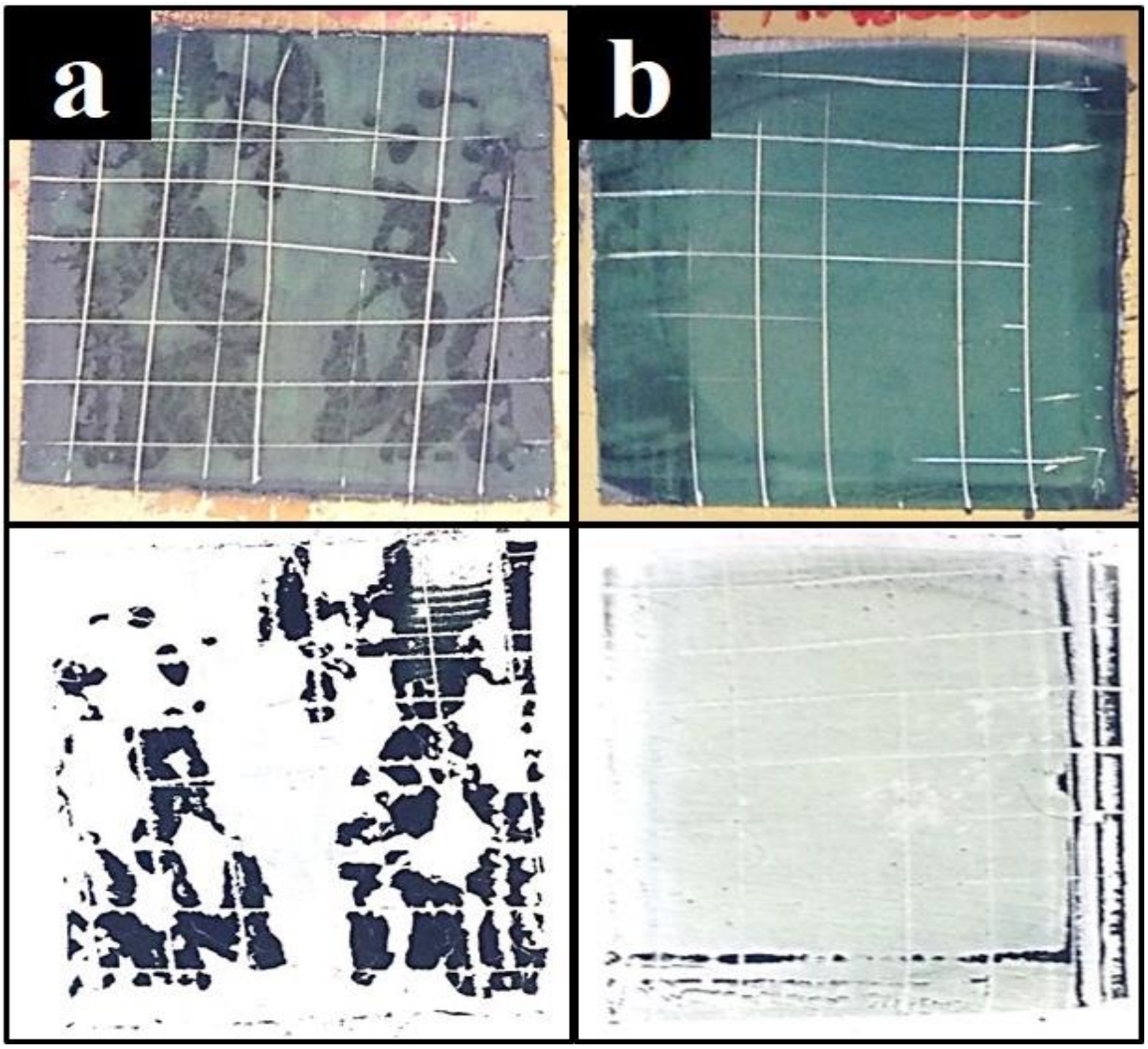

Figure 3.16 Cross hatch scotch tape tested samples for adhesion as per ASTM D3359, polyaniline coating with their corresponding area removed after testing; a) with no dopamine and b) with dopamine in monomer solution.

The adhesive dopamine moieties present in the coating are strongly interacting with steel surface is the reason for improved adhesion. Therefore, the strongly adhered produced coating were stable and have improved corrosion protection.

3.4 Conclusion

In conclusion, we reported a method for electrochemical dopant exchange from polyaniline coating which was electropolymerized on stainless steel. The anion exchange was carried out in respective phosphate electrolyte via cyclic voltammetry technique. The presence of phosphates was supported by FT-IR spectroscopy and has certainly improved the anticorrosion performance of polyaniline coating. Its anticorrosion performance was proved to be the best after HSO_4^- was exchange to phytic acid anion. The size of dopant anion has an influence on exchange efficiency and corrosion performance. The bigger anions prevent the ingress of negatively charged chloride ions. The bigger anions can be exchanged by smaller anions at faster rate due to size memory effect of PAni. On the other hand, smaller anion can still be exchanged by bigger anions at slower rate. Our work also demonstrated the protection provided by PAni/Sf was anodic and barrier, however, PAni/Sf-Ph provided additional inhibition protection due to the presence of phosphates inhibitors in the coating. Further, preliminary study suggests by addition of small quantity of dopamine, the corrosion performance of coating enhanced. Moreover, without affecting the corrosion performance, dopamine enhanced the adhesion of the coating by significant extent. Besides this coating system can be used in combination of commercially available organic paints top coat to provide best corrosion protection. It can also be used as a replacement of toxic metals like Cr (considered hazardous to many living being) as anticorrosive agent and improving environmental friendliness.

Chapter 4

Poly(3,4-ethylenedioxythiophene) coating as anticorrosive agent

Abstract: The poly(3,4-ethylenedioxythiophene) (PEDOT) coating was electrosynthesized on stainless steel surface using sulfuric acid (SA) and p-toluene sulfonic acid (p-TSA) as dopants. The PEDOT coating was evaluated as an anticorrosive agent by investigating the effect of dopants on corrosion performance. The electropolymerization potential was optimized to the lowest and performance of the coating was evaluated. The lower potential yields best coating as higher potential overoxidized the conducting polymers. Further, the corrosion performance was tested in 3.5% NaCl by using linear sweep voltammetry. The bigger dopants were effective for providing better corrosion protection synergistically with PEDOT.

4.1 Introduction

Unlike previous chapters, in this chapter we discussed sulfur based conducting polymer (polythiophenes) because their high tendency to interact with metals. Generally, polythiophenes (PTh) are considered as comparatively more stable than other conducting polymers, however, its conductivity decreases with longer exposure that limits its commercial use. This stability can be enhanced by substituting the monomer that decreases its oxidation potential. The substituted monomer (thiophene) can be obtained by introducing electron donating groups such as ethers that

decreases its oxidation potential. Amongst various substituted polythiophenes such as poly (3-alkoxy thiophene), poly (3,4-alkoxy thiophene) etc., poly (3,4-ethylenedioxythiphoenes) (PEDOT) proved to be most stable and found many applications in the field of energy storage, energy harvesting, corrosion protection etc. The structure of repeating monomer unit (EDOT) makes is more stable and less distorted polymer (PEDOT) chain upon polymerization as compared to other substituted thiophenes (figure 1).

It is the most widely used material in practical applications due to several advantages of its structural and electrochemical properties. Similar to polyaniline, it changes color when doped (conducting) and dedoped (insulating) repeatedly from translucent light blue to opaque dark blue, respectively. This color change upon doping found its use in electrochromic devices [105]. Since the structure of monomeric unit (EDOT) have 3,4 positions occupied by ether group, therefore only 2,5 coupling can be obtained upon polymerizing. This eliminates the competition of polymerization through 3,4 that is believed to have lesser defect compared to other thiophenes derivatives. This gives PEDOT enhanced thermal and chemical stability. The electrical properties of PEDOT remain unaltered even after aging in harsh conditions. This is due the presence of oxygen atom at 3,4 position that stabilizes the positive charge on polymer backbone. This behavior lowers the band gap (~1.5eV) of the polymer thus increasing its electrical conductivity as high as $550 S \cdot cm^{-1}$ in doped state [106]. The PEDOT have excellent electrochemical properties compared to other conducting polymers. It has been reported to have low redox couple and remain unaltered during cycling [107].

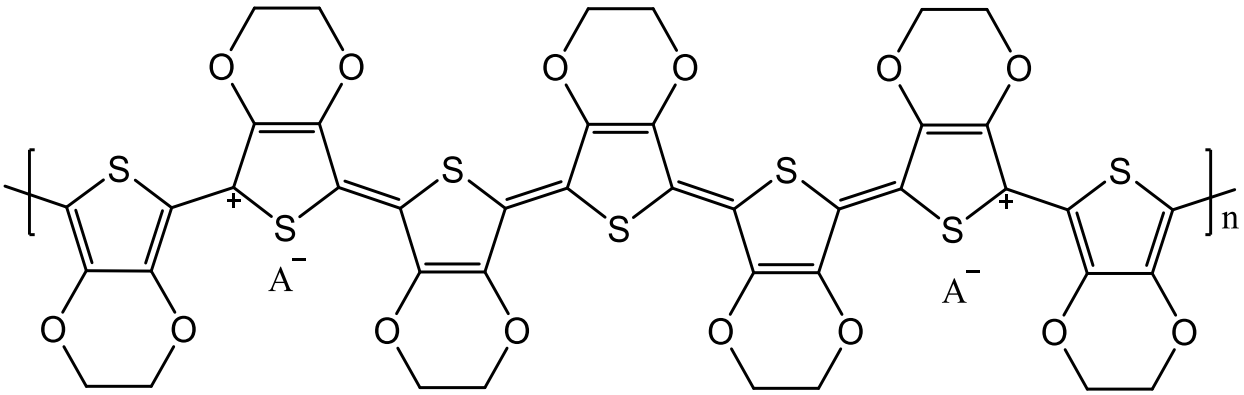

Conducting PEDOT

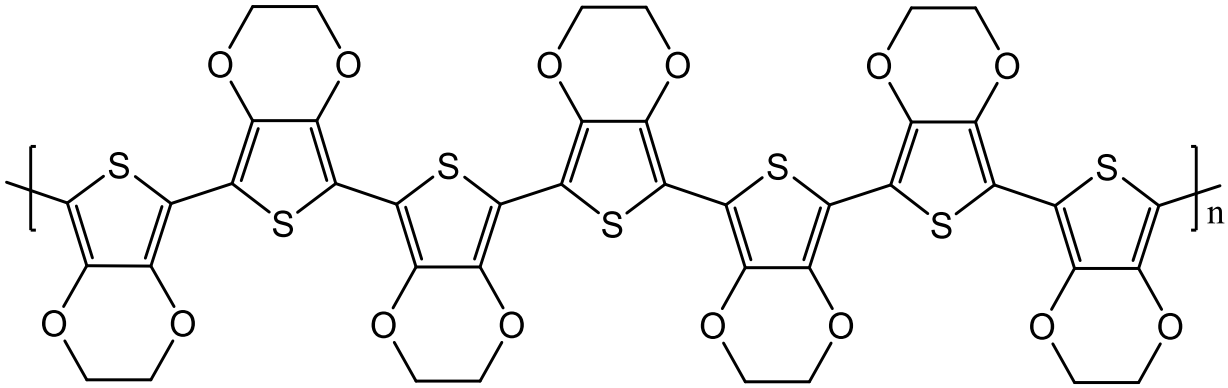

Neutral PEDOT

Figure 4.1 Chemical structure of poly (3,4-ethylenedioxythiophene) in conducting and neutral state.

It inspired a great research interest and range of applications due to above discussed properties of PEDOT. It is an attractive choice of material to be used in electrochromic devices, actuators etc. because of its repetitively doped and dedoped property [108,109]. Using polymeric counter-ion for PEDOT such as polystyrene sulfonate (PSS) makes it water dispersed conducting material that has been used broadly electrode material for flexible displays, organic light emitting diodes (OLED), solar cells and energy storage etc. [110] Typically, OLED is a device where light is generated with combination of electrons and holes, which are inserted from opposite directions into an emissive layer. The generated light will then leave from either of electrodes used (anode or cathode). PEDOT can either serve as hole transporting layer or can be used as a replacement of typically used ITO anode electrode [111]. Using PEDOT as a replacement will certainly reduce the cost of a device. Similarly, in organic solar cells it aids hole transport and can be used as current collectors simultaneously [112]. The other highly conductive optical properties of PEDOT has been reported elsewhere [113]. For energy storage devices, it has proven modification of electrode material with PEDOT, it can reduce the cost, introduce flexibility in the electrodes and can operated in wide range of potential [114,115]. It can be used for high energy density with high power density device with excellent cyclability up to more than 50,000cycles [116]. In combination with first redox material (ruthenium oxide) for such application, it reduces the cost by reducing the amount of expensive Ru in its matrix. The embedded ruthenium oxide in PEDOT matrix has shown significant increase in specific capacitance of 650F/g [117]. The PEDOT is insoluble in water, therefore limits its film forming ability. However, using PSS as a dopant it can be disperse in water and can cast a conducting film of PEDOT:PSS. The presence of PSS in the polymer backbone lowers the ionic resistance. On the other hand, due to incompatibility between polymer and electrolyte it increases the interfacial resistance which decreases the electrochemical activity of

the polymer [118,119]. There has been significant amount of work reported on PEDOT in various applications, however, report on its anticorrosive property is limited. Like PAni and PPy, PEDOT can also be used as a replacement of toxic coating contains chromates. Due to low solubility of monomer (EDOT), it has been mostly electropolymerized in organic solvents such as acetonitrile. To improve the solubility, researchers used surfactant that solubilizes EDOT in micelles and propel the polymerization [120,121]. The comparative study showed the PEDOT has better corrosion inhibiting property when electropolymerized in aqueous electrolyte than organic one [122]. The impedance study suggested the pore resistance is large in aqueous than that of organic electrolyte. This makes aqueous electrolyte best choice for electropolymerization of PEDOT.

4.2 Experimental section

4.2.1 Materials. 3,4-Ethylenedioxythiophene (EDOT) (M_w= 142.17 g·mol^{-1}, density = 1.33 g·cm^{-3}), platinum (Pt) gauze (100 mesh, 99.9% metal basis), p-toluenesulfonic acid (p-TSA) was obtained from Alfa Aesar, USA. Sulfuric acid (SA) was purchased from Anachemia. All chemicals were used without further treatment or purification. Stainless steel sheet (SS316L, 1 mm thick) was used for electrodeposition surface.

4.2.2 Sample preparation. The steel samples of 1.5 cm × 0.5 cm were cut from 1 mm thick sheet and cold mounted into acrylic resin so that only one surface was exposed. The embedded sample was then polished by emery papers of different grit size starting from 800, 1000, and 1200. It was followed by ultrasonic cleaning in deionized (DI) water for 1 min (DI water with ~18.2 Ω·cm resistivity).

4.2.3 Electrochemical synthesis. Poly (3,4-ethylenedioxythiophene) (PEDOT) coating was electrochemically deposited using electrolyte containing 0.1M EDOT and 0.5M dopant (SA and p-TSA). The electrochemical cell set-up used was a single compartment with three-electrode system, where SS (1.5 cm x 0.5 cm) was used as a working electrode, Pt as a counter electrode, Silver/Silver chloride/KCl (3 M) (Ag/Ag^{+}, E° = +205 mV vs. SHE) was used as reference electrodes.

4.2.4 Characterization. The corrosion tests were performed in 3.5% NaCl with linear sweep voltammetry (LSV) at a scan rate of 1 $mV \cdot s^{-1}$, scanning ±150 mV from the open circuit potential (OCP).

4.3 Results and discussion

4.3.1 Electropolymerization. The potentiostatic deposition was adopted to electropolymerized poly(3,4-ethylenedioxythiophene) (PEDOT) coating on stainless steel (SS). Electropolymerization was carried by applying three different potentials of 1, 1.2 and 1.4 V for 10min to optimize the electrodeposition of PEDOT. The dopants used in this study are kept same as in last project i.e. sulfuric acid (SA) and p-toluenesulfonic acid (p-TSA).

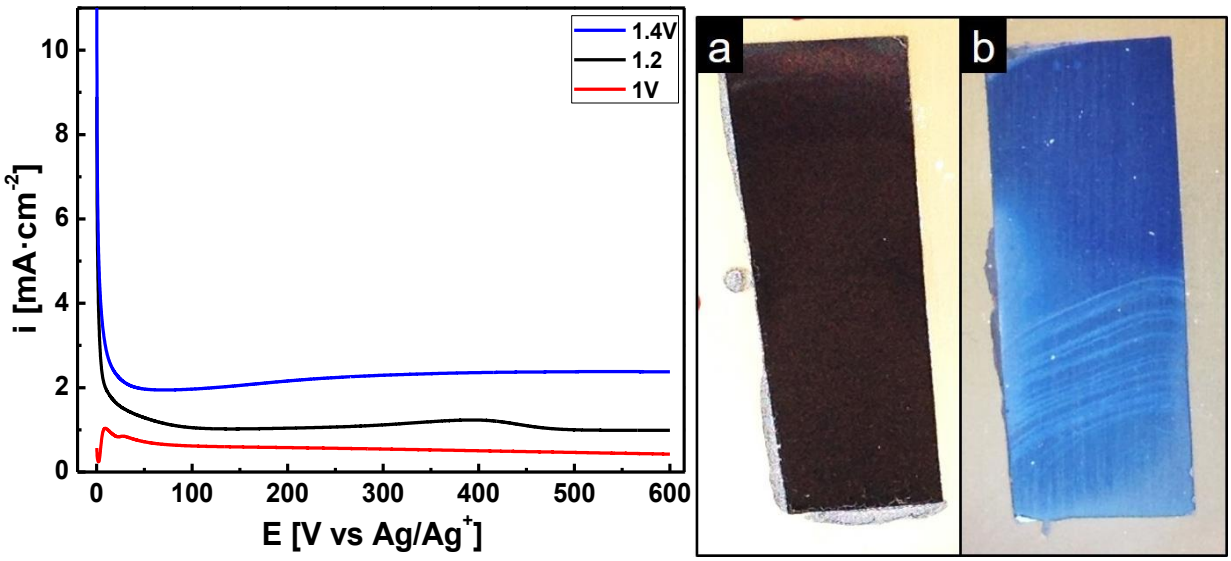

Figure 4.2 Chronoamperometric curves for electrodeposition of PEDOT on stainless steel at different potentials (left) and PEDOT coating electropolymerized at 1.4V (a) and 1V (b) (right).

Typical, potentiostatic deposition curves of PEDOT on stainless steel at different potential are shown in figure 4.2. When PEDOT was electropolymerized at 1.4 V there is a sudden drop in current density at start from 11 $mA \cdot cm^{-2}$ to 2 $mA \cdot cm^{-2}$. This an indicator of formation of passive layer and EDOT oxidation has occurred on the surface. The current gradually increases during electrodeposition, this indicates the growth of PEDOT film. However, higher potential causes the overoxidation of PEDOT film thus reduces its electrochemical activity [123]. The overoxidation of PEDOT coating can be seen as dark blue color in figure 4.2a. Similar coating was obtained for 1.2 V electrodeposition, however, if deposition was carried out at 1 V we can see translucent light blue color conductive PEDOT coating. In figure 4.2 (left), at 1 V the current density was initially at 0.5 $mA \cdot cm^{-2}$ and dropped to almost zero. This decrease in current density is the confirmation of passive layer formation on steel. It increases to 1.2 $mA \cdot cm^{-2}$ when EDOT oxidation occurs and then gradually decreases with time, which can be attributed to PEDOT growth.

4.3.2 Anticorrosive property.

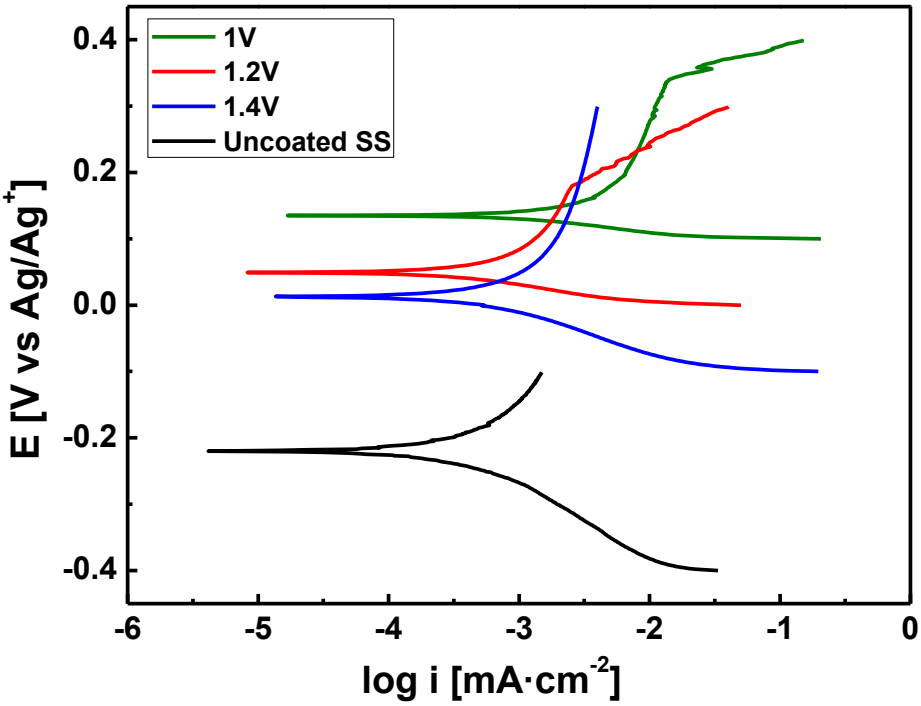

Figure 4.3 Tafel curves of PEDOT coating on stainless steel electrodeposited at different potentials.

The corrosion performance was evaluated in 3.5% wt. NaCl by using linear sweep voltammetry at $1mV \cdot s^{-1}$. Figure 4.3 shows the Tafel curves of PEDOT coating obtained after deposited at different potentials. All three PEDOT coating have higher corrosion potential than that of uncoated steel. This proves that PEDOT have good corrosion performance like other conducting polymers. The maximum anodic shift was obtained for PEDOT (deposited@1 V) which has corrosion potential approximately 270 mV positive than that of bare steel. The corrosion potential of PEDOT coated SS decreases by increasing the deposition potential. This is due to the decrease in electrochemical activity of the polymer at higher potentials. Therefore, for p-TSA electrodeposition potential of 1V was chosen to electropolymerize PEDOT coating on SS.

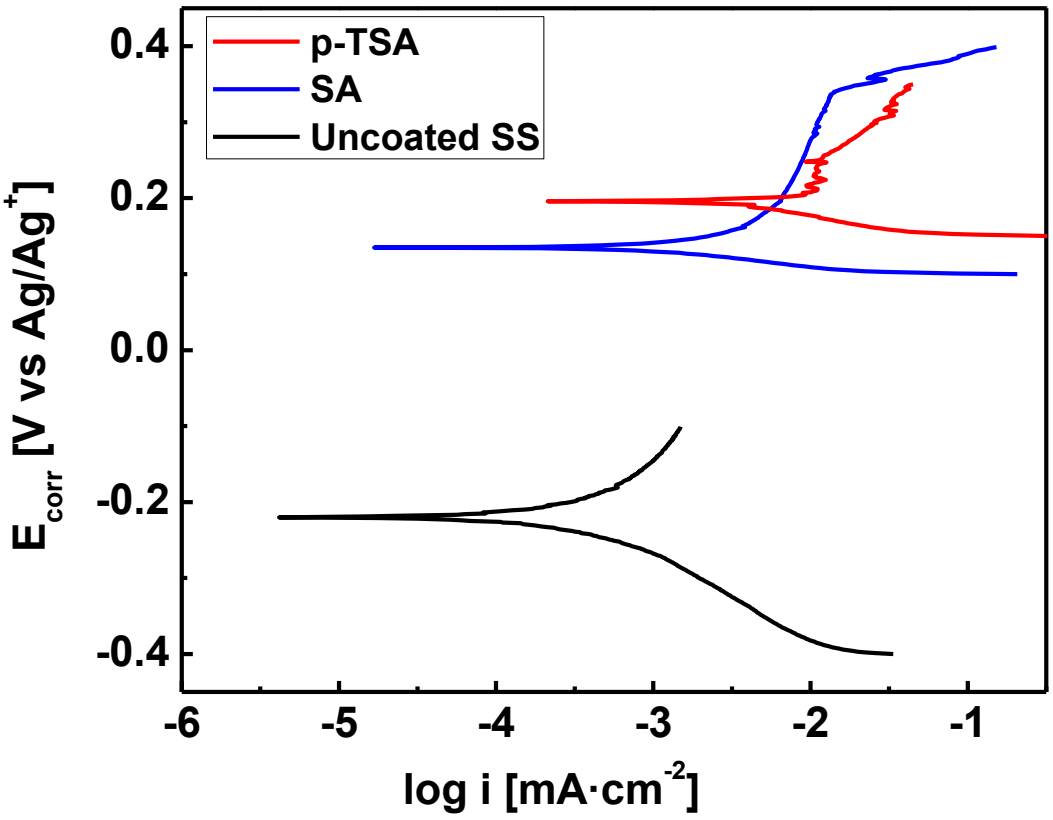

Figure 4.4 Tafel curves of PEDOT coating on stainless steel doped with SA and p-TSA.

In figure 4.4, the comparison of PEDOT coating doped with SA and p-TSA was shown when deposited at 1V. When SA was used as dopant for electrodeposition of PEDOT on SS surface, the corrosion potential was anodically shifted to 0.16 V. This corrosion potential ennobled the surface by 350mV positive to uncoated SS (E_{corr} = -0.19V). Further, this protection was enhanced when dopant was changed to p-TSA. The corrosion potential was slightly higher than that of PEDOT/SA and have better protection. This is due to the presence of benzene ring in p-TSA that form lamellar structure by forming π- π stacking. This lamellar structure prevents the ingress of chloride ion from the surroundings and protect the steel surface. Additionally, the benzene ring in p-TSA increases the electron density in the coating that repel negatively charged chloride. The SA and p-TSA are used in this study to electrodeposit PEDOT showed excellent corrosion protection of stainless steel.

4.4 Conclusion

The PEDOT coated steel showed great potential to be used as an alternative for anticorrosive agent. The dopant used for conducting polymer coating significantly affecting the corrosion performance of the coating. The bigger size dopant provides better protection than that when smaller sized dopants were used. In addition, the presence of aromatic group such as benzene ring that increases the electron density in the coating system. This increases the repulsion between negatively charged chloride ion and coating system that prevents metal surface. Besides, the produced coating helps in reducing the use of primer coating (containing chromium) prior to top coat. These primers are toxic and are hazardous due to the presence of chromium. Additionally, there is limited study of anticorrosion performance of PEDOT our study can be used to further enhance the corrosion performance of PEDOT using other dopants.

Chapter 5

Conducting Polymers: A Suitable Electrode Material for Energy Storage Devices

Abstract: The performance of polyaniline (PAni) was investigated as a suitable electrode material for energy storage devices. The influence of dopants: hydrochloric acid (HCl), perchloric acid (PrA), sulfuric acid (SA), p-toluene sulfonic acid (p-TSA), phosphoric acid (PhAc) and phytic acid (PA), on electrochemical performance of polyaniline was evaluated here. The specific capacitance of polyaniline was influenced by the type of dopant used. The smaller dopant results in compact PAni that degrades the polymer faster during charge-discharge process. On the other hand, the bigger size dopants give more swollen polyaniline and degradation was slower than that of smaller dopants. The highest specific capacitance of 1200 $F \cdot g^{-1}$ was calculated for HCl and PhAc. The cycling stability was excellent when bigger size dopants were used.

5.1 Introduction

Corrosion is major world problem that has been costing us billions of dollars to protect metal structures from degradation. In previous chapters, we have seen how we can enhance metal life by coating them with conducting polymer that provides active protection thus increases the usage life. Likewise, over the past few decades, there have been significant increase in scientific developments demanding the use of energy. As stated by International Energy Agency (IEA), the energy consumption in household has been doubled since 1980 and projected to be tripled by 2030 that costs hundreds of billions of USD over few hundred gigawatts of new energy [124]. It is

imperative to save the energy to reduce the cost of energy production and energy consumption as life becomes more dependent on electronics. Therefore, it is desirable to have clean and efficient energy device due to energy and environmental crisis. We have seen rapid increase in development of clean and sustainable energy technology such as solar energy, wind energy, biomass fuels etc. in past decades. However, the increase in advancement in energy storage and conversion technologies have been dominant in last few years mainly on lithium-ion batteries, supercapacitors and fuel-cells.

For better performance of an energy storage devices, the electrode materials should be of high interest. Currently, there are three majorly used electrode materials of which carbon-based materials are most widely used including conducting polymers alongside metal compounds. Carbon based electrodes includes activated carbon, graphene, carbon nanotubes etc. provide high power density, excellent cyclability, are suitable electrode materials for supercapacitors, anode materials for battery, fuel cells etc. However, due to low energy density of these materials the charge storage mechanism is limited. Metal compounds proved to displayed excellent performance as supercapacitor electrode materials. The good intrinsic electrochemical properties make them best materials for batteries. However, due to toxicity of some metal compounds (such cobalt etc.), high cost and limited abundance limits their commercial use.

Conducting polymers (CP) have attracted great interest of many researchers in energy storage, sensors, electrochromic devices, corrosion protection etc. since their discovery [18,125–130]. They have a wide range of properties not limited to facile production, adjustable electrical conductivity, easy scalable from few microns to nano level, excellent capacitive properties. As shown in Ragone plot (figure 5.1), conducting polymers are among the materials that are bridging the gap between batteries and capacitors as they exhibited high specific capacitance than electrolytic capacitors and

have faster kinetics than inorganic batteries (Li-ion). They have been used in various energy storage device to enhance the electrochemical performance of a device. However, they are widely used as an electrode material for supercapacitors to provide high energy density.

Supercapacitors are high performance energy storage devices that have longer cycle life than conventional electrolytic capacitors and batteries. This is due to their high power and energy density that is useful for faster charge-discharge rates [131–134]. Unlike traditional capacitors, they can store more charge by taking advantage of high surface are of electrodes and decreased distance between them. Generally, they are categorized in to two based on their charge storage mechanism: electrochemical double layer capacitors (EDLC) and pseudocapacitor. EDLC uses the concept of adsorption and desorption of ions on the electrode surface thus creates a double layer at electrode/electrolyte interface where they store electrical charge. The materials having high specific surface area are usually used as its electrode material. Porous carbon materials are excellent material for EDLC due to their low cost and high mechanical and chemical stability. On the other hand, pseudocapacitors utilizes the fast and reversible redox reactions to store charge.

In *EDLC*, charging-discharging process involves the movement of ions (in electrolyte) between the electrodes and electrons travels through external circuit. Cations moves towards negative electrode while anion towards positive one, creates double layers. This double layer stores the electrical energy. There is no electron transfer at electrode/electrolyte interface and no ion exchanged between the electrodes. The electrical energy stored can be calculated as:

$$\mathrm{E} = \frac{1}{2}\mathrm{CV}^2$$

where E is energy density, C is the specific capacitance and V is the voltage window of the capacitor. This specific capacitance is referred as double layer capacitance and can be expressed as:

$$C = \frac{A\varepsilon}{4\pi d}$$

where A is the surface of the electrode, ε is the dielectric constant of electrolyte, d is the distance between the electrodes. Typically, thickness of double layer is of few nanometers that makes specific capacitance higher than conventional capacitors.

Pseudocapacitors are type of supercapacitors that store electrical energy through redox reaction occurs at electrode/electrolyte. It involves electron/charge transfer by three steps; charge adsorption, intercalation of charge and fast reversible faradic redox reaction at electrode surface. There is no reaction between the ions and electrode material, only charge transfer between them. They have much higher specific capacitance than EDLC (10-1000x) because both surface and bulk are involved in electrochemical process. However, their low cycling stability impedes their application as compared to EDLC. Their electrochemical performance is dependent on affinity between electrode materials and ions. The type of materials exhibit redox behavior are transition metal oxides and conducting polymers. The transition metal oxides were used as electrode material for supercapacitors because their multiple oxidation states. They can take part in electron transferring reaction by changing their oxidation states at specific potentials [135–137].

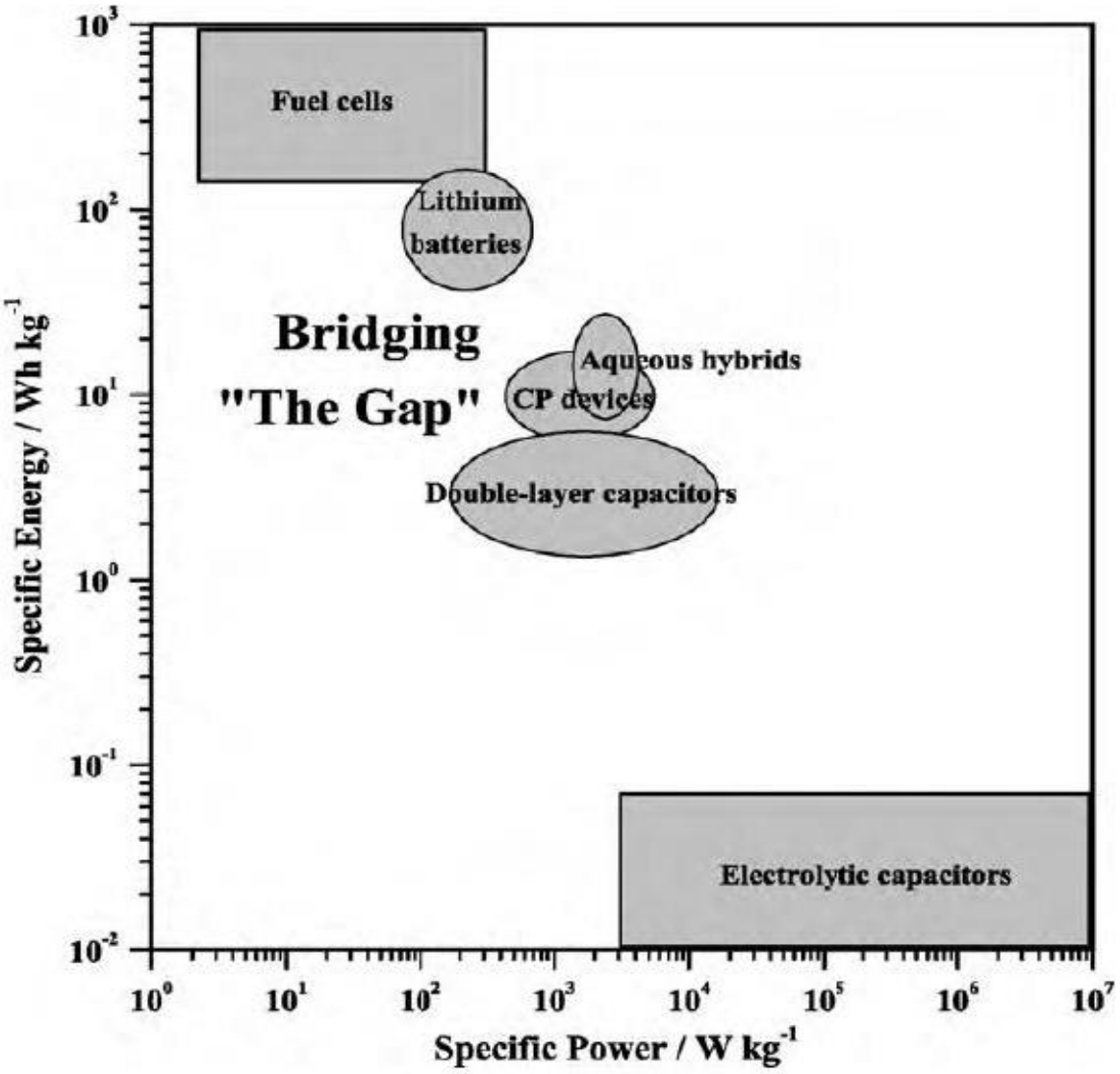

Figure 5.1 Ragone plot for different energy storage devices.

Ruthenium oxide (RuO_2) is considered as excellent supercapacitors electrode material with highest specific capacitance of 1400F·g^{-1} even after thousands of cycle of charge-discharge [138,139]. However, their application is limited due to their higher resistivity, poor cyclability, toxicity and high cost involves than other available materials [140]. The high resistivity can be addressed by adding conductive agent that enhances the charge transfer rate. However, toxicity and high cost still limits their used in wide application areas. Conducting polymers (CP) exhibited the same redox behavior through faradic reaction. The charge storage mechanism involves polymer to

switch between its doping states (doped and dedoped) when ions are inserted/extracted from polymer backbone. During charging process, polymer is oxidized and become positively charge that attract anions from electrolyte to achieve electroneutrality. The process is reversed during discharging, polymer is getting reduced. They have higher specific capacitance than transition metal oxides because whole polymer chain is involved in doping/de-doping process, unlike metal oxides.

Polyaniline (PAni) has been widely studied in energy storage devices including pseudocapacitors and batteries. It can exist in different oxidation states: leucoemeraldine, emeraldine, pernigraniline. Of these three only emeraldine proved high stability and is conducting after protonation. It can be chemically polymerized in various morphologies such as nanofibers, nanorods, nanospheres, nanoflowers, nanoflakes etc. and can be controlled by oxidants and templates [141]. However, electrochemical polymerization is considered as fast and environmentally friendly due to oxidant and additive free polymer formation. The binder-free electrode film can be obtained using electrochemical polymerization.

Table 5.1 Different types of supercapacitor devices with their charge storage mechanism and type of electrode materials used.

Types of supercapacitor	Charge storage mechanism	Electrode materials
Electrochemical Double layer capacitor (EDLC)	Charge adsorption in electrochemical double layer (EDL), non-Faradaic process	Carbon
Pseudocapacitance	Electron transfer via redox reactions, Faradaic process	Transition metal oxides, conducting polymers
Hybrid supercapacitor	Both redox reaction and EDL	Carbon, conducting polymers, transition metal oxides

PAni stores charge via redox reaction as it transitions between its oxidation states. Unlike other conducting polymers (stores charge at their surface), PAni involves bulk volume in charge storage that helps in achieving specific capacitance more than 1000 $F \cdot g^{-1}$. However, charge-discharge process involves insertion/extraction of charged ions in/out of the polymer, this leads to swelling and shrinkage of the polymer. Thus, damaging the integrity of polymer electrode and reduces the cycling stability. In addition, PAni degradation may occur at relatively lower potentials (~1.2V) limiting it use in lower potentials devices. Many efforts have been made on nanotechnology that helps improving the electrochemical performance such as PAni nanofibers [142], PAni nanowires [143,144] or nanocomposite with PAni [145,146]. The high aspect ratio of PAni chain makes disordered structure that slows down the ion diffusion within the electrode. Therefore, ordered nanomaterials were added along with PAni that makes diffusion relatively fast in a desired direction for better accessibility of redox sites. Besides the morphology, dopants influence the structural and electrical properties of polyaniline that affect the electrochemical performance of the polymer. [147,148] In this study, the effect of counter ion (dopant) on electrochemical performance has been investigated.

5.2 Experimental section

5.2.1 Materials. Aniline (M_w= 93.13 $g \cdot mol^{-1}$, density = 1.02 $g \cdot cm^{-3}$), platinum (Pt) gauze (100 mesh, 99.9% metal basis), p-toluenesulfonic acid (p-TSA) was obtained from Alfa Aesar, USA. Sulfuric acid (SA) was purchased from Anachemia. Phosphoric acid (PhAc) was purchased from EM Science, USA, Phytic acid (PA) was obtained from Tokyo Chemical Industry. Hydrochloric acid (HA) was obtained from BDH chemicals. All chemicals were used without further treatment or purification. Carbon cloth (40 cm X 40 cm) was purchased from Fuel Cell Earth LLC, MA.

5.2.2 Electrode preparation. The electrodes were prepared using carbon cloth (CC) (1 cm × 2 cm) as current collector. Prior to electrodeposition, they were immersed in 6 M HNO_3 solution for 24h followed by washing with DI water drying for 30 min in vacuum at 60°C. This treated CC was used for electrodeposition surface with projected area of 1 cm^{-2} (DI water with ~18.2 Ω·cm resistivity).

5.2.3 Electrochemical synthesis. Polyaniline coating was electrochemically deposited using electrolyte containing 0.1 M aniline and 0.5 M dopant (Figure 5.2). The electrochemical cell set-up used was a single compartment with three-electrode system, where CC was used as a working electrode, Pt as a counter electrode, Silver/Silver chloride/KCl (3 M) (Ag/Ag^+, E° = +205 mV vs. SHE) was used as reference electrodes. Electrodeposition was carried out on CH Instruments (CHI 760D) potentiostat using Electrochemical Analyzer software (version 17.06) by applying constant potential of 1 V for 5 min.

5.2.4 Characterization. The electrochemical characterization was carried out based on a three-electrode system. CVs were performed within potential range of −0.2 to +0.8 V vs. Ag/AgCl reference electrode with scan rate of 5-100 $mV \cdot s^{-1}$. Electrochemical Impedance Spectroscopy (EIS) was performed at open circuit potential (0.4 V) within the frequency range of 100kHz to 10mHz with 5mV amplitude. All electrochemcial characterization were performed in 1M H_2SO_4 as an electrolyte.

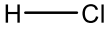

Hydrochloric Acid (HA)

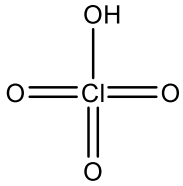

Perchloric Acid (PrA)

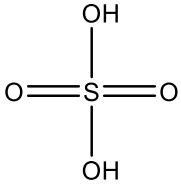

Sulfuric Acid (SA)

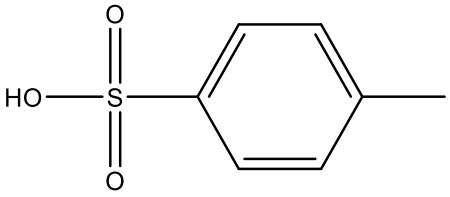

p-Toluenesulfonic Acid (p-TSA)

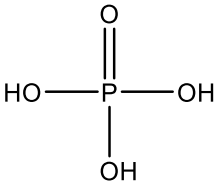

Phosphoric Acid (PhAc)

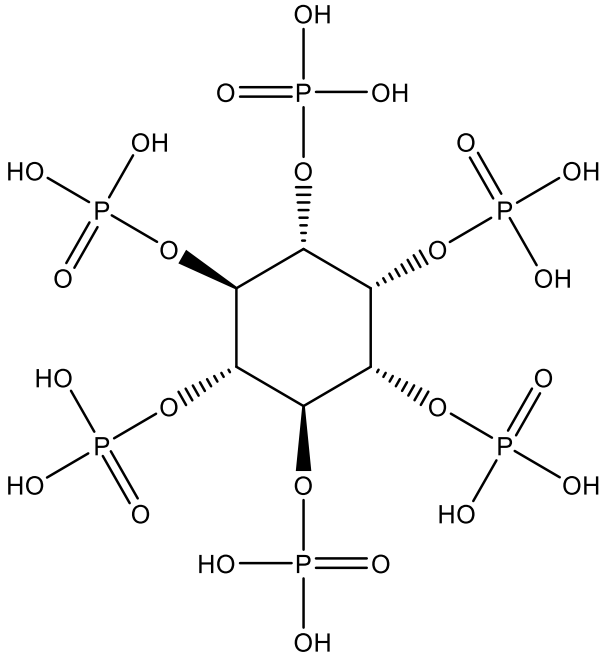

Phytic Acid (PA)

Figure 5.2 Chemical structure of doping agent for polyaniline used in this study

5.3 Results and Discussions

The electrochemical performance of an electrode material to be used as energy storage devices can evaluated using cyclic voltammetry (CV), galvanostatic charge-discharge (GCD), electrochemical impedance spectroscopy (EIS). The operating potential window of any material can be determined by performing CV whereas cycling stability is measured by GCD. The resistance offered by the material in redox reaction, electrolyte etc. can be investigated by applying constant potential as function of frequency.

The specific capacitance of an electrode material is used as an ability to store electrical energy and can be calculated using CV following equations:

$$C_s = \frac{2i_c}{\nu m}$$

Where C_s is specific capacitance, i_c is average cathodic current (in A) (during negative sweep), ν is scan rate (in $mV \cdot s^{-1}$) and m is the mass of an active material (in g), this gives specific capacitance in $F \cdot g^{-1}$. The specific capacitance of an electrode material using GCD can be calculated:

$$C_s = \frac{4It_d}{mV_{max}}$$

Where C_s is specific capacitance, I being the constant charge/discharge current (in A), t_d is discharge time (in sec) m is the mass of an active material (in g) and V_{max} is max potential (in V). When calculating specific capacitance from GCD the charge-discharge curves are considered a linear and triangular. However, in case of conducting polymers the charge-discharge profiles are not linear. The slope of discharge curve changes all along the curve due to different oxidation

states of conducting polymer. This indicates the faradaic process during charge-discharge. Also, CV is considered as best tool to measure the performance of a conducting polymer. The supercapacitive behavior of polyaniline was studied using CV within potential range of -0.2 to +0.8V with varying scan rates. Cycling stability was studied by charge-discharge within 0 to 0.8V at varying current densities.

5.3.1 Cyclic voltammetry. The cyclic voltammetry curves of PAni at different scan rates from 5-100mV·s^{-1} are shown in figure 5.3. Typical shape of polyaniline CV curves was observed that tells the oxidation-reduction reaction of PAni electrodes. There are two pair of clear redox indicates the transformation of different oxidation of PAni which is different than rectangular CV of ideal capacitor. In figure 5.3a, for 5mV·s^{-1}, first redox pair can be seen at 0.2V which is transition between leucoemeraldine and emeraldine while transition between emeraldine salt to pernigraniline can be seen at 0.5 V. This redox pair shift positive with increase in scan rate. The presence of redox peaks indicates the pseudocapacitive behavior of polyaniline electrode and is main contributor in the capacitance. Also, it was observed the area of the obtained voltammogram increases with increase in scan rates for both chlorates. This signifies the ideal capacitive behavior where voltammetric current is proportional to scan rate. From figure 5 a & b, the highest specific capacitance for PAni doped chlorates was calculated as 1200 F·g^{-1} and 840 F·g^{-1} for HCl and $HClO_4$ dopant, respectively.

The HCl doped PAni have better capacitive behavior than that when doped with perchloric acid. This is due to hydrochloric acid provide maximum conductivity to polyaniline chain. Smaller chloride ion has highest mobility along the chain as compared to perchloric acid, hence faster charge transfer. In figure 5.3 c & d, similar PAni CV curves were observed for both sulfuric acid and p-TSA. The presence redox pair in CV indicates the transition between the oxidation states of

polyaniline within operating potential range. This redox pair contributes to the capacitance of the produced electrode and exhibited the pseudocapacitive behavior. The peak positions are similar with chlorates, however, peak currents in sulfates are lower. This is due to low mobility of sulfates within the polymer that increases the ionic resistivity at electrode/electrolyte interface, reduces the specific capacitance. [82] On comparing SA and p-TSA, area within the CV curve is more in SA because of smaller size and charge of hydrogen sulfate than tosylate ion. The higher charge on tosylate reduces the charge transport.

The cyclic voltammetric curves for PAni doped with PhAc and PA are shown in figure 5.3 e & f, respectively. The curves shown distinct redox peak even at higher scan rates. This indicates excellent electrochemical reversibility of PAni. Besides, phosphates are more stable than chlorates and sulfates, therefore provide the stability to the polymer oxidation-reduction reaction occurring during CV.

5.3.2 Scan rates: The specific capacitance of polyaniline decreases with increase in scan rate for all the dopants (Figure 5.4). This is due to the, at higher scan rates, diffusion of protons within the electrode prevents some active sites to transform between the oxidation states of PAni. This leads to high ionic resistivity that decrease the capacitance at higher scan rates. [149] Therefore, at slower scan rates the specific capacitance is highest as accessible actives are maximum within the polymer (Table 5.2).

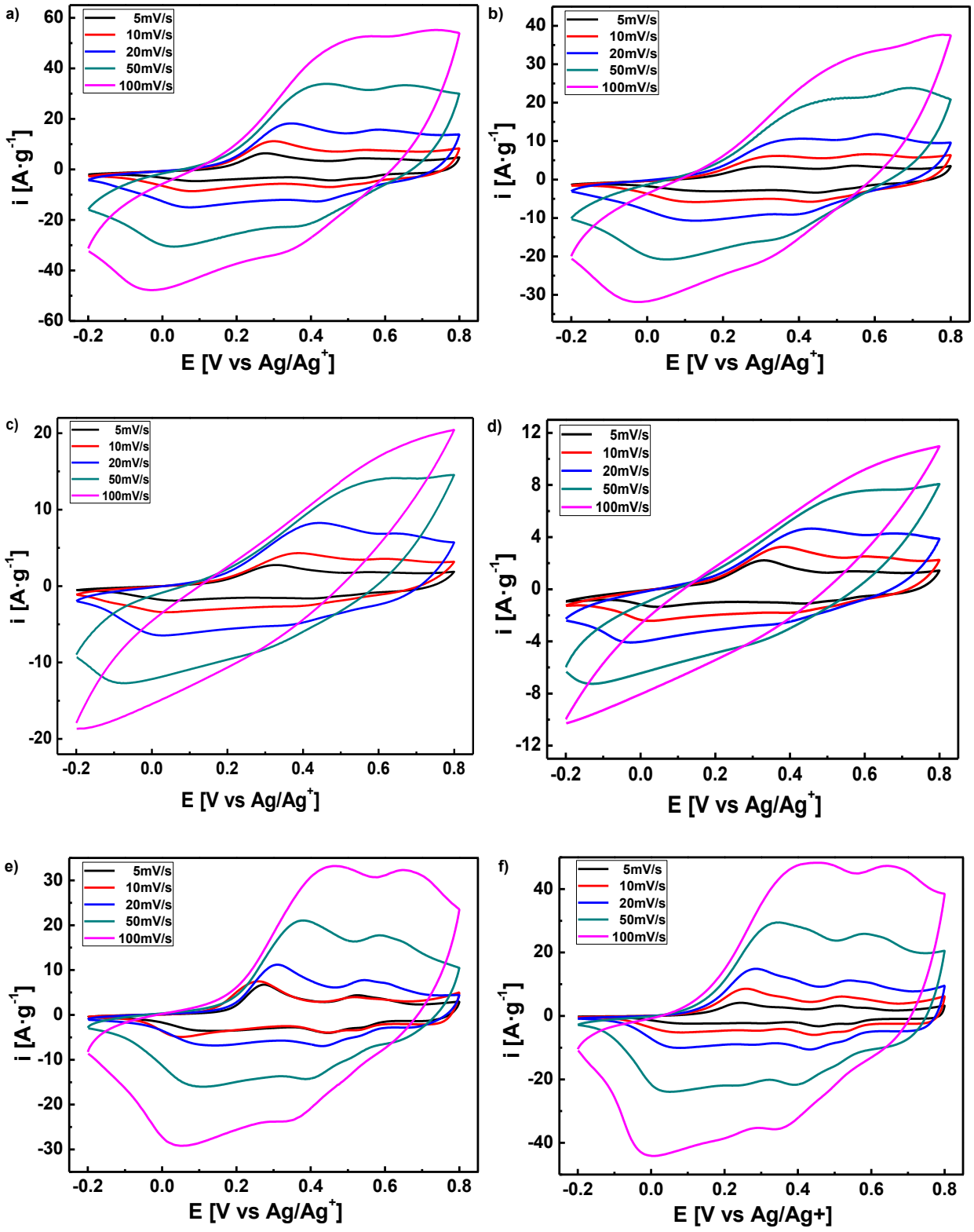

Figure 5.3 Cyclic voltammogram for polyaniline doped with: a) HCl, b) $HClO_4$, c) SA, d) p-TSA, e) PhAc and f) PA.

The relation between redox peak current and scan rate for all dopants are shown in figure 5.4. The electrochemical reaction of PAni diffusion controlled that indicates the ideal capacitive behavior. This can be corroborated with plot where peak current densities are directly proportional to the square root of scan rate following equation [150]:

$$i_p = 2.69x10^5 AC\sqrt{D\nu n^3}$$

Where i_p is the peak current (A), A is area of an electrode (cm^2), C is concentration of electrolyte ($mol \cdot L^{-1}$), D is diffusion coefficient ($cm^2 \cdot s^{-1}$), ν is scan rate ($mV \cdot s^{-1}$) and n is the number of electron transferred in redox reaction.

Table 5.2 The specific capacitance of polyaniline at different scan rates.

Scan rate ($mV \cdot s^{-1}$)	**Specific capacitance ($F \cdot g^{-1}$)**					
	HCl	***$HClO_4$***	***SA***	***p-TSA***	***PhAc***	***PA***
5	1199.6	837.8	490.0	350.1	904.7	666.4
10	1066.7	766.0	440.3	303.6	537.8	708.8
20	966.8	663.5	414.8	249.2	425.3	668.3
50	771.4	513.3	321.7	174.6	392.7	615.5
100	608.9	399.9	211.2	110.9	357.1	552.6

The dependence of specific capacitance on scan rate are plotted in figure 5.5. The decrease in specific capacitance value for PAni was observed for all the dopant that were used to produce PAni with increase in scan rate. The decrease in specific capacitance is in the agreement with our cyclic voltammetry data where anodic peak currents decreases with increase in scan rate. This decrease is evident of active sites in the polymer that cannot be accessed due to diffusion of protons at

higher scan rates. [151] The decrease in specific capacitance was more when sulfates were used because of lower stability of sulfates at higher scan rates. This is due to the small envelope of electron around the sulfates ion, that does not break the water molecules when inserted to the polymer chain. This decreases the electrochemical activity of polyaniline and as a result, more polymer degradation was observed. [152]

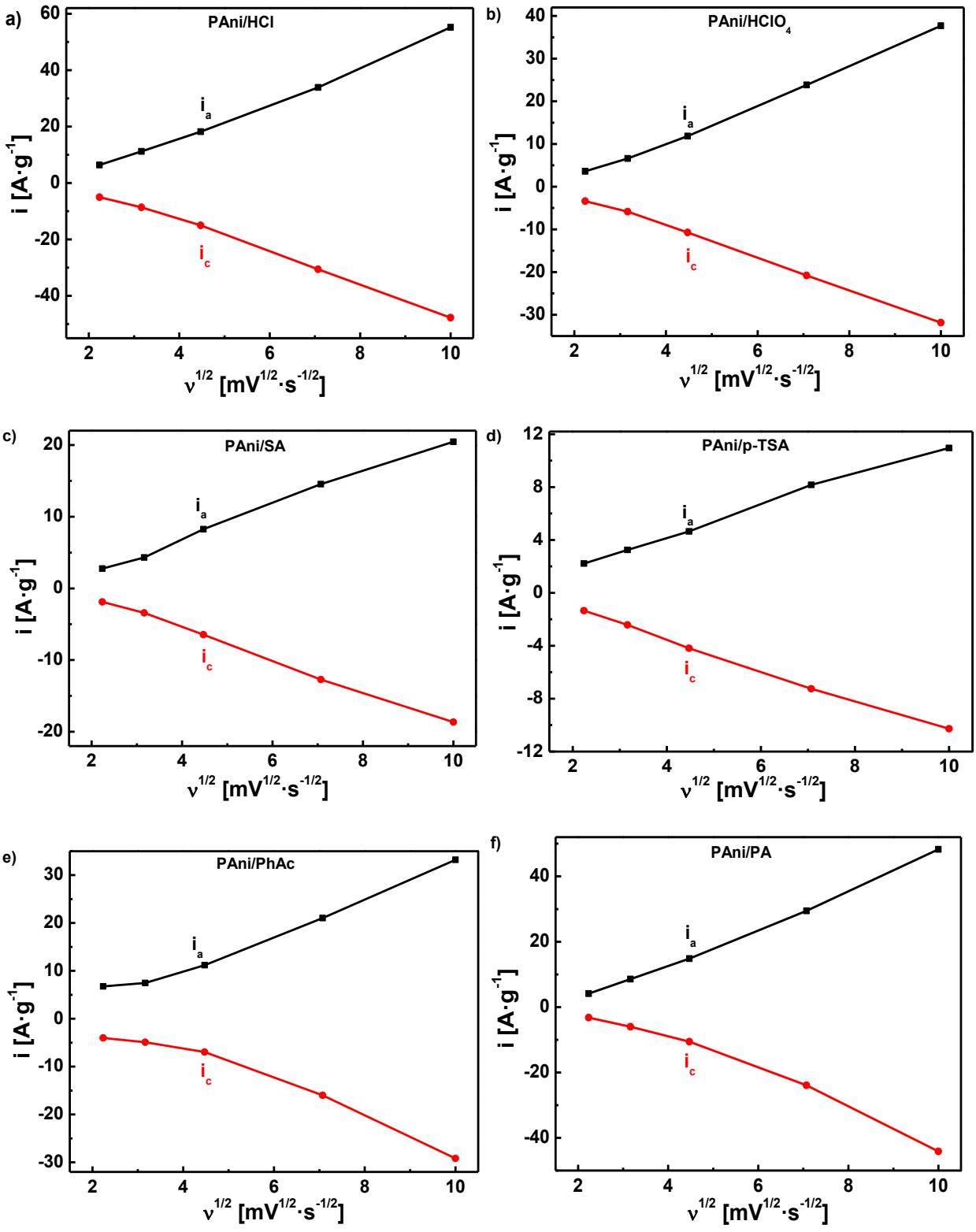

Figure 5.4. The plot of oxidation and reduction peak current versus the square root of scan rate for PAni: a) HCl, b) $HClO_4$, c) SA, d) p-TSA, e) PhAc and f) PA.

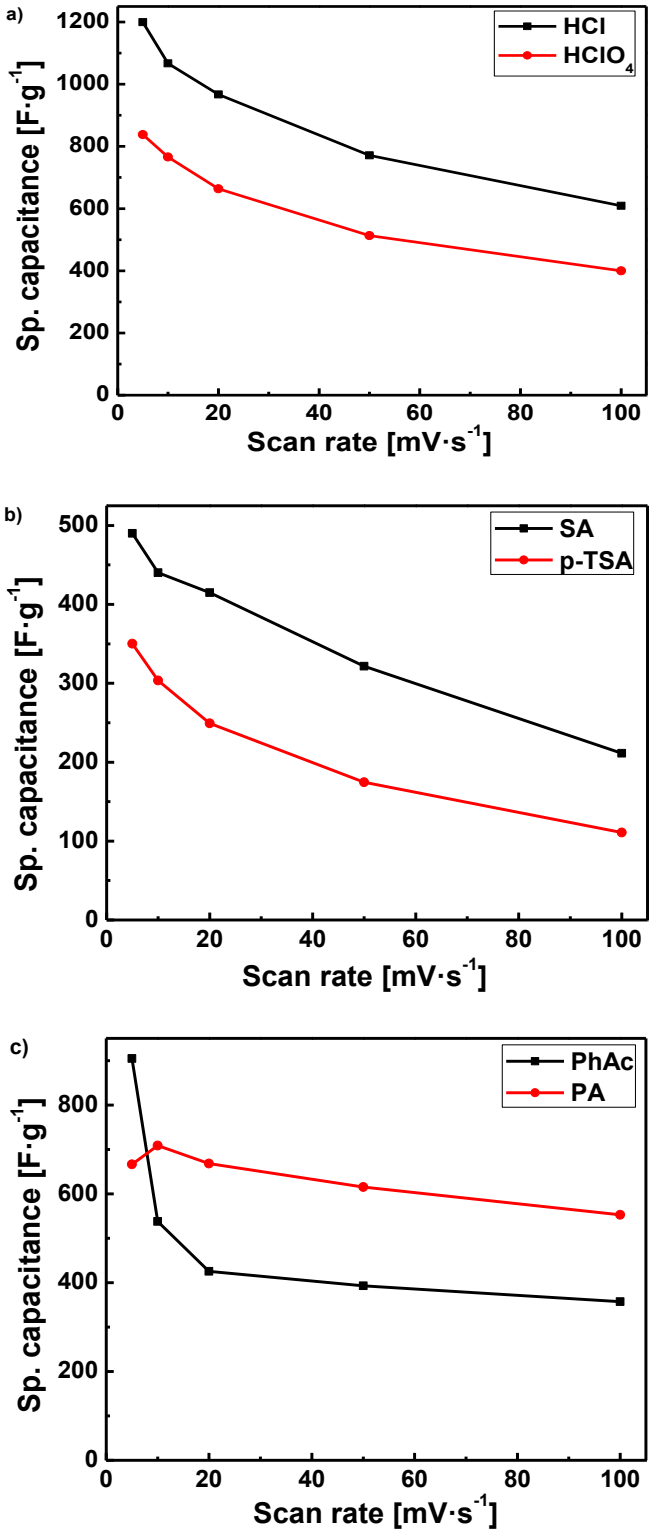

Figure 5.5 Variation of specific capacitance of polyaniline with different scan rate: a) chlorates, b) sulfates and c) phosphates.

5.3.3 Cyclability. The cycling stability is one of the key test to be performed on supercapacitor electrode materials. The stability of an electrode was evaluated using galvanostatic charge-discharge for 2000 cycles within potential range of 0 to 0.8V. The charge-discharge was carried out at 2 $A \cdot g^{-1}$ for sulfates and 10 $A \cdot g^{-1}$ for phosphates. The charge-discharge of chlorates doped PAni was carried out, however the electrodes are unstable at all current densities (not shown here). This is due to smaller size of chlorates makes compact and uniform polyaniline that damages the coating much faster during charge-discharge test because of swelling-shrinking of the electrode during the process.

Figure 5.6 shows the charge-discharge curves for PAni, both charge and discharge curve are behaving in a similar manner indicating the capacitive nature of PAni electrodes. However, non-linear curves showed that process is faradaic and reversible. This indicates the pseudocapacitive behavior of PAni thin films. During discharge, there is IR drop from approximately 0.8 to 0.7 V that results in asymmetric charge-discharge curves. The resistance from electrolyte and PAni film increases during the process resulting in IR drop increase. This IR drop is attributed to equivalent series resistance offered by electrolyte and electrode, which increases with increase in number of cycle for charge-discharge. The decrease in capacitance value was attributed to this increase in series resistance. In figure 5.6a & b, the IR drop is large in smaller size (SA, PhAc) dopant than that of bigger size (p-TSA, PA) because bigger size dopants are loosely bonded to PAni chain. This require lower energy for them to release and increases the charge diffusion in and out of the polymer electrode. As a result, the cycling stability is high when PAni is doped with bigger size dopants that allows faster and effective charge transport and contributes to higher rate performance.

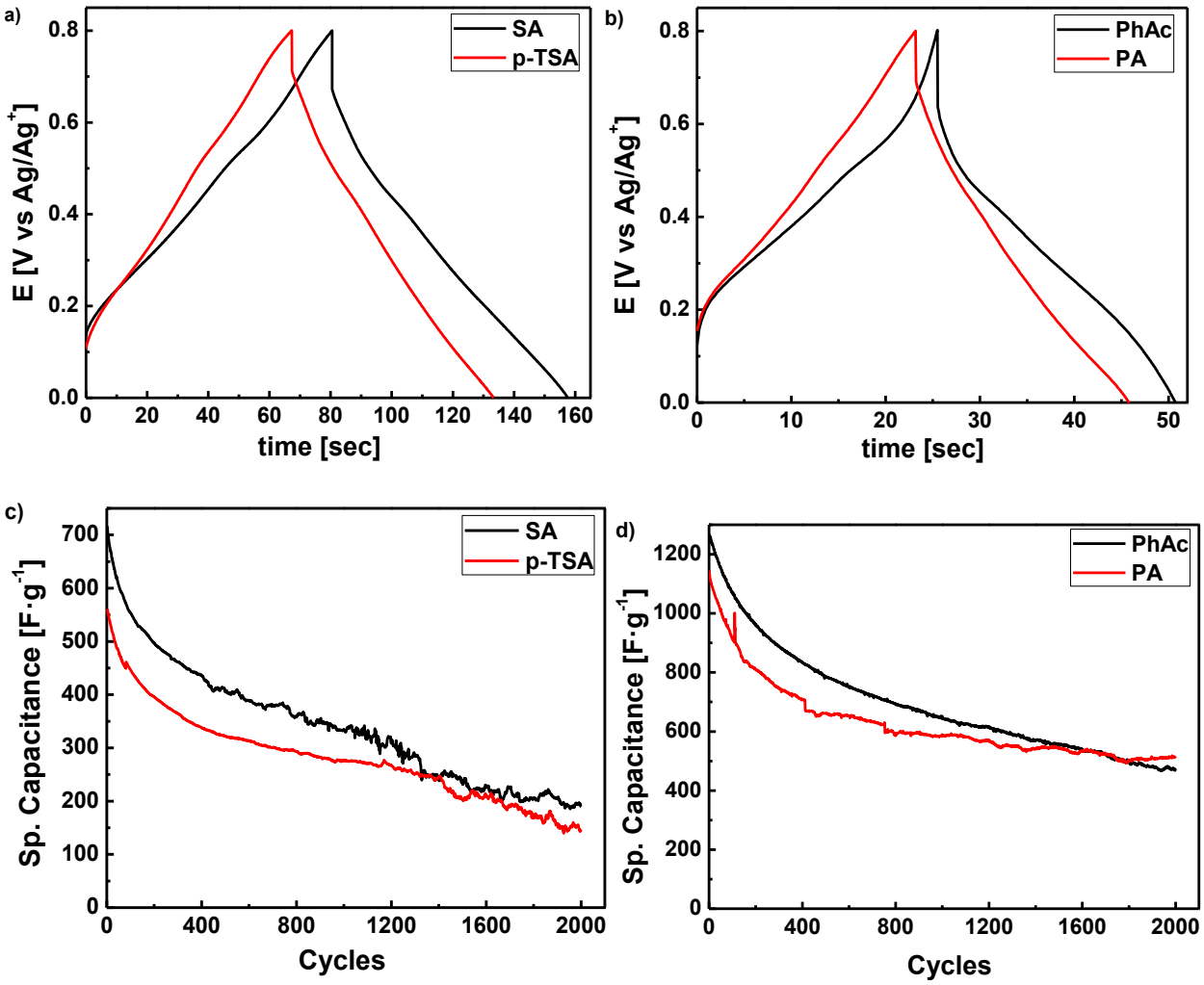

Figure 5.6 Galvanostatic charge-discharge curves for PAni (a, b). Cycling stability of PAni (c, d) with different dopants

The cycling performance can be seen in figure 5.6 c &d for PAni doped sulfates and phosphates. The capacitance decreases faster for first 400 cycles for all the dopants used and get decreases gradually afterwards. This sharp decrease can be attributed to the degradation of electrode as polyaniline films swells and shrink during the charge and discharge due to ion diffusion in and out of the polymer matrix that compromised the integrity of electrode. [153] The capacitance decreases faster with sulfates than that of phosphates due to low mobility of sulfates in polymer. This is the

reason of lower specific capacitance when compared to phosphates. The decrease of specific capacitance is slow for phosphate doped PAni because of their stability at higher scan rates and current densities. The capacitance retention is higher with phosphates (50%) after 2000 cycles than that of sulfates (30%). Even after 2000 cycles the phosphates showed higher specific capacitance of 600 $F \cdot g^{-1}$ which is higher for thin film deposited on carbon based electrodes. [154] The initial decrease of specific capacitance can be attributed to the electrode is getting stabilized before it starts to show stability over 1000 cycles.

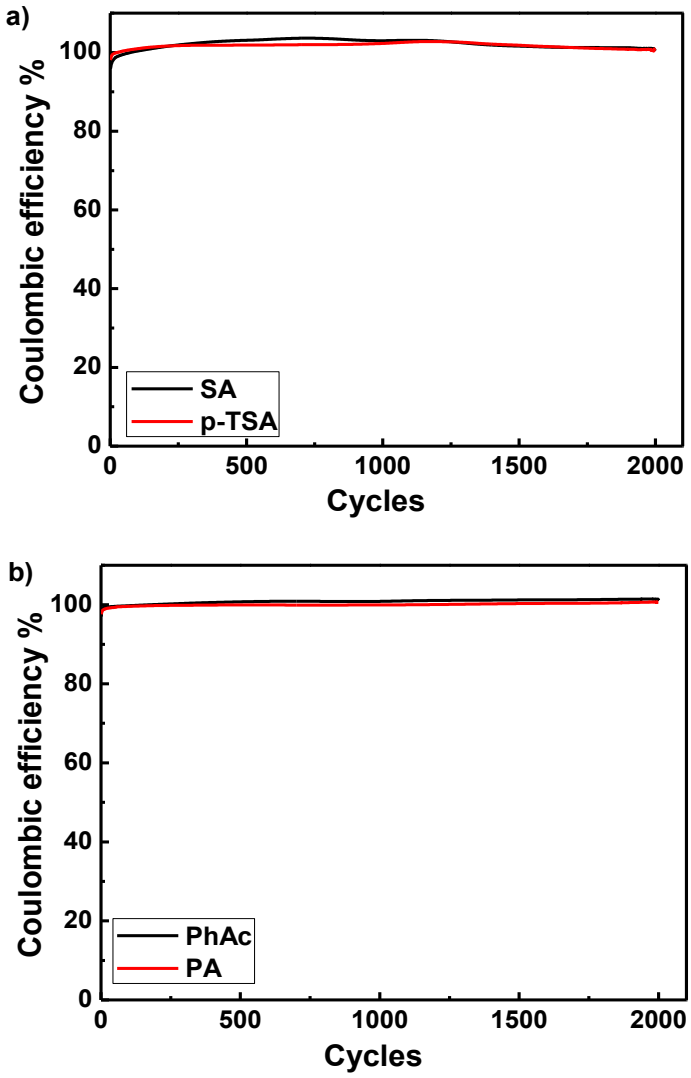

Figure 5.7 Coulombic efficiency of PAni electrodes doped with: a) sulfates and b) phosphates

Moreover, the coulombic efficiency is one of the parameters that can be studied for the cycle stability of an electrode materials for supercapacitors. The coulombic efficiency (η) can be calculated using following equation:

$$\eta\ (\%) = \frac{t_d}{t_c} \times 100$$

where t_d & t_c are charge and discharge time calculated from GCD curves. Figure 5.7 showed the coulombic efficiency for PAni where all the dopants used. For all the dopants, 100% efficiency after 2000 cycles indicates the excellent stability of PAni thin films produced. This indicates the decrease in capacitance is solely due to degradation of the polymer electrodes.

5.3.4 Electrochemical Impedance Spectroscopy. The electrochemical impedance spectroscopy (EIS) is as useful technique to evaluate the electrochemical performance of an electrode with certain frequency range. It is used to understand the mechanism and kinetics of the electrode materials. The EIS of PAni electrode was performed at open circuit potential in the frequency range of 100kHz to 10mHz and plotted as Nyquist plot. A typical Nyquist plot comprises of semi-circle at high frequency range and vertical line in low frequency region. In high frequency region the intercept with X-axis is the solution resistance (R_s) and diameter of the semi-circle is the charge transfer resistance (R_{ct}) of the electrode. In Figure 5.8, Nyquist plot of polyaniline electrode doped with chlorates, sulfates and phosphates were compared. All the impedance spectra showed very low solution resistance and charge transfer resistance indicating electrodes are conductive and rate of ion-diffusion is faster. The strong electrolyte 1M sulfuric acid was used for all the experiments therefore it exhibited low solution resistance of ~5Ω for all the PAni electrode.

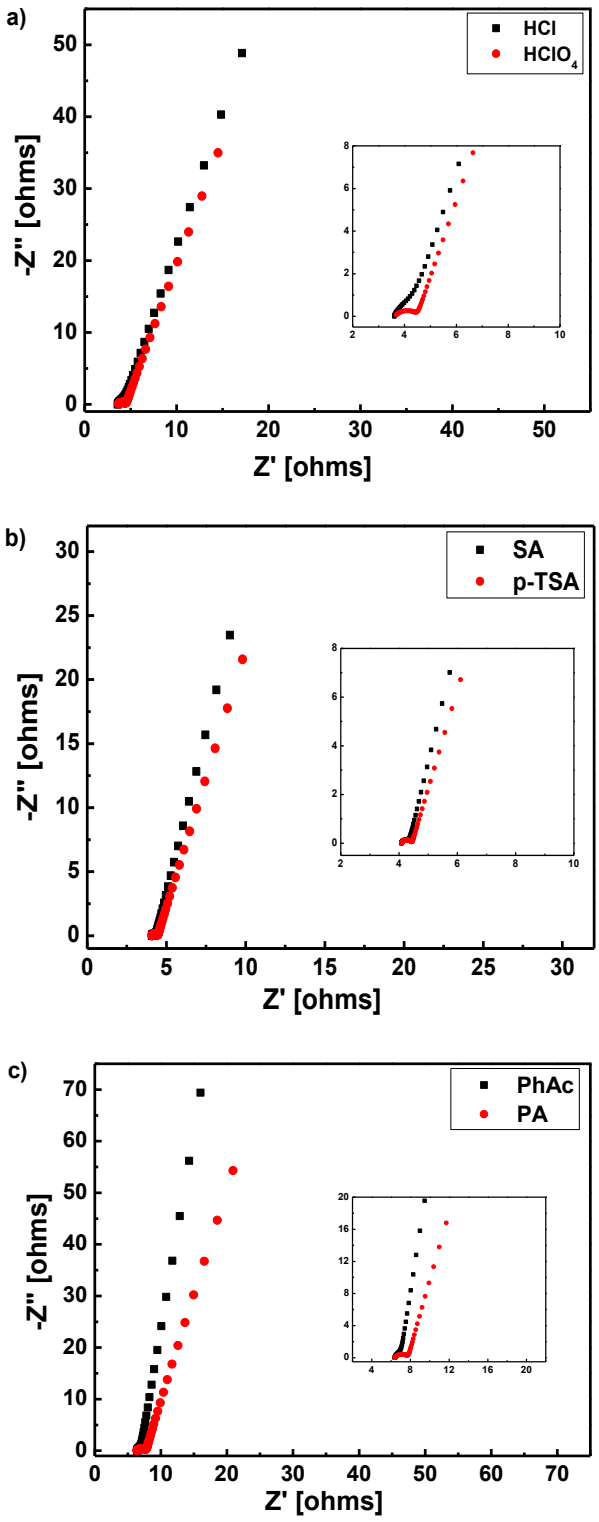

Figure 5.8 Impedance spectra of PAni electrodes doped with: a) chlorates, b) sulfates and c) phosphates, obtained at open circuit potential.

The charge transfer resistance at high frequency region showed excellent penetration of electrolyte ions in polymer has occurred. As a result, redox sites available in the polymer can be accessed easily by fast ion transport from bulk electrolyte to the polymer. In figure 5.8a, the charge transfer of PAni/HCl was found to be 0.2 Ω lower than that of PAni/$HClO_4$. This is in agreement with specific capacitance from cyclic voltammetry (figure 5.5a) where HCl dopant showed higher capacitance value than $HClO_4$. On the other hand, figure 5.8b, both SA and p-TSA showed same charge transfer resistance and similar capacitance behavior. PAni/SA showed more supercapacitor than PAni/pTSA because of straight line in low frequency region for PAni/SA is closer to vertical, which ideal capacitor behavior. Similar behavior was observed when phosphates were compared for specific capacitance (figure 5.8c). However, PAni/PA showed slight higher charge transfer resistance due to bigger size of phytic acid that showed to the stability of polyaniline electrode during charge-discharge. Therefore, even though PAni/PA have slightly sluggish ion diffusion, they exhibited excellent cycling stability.

For polyaniline to be used as supercapacitor electrode, it must display excellent cycling stability of at least 2000 cycles with more than 75% of capacitance retention. Our study investigated the performance of different dopants used for polyaniline with varying size. The bigger size dopant certainly has better stability during charge-discharge as there is more open structure that can withstand swelling-shrinking of polymer for prolonged period. On the other hand, if smaller sized dopants were used, the more compact polymer chains were obtained. As a result, more polymer is contributing to the faradaic process resulting higher specific capacitance at the cost of cycling stability.

5.4 Conclusion

In this study, we investigated the performance of polyaniline as supercapacitor electrode materials. The effect of dopant on the performance of polyaniline has been evaluated. The chlorates showed to have better conductivity than sulfates and phosphates because of high mobility of chloride ion along the polyaniline chain. The scan rates effect was studied on all the dopant used and phosphates exhibited highest stability at higher scan rates. The sulfates are not stable at higher scan rates due to their sluggish movement in the polymer as sulfates have lowest mobility in the polymer. The chlorates were stable at higher scan rates; however, their cycling stability is lower than sulfate as faster degradation of polyaniline was observed when chlorates was used as a dopant. This make electrode unstable during charge-discharge test. This is due to smaller size of chlorates make compact and uniform coating. This damages the electrode during cycling test because of swelling-shrinking of electrode occurs during the process. Moreover, the phosphates showed excellent capacitance retention than sulfates because of higher stability at higher scan rates. The effect of dopant was investigated in this study showed that dopant plays and important role in the performance of polyaniline as energy storage device. The smaller size dopant makes compact coating and can easily diffuse in and out of the polymer. However, during charge-discharge process the polymer swell and shrinks that makes its degradation faster. On the other hand, bigger size dopant showed stability at higher scan rates and current densities. This indicates that bigger size dopants are best for polyaniline that can be used for corrosion protection and energy storage device at the same time. Besides, work done in the thesis will benefit material interface related researches in general, and lead to in-depth studies of fundamental and applied sciences and technologies.

Chapter 6

Conclusions and outlook

In conclusions, we have demonstrated and discussed the performance of conducting polymer that can be used for multipurpose with single layer of coating. The electrochemical performance of conducting polymers is greatly influenced by type of dopants used for electrosynthesis. Additionally, these dopants affect the passivation behavior of steel used by forming metal oxide (passive layer) at different rates with varying concentrations. Furthermore, the presence of aromatic ring in dopant ions enhances conducting polymer performance. This is due to aromatic ring forms π- π stacking within the molecule along the polymer chain to create lamellar structures, which prevent the ingress of chloride ions in the coating system. In addition, size of dopant plays key role in anion exchange where bigger size dopant ions can partially replace smaller size dopant. On the other hand, small size dopants can completely replace bigger size dopant because bigger size dopant leave bigger pore when released. This creates a size memory effect in the polymer chain that can accommodate similar or small size dopants. Moreover, bigger dopants result in more open structure in polymer chains that promotes the ion transport. This makes redox sites in the polymer to be easily accessed.

The outcomes of this study can be further used in combination of commercially available organic paint topcoat to have longer life and higher corrosion potential with excellent biocidal properties. The coatings have shown excellent stability in chlorine-based bleach solution and can withstand

more than 100 ℃ for more than 30min. Our system can also be used as replacement of toxic metal primer, which is hazardous to many living organisms including human being and can be useful if used as an antibacterial or antifouling coating. Besides, work done in the thesis will benefit material interface related researches in general, and lead to in-depth studies of fundamental and applied sciences and technologies.

References

(1) Shirakawa, H.; Louis, J.; Macdiarmid, A. G. Synthesis of Electrically Conducting Organic Polymers : Halogene Derivatives of Polyacetylene, (CH)X. *J. C. S. Chem. Comm* **1977**, No. 578, 578–580.

(2) Skotheim, T. A.; Reynolds, J. R. *Handbook of Conducting Polymers: Conjugated Polymers Processing and Applications*; 2007.

(3) Dai, L. Chapter 2 Conducting Polymers. *Intelligent Macromolecules for Smart Devices* **1975**, *1980*, 1–41.

(4) Bufon, B. C. C.; Vollmer, J.; Heinzel, T.; Espindola, P.; John, H. Relationship between Chain Length , Disorder , and Resistivity in Polypyrrole Films. *Journal of Physical Chemistry B* **2005**, *109*, 19191–19199.

(5) Meerholz, K.; Heinze, J. Influence of Chain Length and Defects on the Electrical Conductivity of Conducting Polymers. *Synthetic Metals* **1993**, *57* (2–3), 5040–5045.

(6) Bufon, B. C. C.; Heinzel, T.; Espindola, P.; Heinze, J. Influence of the Polymerization Potential on the Transport Properties of Polypyrrole Films. *Journal of Physical Chemistry B* **2010**, *114*, 714–718.

(7) Heinze, J.; Frontana-Uribe, B. A.; Ludwigs, S. Electrochemistry of Conducting Polymers - Persistent Models and New Concepts. *Chemical Reviews* **2010**, *110*, 4724–4771.

(8) Otero, T. F.; Grande, H.; Rodriguez, J. Electrochemical Oxidation of Polypyrrole under Conformational Relaxation Control. Electrochemical Relaxation Model. *Synthetic Metals* **1996**, *76* (1–3), 285–288.

(9) Otero, T. F.; De Larreta, E. Electrochemical Control of the Morphology, Adherence, Appearance and Growth of Polypyrrole Films. *Synthetic Metals* **1988**, *26* (1), 79–88.

(10) Pan, L.; Yu, G.; Zhai, D.; Lee, H. R.; Zhao, W.; Liu, N.; Wang, H.; Tee, B. C.-K.; Shi, Y.; Cui, Y.; Bao, Z. Hierarchical Nanostructured Conducting Polymer Hydrogel with High Electrochemical Activity. *Proceedings of the National Academy of Sciences of the United States of America* **2012**, *109* (24), 9287–9292.

(11) Shi, Y.; Pan, L.; Liu, B.; Wang, Y.; Cui, Y.; Bao, Z.; Yu, G. Nanostructured Conductive Polypyrrole Hydrogels as High-Performance, Flexible Supercapacitor Electrodes. *Journal of Materials Chemistry A* **2014**, *2* (17), 6086.

(12) Arenas, M. C.; Sánchez, G.; Nicho, M. E.; Elizalde-Torres, J.; Castaño, V. M. Engineered Doped and Codoped Polyaniline Gas Sensors Synthesized in N,N,Dimethylformamide Media. *Applied Physics A: Materials Science and Processing* **2012**, *106* (4), 901–908.

(13) Choi, H. H.; Lee, J.; Dong, K.-Y.; Ju, B.-K.; Lee, W. Gas Sensing Performance of Composite Materials Using Conducting Polymer/Single-Walled Carbon Nanotubes. *Macromolecular Research* **2012**, *20* (2), 143–146.

(14) Tyler McQuade, D.; Pullen, A. E.; Swager, T. M. Conjugated Polymer-Based Chemical Sensors. *Chemical Reviews* **2000**, *100* (7), 2537–2574.

(15) Peng, H.; Zhang, L.; Soeller, C.; Travas-Sejdic, J. Conducting Polymers for Electrochemical DNA Sensing. *Biomaterials* **2009**, *30* (11), 2132–2148.

(16) Liu, Z.; Wang, J.; Kushvaha, V.; Poyraz, S.; Tippur, H.; Park, S.; Kim, M.; Liu, Y.; Bar, J.; Chen, H.; Zhang, X. Poptube Approach for Ultrafast Carbon Nanotube Growth. *Chemical Communications* **2011**, *47* (35), 9912.

(17) Zhang, X.; Manohar, S. K. Microwave Synthesis of Nanocarbons from Conducting

Polymers. *Chemical Communications* **2006**, No. 23, 2477.

(18) Spinks, G. M.; Dominis, A. J.; Wallace, G. G.; Tallman, D. E. Electroactive Conducting Polymers for Corrosion Control: Part 1. Non Ferrous Metals. *Journal of Solid State Electrochemistry* **2002**, *6* (2), 85–100.

(19) Çolak, N.; Özyilmaz, a. T. Polyaniline Coating on Iron–Synthesis and Characterization. *Polymer-Plastics Technology and Engineering* **2005**, *44* (8–9), 1547–1558.

(20) Tallman, D. E.; Spinks, G.; Dominis, A.; Wallace, G. G. Electroactive Conducting Polymers for Corrosion Control-Part 1. Genral Intro and Non-Ferrous Metals. *Journal of Solid State Electrochemistry* **2002**, *6* (2), 73–84.

(21) Özyilmaz, A. T.; Erbil, M.; Yazici, B. The Influence of Polyaniline (PANI) Top Coat on Corrosion Behaviour of Nickel Plated Copper. *Applied Surface Science* **2005**, *252* (5), 2092–2100.

(22) Pawar, P.; Gaikawad, A. B.; Patil, P. P. Electrochemical Synthesis of Corrosion Protective Polyaniline Coatings on Mild Steel from Aqueous Salicylate Medium. *Science and Technology of Advanced Materials* **2006**, *7* (7), 732–744.

(23) Saravanan, K.; Sathiyanarayanan, S.; Muralidharan, S.; Azim, S. S.; Venkatachari, G. Performance Evaluation of Polyaniline Pigmented Epoxy Coating for Corrosion Protection of Steel in Concrete Environment. *Progress in Organic Coatings* **2007**, *59* (2), 160–167.

(24) Bruyne, A. De; Delplancke, J. L.; Winand, R. Comparison between Polypyrrole Films Obtained on Mild Steel by Electropolymerization from Oxalic Acid and Sodium Sulphate Aqueous Solutions. *Surface and Coatings Technology* **1998**, *99* (1), 118–124.

(25) Brusic, V. Use of Polyaniline and Its Derivatives in Corrosion Protection of Copper and

Silver. *Journal of The Electrochemical Society* **1997**, *144* (2), 436.

(26) Kinlen, P. J.; Menon, V.; Ding, Y. A Mechanistic Investigation of Polyaniline Corrosion Protection Using the Scanning Reference Electrode Technique. *Journal of The Electrochemical Society* **1999**, *146* (10), 3690.

(27) Nautiyal, A.; Qiao, M.; Cook, J. E.; Zhang, X.; Huang, T.-S. High Performance Polypyrrole Coating for Corrosion Protection and Biocidal Applications. *Applied Surface Science* **2018**, *427*, 922–930.

(28) Nautiyal, A.; Parida, S. Comparison of Polyaniline Electrodeposition on Carbon Steel from Oxalic Acid and Salicylate Medium. *Progress in Organic Coatings* **2016**, *94*, 28–33.

(29) Wang, G.; Zhang, L.; Zhang, J. A Review of Electrode Materials for Electrochemical Supercapacitors. *Chemical Society Review* **2012**, *41*, 797–828.

(30) Yu, G.; Hu, L.; Liu, N.; Wang, H.; Vosgueritchian, M.; Yang, Y. Enhancing the Supercapacitor Performance of Graphene / MnO 2 -Nanostructured Electrodes by Conductive Wrapping. *Nano Letters* **2011**, *11*, 1–3.

(31) Bobacka, J. Conducting Polymer-Based Solid-State Ion-Selective Electrodes. *Electroanalysis* **2006**, *18* (1), 7–18.

(32) Shown, I.; Ganguly, A.; Chen, L.-C.; Chen, K.-H. Conducting Polymer-Based Flexible Supercapacitor. *Energy Science & Engineering* **2015**, *3* (1), 2–26.

(33) Ding, K.; Jia, H.; Wei, S.; Guo, Z. Electrocatalysis of Sandwich-Structured Pd/Polypyrrole/Pd Composites toward Formic Acid Oxidation. *Industrial and Engineering Chemistry Research* **2011**, *50* (11), 7077–7082.

(34) Yoon, H. Current Trends in Sensors Based on Conducting Polymer Nanomaterials. *Nanomaterials* **2013**, *3* (3), 524–549.

(35) Shao, L.; Cheng, X.; Wang, Z.; Ma, J.; Guo, Z. Tuning the Performance of Polypyrrole-Based Solvent-Resistant Composite Nanofiltration Membranes by Optimizing Polymerization Conditions and Incorporating Graphene Oxide. *Journal of Membrane Science* **2014**, *452*, 82–89.

(36) Fontana, M. G. *Corrosion Engineering*; 1987.

(37) Schirmeisen, M.; Beck, F. Electrocoating of Iron and Other Metals with Polypyrrole. *Journal of Applied Electrochemistry* **1989**, *19* (3), 401–409.

(38) Rizzi, M.; Trueba, M.; Trasatti, S. P. Polypyrrole Films on Al Alloys: The Role of Structural Changes on Protection Performance. *Synthetic Metals* **2011**, *161* (1–2), 23–31.

(39) Hülser, P.; Beck, F. Electrodeposition of Polypyrrole Layers on Aluminium from Aqueous Electrolytes. *Journal of Applied Electrochemistry* **1990**, *20* (4), 596–605.

(40) Troch-Nagels, G.; Winand, R.; Weymeersch, A.; Renard, L. Electron Conducting Organic Coating of Mild Steel by Electropolymerization. *Journal of Applied Electrochemistry* **1992**, *22* (8), 756–764.

(41) DeBerry, D. W. Modification of the Electrochemical and Corrosion Behavior of Stainless Steels with an Electroactive Coating. *Journal of The Electrochemical Society* **1985**, *132* (5), 1022.

(42) Shabani-Nooshabadi, M.; Mollahoseiny, M.; Jafari, Y. Electropolymerized Coatings of Polyaniline on Copper by Using the Galvanostatic Method and Their Corrosion Protection Performance in HCl Medium. *Surface and Interface Analysis* **2014**, *46* (7), 472–479.

(43) Shabani-Nooshabadi, M.; Ghoreishi, S. M.; Behpour, M. Electropolymerized Polyaniline Coatings on Aluminum Alloy 3004 and Their Corrosion Protection Performance. *Electrochimica Acta* **2009**, *54* (27), 6989–6995.

(44) Rahman, S. U.; Abul-Hamayel, M. A.; Abdul Aleem, B. J. Electrochemically Synthesized Polypyrrole Films as Primer for Protective Coatings on Carbon Steel. *Surface and Coatings Technology* **2006**, *200* (9), 2948–2954.

(45) Biallozor, S.; Kupniewska, A. Conducting Polymers Electrodeposited on Active Metals. *Synthetic Metals*. 2005, pp 443–449.

(46) Idla, K.; Talo, A.; Niemi, H. E.-M.; Forsén, O.; Yläsaari, S. An XPS and AFM Study of Polypyrrole Coating on Mild Steel. *Surface and Interface Analysis* **1997**, *25* (11), 837–854.

(47) Bruyne, A. De; Delplancke, J. L.; Winand, R. Comparison between Polypyrrole Films Obtained on Mild Steel by Electropolymerization from Oxalic Acid and Sodium Sulphate Aqueous Solutions. *Surface and Coatings Technology* **1998**, *99* (1), 118–124.

(48) Asan, A.; Kabasakaloglu, M. Electrochemical and Corrosion Behaviors of Mild Steel Coated with Polypyrrole. *Materials Science* **2003**, *39* (5), 643–651.

(49) Videla, H. A. Microbially Induced Corrosion: An Updated Overview. *International Biodeterioration & Biodegradation* **2001**, *48* (1), 176–201.

(50) Little, B. J.; Lee, J. S. Microbiologically Influenced Corrosion. In *Kirk-Othmer Encyclopedia of Chemical Technology*; 2009; pp 1–42.

(51) Heitz, E.; Flemming, H.-C.; Sand, W. Microbially Influenced Corrosion of Materials: Scientific and Engineering Aspects. *Solid State Electrochem* **1997**, 1.

(52) Enning, D.; Garrelfs, J. Corrosion of Iron by Sulfate-Reducing Bacteria: New Views of an Old Problem. *Applied and Environmental Microbiology* **2014**, *80* (4), 1226–1236.

(53) Da Silva, F. A. G.; Queiroz, J. C.; Macedo, E. R.; Fernandes, A. W. C.; Freire, N. B.; Da Costa, M. M.; De Oliveira, H. P. Antibacterial Behavior of Polypyrrole: The Influence of

Morphology and Additives Incorporation. *Materials Science and Engineering C* **2016**, *62*, 317–322.

(54) Qiao, M.; Ren, T.; Huang, T.-S.; Weese, J.; Liu, Y.; Ren, X.; Farag, R. N-Halamine Modified Thermoplastic Polyurethane with Rechargeable Antimicrobial Function for Food Contact Surface. *RSC Adv.* **2017**, *7* (3), 1233–1240.

(55) Rammelt, U.; Nguyen, P. T.; Plieth, W. Corrosion Protection by Ultrathin Films of Conducting Polymers. *Electrochimica Acta* **2003**, *48* (9 SPEC.), 1257–1262.

(56) Iroh, J. O.; Su, W. Corrosion Performance of Polypyrrole Coating Applied to Low Carbon Steel by an Electrochemical Process. *Electrochimica Acta* **2000**, *46* (1), 15–24.

(57) Yang, Iuan-Jou; Teng, M.-Y. Passivation of Iron-Based Alloys in Para-Toluene Sulfonic Acid. *J. Electrochem. Soc.* **1993**, *140* (6), 1556–1561.

(58) Camalet, J. L.; Lacroix, J. C.; Aeiyach, S.; Lacaze, P. C. Characterization of Polyaniline Films Electrodeposited on Mild Steel in Aqueous P-Toluenesulfonic Acid Solution. *Journal of Electroanalytical Chemistry* **1998**, *445* (1–2), 117–124.

(59) Bernard, M. C.; Hugot-LeGoff, A.; Joiret, S.; Dinh, N. N.; Toan, N. N. Polyaniline Layer for Iron Protection in Sulfate Medium. *Synthetic Metals* **1999**, *102* (1–3), 1383–1384.

(60) Nguyen Thi Le, H.; Garcia, B.; Deslouis, C.; Le Xuan, Q. Corrosion Protection and Conducting Polymers: Polypyrrole Films on Iron. *Electrochimica Acta* **2001**, *46* (26–27), 4259–4272.

(61) Cohen, M. The Formation and Properties of Passive Films on Iron. *Canadian Journal of Chemistry* **1959**, *37* (1), 286–291.

(62) Oswin, H.G.; Cohen, M. Study of the Cathodic Reduction of Oxide Films on Iron. *Journal of Electrochemical Society* **1957**, *10* (1), 9–16.

(63) Free, M. L. Understanding the Effect of Surfactant Aggregation on Corrosion Inhibition of Mild Steel in Acidic Medium. *Corrosion Science* **2002**, *44* (12), 2865–2870.

(64) Shustak, G.; Domb, A. J.; Mandler, D. Preparation and Characterization of N-Alkanoic Acid Self-Assembled Monolayers Adsorbed on 316L Stainless Steel. *Langmuir* **2004**, *20* (18), 7499–7506.

(65) Shustak, G.; Domb, A. J.; Mandler, D. N-Alkanoic Acid Monolayers on 316L Stainless Steel Promote the Adhesion of Electropolymerized Polypyrrole Films. *Langmuir* **2006**, *22* (12), 5237–5240.

(66) Cords, B. R.; Burnett, S. L.; Hilgren, J.; Finley, M.; Magnuson, J. Surface-Active Agents , and Peroxides. In *Antimicrobials in Food*; 2005; pp 533–536.

(67) Qiao, M. Application and Toxicity Assessment of Antimicrobial N-Halamines for Food Safety Controls, Auburn University, 2017.

(68) Igual Muñoz, A.; García Antón, J.; Guiñón, J. L.; Pérez Herranz, V. Inhibition Effect of Chromate on the Passivation and Pitting Corrosion of a Duplex Stainless Steel in LiBr Solutions Using Electrochemical Techniques. *Corrosion Science* **2007**, *49* (8), 3200–3225.

(69) Ding, M.; Shi, X. Molecular Mechanisms of Cr (VI) Induced Carcinogenesis. *Molecular and Cellular Biochemistry* **2002**, *234* (1), 293–300.

(70) Schirmeisen, M.; Beck, F. Electrocoating of Iron and Other Metals with Polypyrrole. *Journal of Applied Electrochemistry* **1989**, *19* (3), 401–409.

(71) Wessling, B.; Posdorfer, J. Nanostructures of the Dispersed Organic Metal Polyaniline Responsible for Macroscopic Effects in Corrosion Protection. *Synthetic Metals* **1999**, *102* (1–3), 1400–1401.

(72) Gašparac, R.; Martin, C. R. Investigations of the Mechanism of Corrosion Inhibition by Polyaniline. Polyaniline-Coated Stainless Steel in Sulfuric Acid Solution. *Journal of The Electrochemical Society* **2001**, *148* (4), B138–B145.

(73) Ahmad, N.; MacDiarmid, A. G. Inhibition of Corrosion of Steels with the Exploitation of Conducting Polymers. *Synthetic Metals* **1996**, *78* (2), 103–110.

(74) Wessling, B. Dispersion as the Link between Basic Research and Commercial Applications of Conductive Polymers (Polyaniline). *Synthetic Metals* **1998**, *93* (2), 143–154.

(75) Aeiyach, S.; Zaid, B.; Lacaze, P. C. One-Step Electrosynthesis of PPy Films on Zinc Substrates by Anodic Polymerization of Pyrrole in Aqueous Solution. *Electrochimica Acta* **1999**, *44* (17), 2889–2898.

(76) Huang, W.-S.; Humphrey, B. D.; MacDiarmid, A. G. Polyaniline, a Novel Conducting Polymer. *Journal of the Chemical Society, Faraday Transactions* **1986**, *82*, 2385–2400.

(77) MacDiarmid, A. G.; Epstein, A. J. Polyanilines: A Novel Class of Conducting Polymers. *Faraday Discussions of the Chemical Society* **1989**, *88*, 317.

(78) Salamifar, E.; Mehrgardi, M. A.; Mousavi, M. F. Ion Transport and Degradation Studies of a Polyaniline-Modified Electrode Using SECM. *Electrochimica Acta* **2009**, *54* (20), 4638–4646.

(79) Ayad, M. M.; Salahuddin, N. A.; Abou-Seif, A. K.; Alghaysh, M. O. PH Sensor Based on Polyaniline and Aniline–anthranilic Acid Copolymer Films Using Quartz Crystal Microbalance and Electronic Absorption Spectroscopy. *Polym. Adv. Technol.* **2008**, *19* (April), 1142–1148.

(80) Jin, Z.; Su, Y.; Duan, Y. Improved Optical PH Sensor Based on Polyaniline. *Sensors and*

Actuators, B: Chemical **2000**, *71* (1–2), 118–122.

(81) Kaempgen, M.; Roth, S. Transparent and Flexible Carbon Nanotube/Polypyrrole and Carbon Nanotube/Polyaniline PH Sensors. *Physica Status Solidi (B) Basic Research* **2006**, *243* (13), 3519–3523.

(82) Eftekhari, A.; Afshani, R. Electrochemical Polymerization of Aniline in Phosphoric Acid. *Journal of Polymer Science, Part A: Polymer Chemistry* **2006**, *44* (10), 3304–3311.

(83) Gao, Y.; Syed, J. A.; Lu, H.; Meng, X. Anti-Corrosive Performance of Electropolymerized Phosphomolybdic Acid Doped PANI Coating on 304SS. *Applied Surface Science* **2016**, *360*, 389–397.

(84) Lizarraga, L.; Andrade, E. M.; Molina, F. V. Anion Exchange Influence on the Electrochemomechanical Properties of Polyaniline. *Electrochimica Acta* **2007**, *53* (2), 538–548.

(85) Roobottom, H. K.; Jenkins, H. D. B.; Passmore, J.; Glasser, L. Thermochemical Radii of Complex Ions. *Journal of Chemical Education* **1999**, *76* (11), 1570–1573.

(86) Cao, F.; Wei, J.; Dong, J.; Ke, W. The Corrosion Inhibition Effect of Phytic Acid on 20SiMn Steel in Simulated Carbonated Concrete Pore Solution. *Corrosion Science* **2015**, *100*, 365–376.

(87) Gao, X.; Zhao, C.; Lu, H.; Gao, F.; Ma, H. Influence of Phytic Acid on the Corrosion Behavior of Iron under Acidic and Neutral Conditions. *Electrochimica Acta* **2014**, *150*, 188–196.

(88) Xing, J.; Liao, M.; Zhang, C.; Yin, M.; Li, D.; Song, Y. The Effect of Anions on the Electrochemical Properties of Polyaniline for Supercapacitors. *Physical Chemistry Chemical Physics* **2017**, *19* (21), 14030–14041.

(89) Trchová, M.; Šeděnková, I.; Tobolková, E.; Stejskal, J. FTIR Spectroscopic and Conductivity Study of the Thermal Degradation of Polyaniline Films. *Polymer Degradation and Stability* **2004**, *86* (1), 179–185.

(90) Šeděnková, I.; Trchová, M.; Blinova, N. V.; Stejskal, J. In-Situ Polymerized Polyaniline Films. Preparation in Solutions of Hydrochloric, Sulfuric, or Phosphoric Acid. *Thin Solid Films* **2006**, *515* (4), 1640–1646.

(91) Scheider, W. Theory of the Frequency Dispersion of Electrode Polarization. Topology of Networks with Fractional Power Frequency Dependence. *The Journal of Physical Chemistry* **1975**, *79* (2), 127–136.

(92) Tang, S. J.; Wang, A. T.; Lin, S. Y.; Huang, K. Y.; Yang, C. C.; Yeh, J. M.; Chiu, K. C. Polymerization of Aniline under Various Concentrations of APS and HCl. *Polymer Journal* **2011**, *43* (8), 667–675.

(93) Arora, M.; Gupta, S. K. Vibrational Spectroscopy of PTSA - Doped Polyaniline. *AIP Conference Proceedings* **2008**, *1075*, 118–120.

(94) Jastrzbski, W.; Sitarz, M.; Rokita, M.; Bułat, K. Infrared Spectroscopy of Different Phosphates Structures. *Spectrochimica Acta - Part A: Molecular and Biomolecular Spectroscopy* **2011**, *79* (4), 722–727.

(95) Northcutt, R. G.; Sundaresan, V. B. Phospholipid Vesicles as Soft Templates for Electropolymerization of Nanostructured Polypyrrole Membranes with Long Range Order. *Journal of Materials Chemistry A* **2014**, *2* (30), 11784–11791.

(96) Armes, S. P.; Miller, J. F. Optimum Reaction Conditions for the Polymerization of Aniline in Aqueous Solution by Ammonium Persulphate. *Synthetic Metals* **1988**, *22* (4), 385–393.

(97) Bacon, J.; Adams, R. N. Anodic Oxidations of Aromatic Amines. III. Substituted Anilines in Aqueous Media. *Journal of the American Chemical Society* **1968**, *90* (24), 6596–6599.

(98) Lee, H.; Dellatore, S. M.; Miller, W. M.; Messersmith, P. B. Mussel-Inspired Surface Chemistry for Multifunctional Coatings. *Science* **2007**, *318* (OCTOBER), 426–431.

(99) Lee, H.; Scherer, N. F.; Messersmith, P. B. Single-Molecule Mechanics of Mussel Adhesion. *Proceedings of the National Academy of Sciences* **2006**, *103* (35), 12999–13003.

(100) Liu, Y.; Ai, K.; Lu, L. Polydopamine and Its Derivative Materials: Synthesis and Promising Applications in Energy, Environmental, and Biomedical Fields. *Chemical Reviews* **2014**, *114* (9), 5057–5115.

(101) Kim, R.; Nam, Y. Electrochemical Layer-by-Layer Approach to Fabricate Mechanically Stable Platinum Black Microelectrodes Using a Mussel-Inspired Polydopamine Adhesive. *Journal of Neural Engineering* **2015**, *12* (2).

(102) Łuczak, T. Preparation and Characterization of the Dopamine Film Electrochemically Deposited on a Gold Template and Its Applications for Dopamine Sensing in Aqueous Solution. *Electrochimica Acta* **2008**, *53* (19), 5725–5731.

(103) Yu, F.; Chen, S.; Chen, Y.; Li, H.; Yang, L.; Chen, Y.; Yin, Y. Experimental and Theoretical Analysis of Polymerization Reaction Process on the Polydopamine Membranes and Its Corrosion Protection Properties for 304 Stainless Steel. *Journal of Molecular Structure* **2010**, *982* (1–3), 152–161.

(104) Wang, J. lei; Li, B. chao; Li, Z. jun; Ren, K. feng; Jin, L. jiang; Zhang, S. miao; Chang, H.; Sun, Y. xin; Ji, J. Electropolymerization of Dopamine for Surface Modification of Complex-Shaped Cardiovascular Stents. *Biomaterials* **2014**, *35* (27), 7679–7689.

(105) Reynolds, J. R.; Kumar, A.; Reddinger, J. L.; Sankaran, B.; Sapp, S. A.; Sotzing, G. A. Unique Variable-Gap Polyheterocycles for High-Contrast Dual Polymer Electrochromic Devices. *Synthetic Metals* **1997**, *85* (1–3), 1295–1298.

(106) Groenendaal, B. L.; Jonas, F.; Freitag, D.; Pielartzik, H.; Reynolds, J. R. PEDOT Its Derivatives : Past , Present and Future. *Advanced Materials* **2000**, *12* (7), 481–494.

(107) Dietrich, M.; Heinze, J.; Heywang, G.; Jonas, F. Electrochemical and Spectroscopic Characterization of Polyalkylenedioxythiophenes. *Journal of Electroanalytrcal Chemistry* **1994**, *369*, 87–92.

(108) Pei, Q.; Zuccarello, G.; Ahlskog, M.; Inganäs, O. Electrochromic and Highly Stable Poly(3,4-Ethylenedioxythiophene) Switches between Opaque Blue-Black and Transparent Sky Blue. *Polymer* **1994**, *35* (7), 1347–1351.

(109) Chen, X.; Xing, K. Z.; Inganäs, O. Electrochemically Induced Volume Changes in Poly(3,4-Ethylenedioxythiophene). *Chemistry of Materials* **1996**, *8* (10), 2439–2443.

(110) Sun, K.; Zhang, S.; Li, P.; Xia, Y.; Zhang, X.; Du, D.; Isikgor, F. H.; Ouyang, J. Review on Application of PEDOTs and PEDOT:PSS in Energy Conversion and Storage Devices. *Journal of Materials Science: Materials in Electronics* **2015**, *26* (7), 4438–4462.

(111) Benor, A.; Takizawa, S. ya; Pérez-Bolívar, C.; Anzenbacher, P. Efficiency Improvement of Fluorescent OLEDs by Tuning the Working Function of PEDOT:PSS Using UV-Ozone Exposure. *Organic Electronics: physics, materials, applications* **2010**, *11* (5), 938–945.

(112) Tait, J. G.; Worfolk, B. J.; Maloney, S. A.; Hauger, T. C.; Elias, A. L.; Buriak, J. M.; Harris, K. D. Spray Coated High-Conductivity PEDOT:PSS Transparent Electrodes for Stretchable and Mechanically-Robust Organic Solar Cells. *Solar Energy Materials and Solar Cells* **2013**, *110*, 98–106.

(113) Elschner, A.; Lövenich, W. Solution-Deposited PEDOT for Transparent Conductive Applications. *MRS Bulletin* **2011**, *36* (10), 794–798.

(114) Arbizzani, C.; Mastragostino, M.; Rossi, M. Preparation and Electrochemical Characterization of a Polymer Li1.03Mn1.97O4/PEDOT Composite Electrode. *Electrochemistry Communications* **2002**, *4* (7), 545–549.

(115) Arbizzani, C.; Balducci, A.; Mastragostino, M.; Rossi, M.; Soavi, F. Li1.01Mn1.97O4 Surface Modification by Poly(3,4-Ethylenedioxythiophene). *Journal of Power Sources* **2003**, *119–121*, 695–700.

(116) Liu, K.; Hu, Z.; Xue, R.; Zhang, J.; Zhu, J. Electropolymerization of High Stable Poly(3,4-Ethylenedioxythiophene) in Ionic Liquids and Its Potential Applications in Electrochemical Capacitor. *Journal of Power Sources* **2008**, *179* (2), 858–862.

(117) Huang, L. M.; Lin, H. Z.; Wen, T. C.; Gopalan, A. Highly Dispersed Hydrous Ruthenium Oxide in Poly(3,4-Ethylenedioxythiophene)-Poly(Styrene Sulfonic Acid) for Supercapacitor Electrode. *Electrochimica Acta* **2006**, *52* (3), 1058–1063.

(118) Ghosh, S.; Inganas, O. Conducting Polymer Hydrogels as 3D Electrodes : Applications for Supercapacitors. *Advanced Materials* **1999**, *11* (14), 1214–1218.

(119) Ghosh, S.; Inganäs, O. Electrochemical Characterization of Poly(3,4-Ethylene Dioxythiophene) Based Conducting Hydrogel Networks. *Journal of The Electrochemical Society* **2000**, *147* (5), 1872.

(120) Choi, J. W.; Han, M. G.; Kim, S. Y.; Oh, S. G.; Im, S. S. Poly(3,4-Ethylenedioxythiophene) Nanoparticles Prepared in Aqueous DBSA Solutions. *Synthetic Metals* **2004**, *141* (3), 293–299.

(121) Sadki, S.; Chevrot, C. Electropolymerization of 3,4-Ethylenedioxythiophene, N-

Ethylcarbazole and Their Mixtures in Aqueous Micellar Solution. *Electrochimica Acta* **2003**, *48* (6), 733–739.

(122) Zhu, G.; Hou, J.; Zhu, H.; Qiu, R.; Xu, J. Electrochemical Synthesis of Poly(3,4-Ethylenedioxythiophene) on Stainless Steel and Its Corrosion Inhibition Performance. *Journal of Coatings Technology and Research* **2013**, *10* (5), 659–668.

(123) Hui, Y.; Bian, C.; Wang, J.; Tong, J.; Xia, S. Comparison of Two Types of Overoxidized PEDOT Films and Their Application in Sensor Fabrication. *Sensors (Switzerland)* **2017**, *17* (3), 2–12.

(124) IEA. *Renewable Energy: Medium-Term Market Report 2014*; 2014.

(125) Osaka, T.; Naoi, K.; Sakai, H.; Ogano, S. Effect of PF6- Anion on the Properties of Lithium-Polypyrrole Battery during Polypyrrole Film Formation. *J. Electrochem. Soc.* **1987**, *134* (2), 285–289.

(126) Kaneto, K.; Maxfield, M.; Nairns, D. P.; Macdiarmid, A. G.; Heeger, A. J. Electrochemistry of Polyacetylene: Characteristics of Polyacetylenes Cathodes. *J. Chem. Soc. Faraday Trans. 1* **1982**, *78*, 3417–3429.

(127) Yoshinos, K.; Kaneto, K.; Takeda, S. Applications of Conducting Polymers as Electronics and Optoelectronics Devices. *Synthetic Metals* **1987**, *18*, 741–746.

(128) Kobayashi, T.; Yoneyama, H.; Tamura, H. Polyaniline Film-Coated Electrodes as Electrochromic Display Devices. *Journal of Electroanalytical Chemistry* **1984**, *161* (2), 419–423.

(129) Spinks, G. M.; Dominis, A. J.; Wallace, G. G.; Tallman, D. E. Electroactive Conducting Polymers for Corrosion Control: Part 2. Ferrous Metals. *Journal of Solid State Electrochemistry* **2002**, *6* (2), 85–100.

(130) Yoon, H. Current Trends in Sensors Based on Conducting Polymer Nanomaterials. *Nanomaterials* **2013**, *3* (3), 524–549.

(131) Simon, P.; Gogotsi, Y. Materials for Electrochemical Capacitors. *Nature Materials* **2008**, *7* (11), 845–854.

(132) Wang, G.; Zhang, L.; Zhang, J. A Review of Electrode Materials for Electrochemical Supercapacitors. *Chem Soc Rev* **2012**, *41* (2), 797–828.

(133) Lukatskaya, M. R.; Dunn, B.; Gogotsi, Y. Multidimensional Materials and Device Architectures for Future Hybrid Energy Storage. *Nature Communications* **2016**, *7*, 12647.

(134) Yu, Z.; Tetard, L.; Zhai, L.; Thomas, J. Supercapacitor Electrode Materials: Nanostructures from 0 to 3 Dimensions. *Energy Environ. Sci.* **2015**, *8* (3), 702–730.

(135) Xu, C.; Li, Z.; Yang, C.; Zou, P.; Xie, B.; Lin, Z.; Zhang, Z.; Li, B.; Kang, F.; Wong, C.-P. An Ultralong, Highly Oriented Nickel-Nanowire-Array Electrode Scaffold for High-Performance Compressible Pseudocapacitors. *Advanced Materials* **2016**, *28* (28), 5777.

(136) Deng, W.; Ji, X.; Chen, Q.; Banks, C. E. Electrochemical Capacitors Utilising Transition Metal Oxides: An Update of Recent Developments. *RSC Advances* **2011**, *1* (7), 1171.

(137) Faraji, S.; Ani, F. N. Microwave-Assisted Synthesis of Metal Oxide/Hydroxide Composite Electrodes for High Power Supercapacitors - A Review. *Journal of Power Sources* **2014**, *263*, 338–360.

(138) Kim, I.-H.; Kim, K.-B. Ruthenium Oxide Thin Film Electrodes for Supercapacitors. *Electrochemical and Solid-State Letters* **2001**, *4* (5), A62–A64.

(139) Zhi, M.; Xiang, C.; Li, J.; Li, M.; Wu, N. Nanostructured Carbon-Metal Oxide Composite Electrodes for Supercapacitors: A Review. *Nanoscale* **2013**, *5* (1), 72–88.

(140) Zeng, W.; Zhang, G.; Hou, S.; Wang, T.; Duan, H. Facile Synthesis of

Graphene@NiO/MoO3 Composite Nanosheet Arrays for High-Performance Supercapacitors. *Electrochimica Acta* **2015**, *151*, 510–516.

(141) Tran, H. D.; D'Arcy, J. M.; Wang, Y.; Beltramo, P. J.; Strong, V. A.; Kaner, R. B. The Oxidation of Aniline to Produce "Polyaniline": A Process Yielding Many Different Nanoscale Structures. *Journal of Materials Chemistry* **2011**, *21* (11), 3534–3550.

(142) Zhang, H.; Zhao, Q.; Zhou, S.; Liu, N.; Wang, X.; Li, J.; Wang, F. Aqueous Dispersed Conducting Polyaniline Nanofibers: Promising High Specific Capacity Electrode Materials for Supercapacitor. *Journal of Power Sources* **2011**, *196* (23), 10484–10489.

(143) Xu, J.; Wang, K.; Zu, S. Z.; Han, B. H.; Wei, Z. Hierarchical Nanocomposites of Polyaniline Nanowire Arrays on Graphene Oxide Sheets with Synergistic Effect for Energy Storage. *ACS Nano* **2010**, *4* (9), 5019–5026.

(144) Wang, K.; Huang, J.; Wei, Z. Conducting Polyaniline Nanowire Arrays for High Performance Supercapacitors. *The Journal of Physical Chemistry C* **2010**, *114* (17), 8062–8067.

(145) Woo, S. W.; Dokko, K.; Nakano, H.; Kanamura, K. Incorporation of Polyaniline into Macropores of Three-Dimensionally Ordered Macroporous Carbon Electrode for Electrochemical Capacitors. *Journal of Power Sources* **2009**, *190* (2), 596–600.

(146) Eftekhari, A.; Fan, Z. Ordered Mesoporous Carbon and Its Applications for Electrochemical Energy Storage and Conversion. *Mater. Chem. Front.* **2017**, *1* (6), 1001–1027.

(147) Kulkarni, M. V.; Viswanath, A. K.; Marimuthu, R.; Seth, T. Synthesis and Characterization of Polyaniline Doped with Organic Acids. *Journal of Polymer Science, Part A: Polymer Chemistry* **2004**, *42* (8), 2043–2049.

(148) Zhang, Z.; Wei, Z.; Wan, M. Nanostructures of Polyaniline Doped with Inorganic Acids. *Macromolecules* **2002**, *35* (15), 5937–5942.

(149) Gujar, T. P.; Kim, W. Y.; Puspitasari, I.; Jung, K. D.; Joo, O. S. Electrochemically Deposited Nanograin Ruthenium Oxide as a Pseudocapacitive Electrode. *International Journal of Electrochemical Science* **2007**, *2* (9), 666–673.

(150) Bard, A. J.; Faulkner, L. R. *Electrochemcial Methods: Fundamentals and Applications*, Second.; John Wiley and Sons, 2001.

(151) Kim, J.; Lee, J.; You, J.; Park, M.-S.; Hossain, M. S. Al; Yamauchi, Y.; Kim, J. H. Conductive Polymers for Next-Generation Energy Storage Systems: Recent Progress and New Functions. *Mater. Horiz.* **2016**, *3* (6), 517–535.

(152) Zhang, A. Q.; Cui, C. Q.; Lee, J. Y. Electrochemical Degradation of Polyaniline in HClO4 and H2SO4. *Synthetic Metals* **1995**, *72* (3), 217–223.

(153) Kötz, R.; Carlen, M. Principles and Applications of Electrochemical Capacitors. *Electrochimica Acta* **2000**, *45* (15–16), 2483–2498.

(154) Chen, W. C.; Wen, T. C.; Teng, H. Polyaniline-Deposited Porous Carbon Electrode for Supercapacitor. *Electrochimica Acta* **2003**, *48* (6), 641–649.